AN ABSTRACT OF THE THESIS OF

Teresa L. Lemmon for the degree of Doctor of Philosophy in Chemistry presented on April 26, 1995. Title: Development of Chemostats and Use of Redox Indicators for Studying Redox Transformations in Biogeochemical Matrices.

Redacted for Privacy

Abstract approved: _____

James D. Ingle Jr.

Two sophisticated reactor systems were developed for the study of redox transformations of organic and inorganic matrix species, organic and inorganic contaminants, and organic redox indicators. These computer-controlled reactor systems allow investigation of samples at different environmental redox levels (as measured with a Pt electrode) under well controlled, quasi steady-state conditions. A unique external flow loop system provides a continuously filtered and recirculated solution for on-line measurements.

The usefulness of twelve redox indicators in solution for the evaluation the redox potential was demonstrated. The speciation (determined by the measured absorbance) of indicators that couple with Fe(II) (dichloroindophenol, methylene blue and thionine) can be utilized to predict the prevalent oxidation state of Fe. Because all reduced indicators couple with Cr(VI), the reduction of the indicator by the matrix correlates to reduced Cr in the sample.

Two of the indicators tested in solution experiments, thionine and phenosafranine, were immobilized on an affinity chromatography gel which demonstrates an innovative use of existing technology. The absorbance of the gel was measured by packing the beads into a spectrophotometric flow cell in the external flow loop of the reactor system. The electronic structure and electrochemical behavior of these indicators were only slightly affected by immobilization on the gel. For both indicators, immobilization caused the formal potential at pH 7 to decrease less than 20 mV ($E^{o'}$ = 52 mV, Thi_{immob}; $E^{o'}$ = -286 mV, $PSaf_{immob}$), and adsorption spectrum to shift less than 40 nm higher (λ_{max} = 640 nm, Thi_{immob}; λ_{max} = 544 nm, $PSaf_{immob}$) with respect to the free (unbound) indicators. These immobilized redox indicators are useful for studying the redox characteristics of geochemical matrices in which adsorption of free indicators on solids would preclude their use.

The reactor system and immobilized thionine (which couples with Fe(II), O_2, and Cr(VI)) were used to study redox transformations in several soil solutions. The measured absorbance can be used to predict the redox status of some species in the solution (e.g., Fe(II) concentration above 30 μM and no detectable Cr(VI) present if indicator is reduced). The solution concentration of Fe(II), Mn(II), and phosphate were monitored and correlated to the measured E_H throughout the experiments. A strong negative correlation is observed between Fe(II) and E_H below 200 mV. There is a positive correlation between the Fe(II) and phosphate concentrations.

Development of Chemostats and Use of Redox Indicators for Studying Redox Transformations in Biogeochemical Matrices

by

Teresa L. Lemmon

A THESIS

submitted to

Oregon State University

in partial fulfillment of
the requirements for the
degree of

Doctor of Philosophy

Completed April 26, 1995
Commencement June 1995

Doctor of Philosophy thesis of Teresa L. Lemmon presented on April 26, 1994

APPROVED:

Redacted for Privacy

Major Professor, representing Chemistry

Redacted for Privacy

Chair of Department of Chemistry

Redacted for Privacy

Dean of Graduate School

I understand that my thesis will become part of the permanent collection of Oregon State University libraries. My signature below authorizes release of my thesis to any reader upon request.

Redacted for Privacy

Teresa L. Lemmon, Author

This thesis is dedicated to the loving memory of my grandfather.

ACKNOWLEDGMENT

I would like to thank Dr. James Ingle Jr. for his support and guidance in both my research and the preparation of this thesis. Jim has been a mentor and teacher and I have enjoyed working with him and learning from him. He has always challenged me to excel, and I am grateful. Financial support for my research was provided by the Western Region Hazardous Substance Research Center. I would like to acknowledge Jim Mobley for his initial evaluation of the indicators which was my starting block, and Mike Schuyler and Armando Heberlin for their programming assistance. I would also like to thank the members of the Ingle group, Eric Clark, Ying Yang, Jameela Al-Mutawah, Mark Bos, and Brian Jones for their friendship, suggestions and distractions. Finally, and most importantly, I wish to thank my husband John for his constant encouragement and faith in me, and my family for all their support.

TABLE OF CONTENTS

Page

1. Introduction 1

2. Historical 6

3. Reactor System for Study of Reductive Dechlorination in Anaerobic Cultures 13

   3.1 Introduction 14
   3.2 Experimental 18

      3.2.1 Instrumentation 18
      3.2.2 Interfacing 22
      3.2.3 Software 22
      3.2.4 Procedure 29

   3.3 Results and Discussion 33
   3.4 Conclusions 40
   3.5 References 42

4. Reactor System for Study of Redox Transformations in Controlled Environmental Conditions 44

   4.1 Introduction 45
   4.2 Experimental 50
   4.2.1 Instrumentation 50

      4.2.2 Interfacing 55
      4.2.3 Software 56
      4.2.4 Procedure 67

   4.3 Results and Discussion 68
   4.4 Conclusions 73
   4.5 References 74

5. Characterization and Immobilization of Redox Indicators 76

   5.1 Introduction 77

TABLE OF CONTENTS (Continued)

Page

5.2 Experimental 83

5.2.1 Chemicals 83
5.2.2 Characterization of Redox Indicators 85
5.2.3 Immobilization of Indicators 89
5.2.4 Characterization of Oxygen Response 100

5.3 Results and Discussion 101

5.3.1 Characterization of Redox Indicators 101
5.3.2 Immobilization of Indicators 115
5.3.3 Characterization of Oxygen Response 122

5.4 Conclusions 128
5.5 References 135

6. Redox Characterization of Soil 137

6.1 Introduction 138
6.2 Experimental 141

6.2.1 Instrumentation 141
6.2.2 Soil Samples 143
6.2.3 Reactor Studies 146

6.3 Results and Discussion 149

6.3.1 Aloha BC soil 149
6.3.2 Aloha A1 154
6.3.3 Bashaw A1 Soil 166

6.4 Conclusions 188
6.5 References 191

7. Conclusions 193

Bibliography 198

TABLE OF CONTENTS (Continued)

Page

Appendices 203

Appendix A Instrumentation 204
Appendix B Colorimetric Procedures 218
Appendix C Detailed Experimental Procedure 220
Appendix D Chromium Reactions in the Environment 226

LIST OF FIGURES

Figure		Page
3.1	Schematic of reactor system	19
3.2	Computer screen display during experiment.	24
3.3	Schematic of pH-stat approach.	26
3.4	Variation of pH (-) and acetate concentrations (▬)during an experiment of about 2 weeks	35
3.5	Total amount of acetate added during a portion of an experiment	36
3.6	Example of wide fluctuations in measured potential when a significant amount of oxidant is consumed in the one minute between reagent addition and measurement of Pt after	38
3.7	Example of changing redox condition during two experiments	39
4.1	Schematic of reactor system	51
4.2	Computer screen display during experiment.	57
4.3	Conceptual approach to E_H- and pH-stat with a liquid	60
4.4	Conceptual approach to E_H-stat with O_2 gas.	65
4.5	Program flow chart.	69
4.6	Example of pH-stat at pH 6 utilizing acid (1 M) and base (1 M).	71
4.7	Example of Eh-stat utilizing H2O2 to maintain various redox potentials	72
5.1	Schematic of reactor system.	86
5.2	Indicators with amine groups not directly involved with the redox chemistry.	90

LIST OF FIGURES (Continued)

Figure		Page
5.3	Reaction scheme for coupling indicators to Spectra/Gel® MAS (MonoAldehyde Surface) beads.	92
5.4	Flow cell packed with immobilized indicator	94
5.5	Flow loop to determine E°' for bound indicators	96
5.6	Two reaction schemes for attaching an indicator to a polymer	99
5.7	Absorption spectrum of Cr(VI) (157 μM) and thionine (5 μM) solution; (a) before and (b) after titration with Fe(II) (50 mM).	102
5.8	Titration of Cr(VI) and thionine (Thi) with Fe(II): (a) absorbance of chromate (372 nm) and Thi (598 nm); (b) potential at a platinum electrode	103
5.9	Additional electrode data obtained during titration of Cr(VI) and Thi experiment: (a) measured DO concentration; (b) pH.	104
5.10	Titration of Cr(VI) and methylene blue (MB) with Fe(II) (a, b), and titration of Cr(VI) and safranine O (SafO) with Ti(III) (c, d).	105
5.11	Titration of Cr(VI) and indicator (indigo carmine (IC) a and b, benzyl viologen (BV) c and d) with Ti(III).	106
5.12	Titration of Cr(VI) and methyl viologen (MV) with Ti(III) (a, b), and titiration of dichloroindophenol (DCIP) (c, d) with Fe(II).	107
5.13	Titration of Cr(VI) and indicator (indigo tetrasulfonic acid (ITESA) a and b, phenosafranine (Psaf) c and d) with Ti(III).	108
5.14	Comparison of observed E_H and computed E_H: ○=DCIP; ●=TB; ▽=THI; ▼=MB; □= ITESA; ■=IC; Δ=PSaf; ▲=SafO; ⧖=BV; ⧗=MV	112
5.15	Absorption spectrum of immobilized indicators: (a) thionine; (b) phenosafranine	117
5.16	Redox cycling of immobilized thionine.	121

LIST OF FIGURES (Continued)

Figure		Page
5.17	Monitored parameters during the determination of oxygen transfer efficiency from gas stream to solution.	124
5.18	Potential scale showing location of redox indicators and important couples.	129
6.1	Schematic of reactor system.	142
6.2	Potential measured at a Pt electrode and pH during the Aloha BC soil experiment.	151
6.3	Total amount of acid, base and glucose added to the reactor during the Aloha BC soil experiment.	153
6.4	Pt electrode potential and pH during first 350 hr of the Aloha A1 #1 experiment.	156
6.5	Pt electrode potential and pH during the last 150 hr of the Aloha A1 #1 experiment.	157
6.6	Total amount of acid added during Aloha A1 #1 experiment to maintain pH 6.	160
6.7	Pt electrode potential and pH during the Aloha A1 #2 experiment.	163
6.8	Monitored parameters during the Bashaw A1 soil experiment: (a) pH, (b) E_H and net amount of acid added (moles acid - moles base).	169
6.9	Measured concentrations of Fe(II) and phosphate in solution during the first 700 hr of the Bashaw A1 soil experiment.	172
6.10	Correlation between solution concentration of Fe(II) and potential measured at a Pt electrode (below 200 mV) during the Bashaw A1 soil experiment.	174

LIST OF FIGURES (Continued)

Figure		Page
6.11	Measured concentrations of Fe(II) in solution (■) and percent of immobilized thionine oxidized (Δ) during the last 400 hr of the Bashaw A1 soil experiment.	176
6.12	Correlation between solution concentration of Fe(II) and potential measured at a Pt electrode (above 200 mV) during the Bashaw A1 soil experiment from 700 to 1100 hr.	177
6.13	Correlation between solution concentration of Fe(II) and phosphate during the Bashaw A1 soil experiment.	179
6.14	Measured concentrations of Fe(II) in solution (■) and the fraction of immobilized thionine oxidized (Δ) during the first 200 hr of the Bashaw A1 soil experiment.	181
6.15	Absorbance of immobilized thionine during Bashaw A1 soil experiment.	182
6.16	Correlation diagram for solution concentration of Fe(II) and % oxidized thionine during the Bashaw A1 soil experiment from 750 to 1100 hr.	184
A.1	Circuit diagram for computer controlled dispense pump	205
A.2	Interface box attached to computer board with ribbon cable.	206
A.3	ADC board analog connector.	209
A.4	Machine drawing of Delrin reactor lid.	210
A.5	Electrode fitting assembly	212
A.6	Machine drawing of Delrin filter holder: (a) inlet side; (b) outlet side.	213
A.7	Assembly of cross-flow filter: (A) filter holer inlet side; (B) Teflon ring; (C) fluorocarbon mesh; (D) Durapore filter; (E) filter holder outlet side.	215
A.8	Circuit diagram for computer controlled solenoid valve.	216

LIST OF TABLES

Table		Page
5.1	Summary of indicators, formal potentials and evaluations	80
5.2	Indicators studied	84
5.3	Experiments conducted in the reactor system	88
5.4	Formal potential for bound (immobilized) indicators	123
6.1	Aloha BC soil experiment summary.	150
6.2	Summary of Aloha Al #1 soil experiment.	158
6.3	Concentrations of Fe(II) and Mn(II) in the Aloha A1 #1 soil solution.	162
6.4	Summary of the Aloha Al #2 soil experiment.	165
6.5	Concentrations of Fe(II) in the Aloha A1 #2 soil solution.	167

Development of Chemostats and Use of Redox Indicators for Studying Redox Transformations in Biogeochemical Matrices

Chapter 1
Introduction

This thesis discusses the development of two new chemostat reactor systems and the use of organic redox indicators such as thionine and phenosafranine to study the redox transformations of matrix components and inorganic and organic contaminants. The redox condition of an environmental site affects the speciation of many organic and inorganic contaminants as well as matrix components and thus their solubility, mobility and toxicity. For example, Cr(VI) is generally very soluble and highly toxic, while Cr(III) is very insoluble and not very toxic (1). Other inorganic priority contaminants that can exist in more than one oxidation state include As, Se, Ag, Cu, Hg, Sb and Tl. Thus, it is clear that an understanding of the redox state and speciation of chemicals is required in virtually all aspects of hazardous waste management: (i) evaluation of disposal options, (ii) risk assessments of contaminated sites, and (iii) evaluation of clean-up options for contaminated sites.

Because most redox transformation reactions are dependent on pH as well as the redox potential (E_H), both conditions must be controlled when conducting laboratory studies to determine when transformations of a given component occur. A sophisticated reactor system is needed to obtain such control of experimental conditions. Although others (2 - 12) have developed

reactors to control the pH and E_H simultaneously, and there are pH/E_H controllers that are commercially available, the systems presented here offer additional options and advantages.

Most unique is an external flow loop which allows solution to be continuously pumped from the reactor, filtered, and returned to the reactor. This arrangement allows on-line spectrophotometric and dissolved oxygen (DO) measurements and provides filtered samples for external analysis techniques.

The flexible, computer-based control system can be used to maintain both the pH and E_H at setpoints by addition of acid and base (pH-stat) and/or additions of oxidants or reductants (E_H-stat). The redox-active reagent can be a solution (e.g., H_2O_2 or Ti(III) citrate) or a gas (e.g., O_2 or H_2). Information stored in computer files includes the monitored parameters (e.g., pH, E_H, DO), reagent addition parameters (e.g., time of addition, volume added, cumulative amount added), and the calculated buffer capacity (pH or redox).

Detailed descriptions of the components and capabilities of the two reactor systems are found in Chapters 3 and 4. Chapter 3 describes the reactor system developed in a collaborative project with Sandra Woods and Sheryl Stuart of the Civil Engineering department. They are investigating the dependence of pentachlorophenol (PCP) degradation rates on the measured E_H and the nutrient concentration. The reactor presented in Chapter 4 was used to study the redox transformations of redox indicators in solution, immobilized redox indicators, and several environmental redox-active components of soils (e.g., Mn and Fe) as detailed in Chapters 5 and 6.

The most common method of determining the redox status of a system is to measure the oxidation-reduction (redox) potential with a Pt electrode (E_H). However, there are several problems with this approach. First, many environmental redox reactions are slow to reach equilibrium. In addition, there is often more than one redox couple present and the measured potential is actually a mixed potential. Finally, many redox couples do not react in a reversible manner at the electrode surface (13). Clearly, a better approach to evaluating the redox status of a system is needed.

In this thesis, one goal was to investigate more thoroughly and quantitatively the feasibility of utilizing redox indicators to develop a spectrochemical redox sensor. Such a sensor could be used to indicate when conditions exist for redox transformations of contaminants to occur and the redox state of some species in the biogeochemical matrix.

Studies of dissolved redox indicators and immobilized redox indicators are presented in Chapter 5. In the first part of Chapter 5, the oxidation and reduction of twelve redox indicators in solution is discussed. For all indicators, the spectral absorption characteristics were monitored and the poising of the potential of a Pt electrode was evaluated. Although these results show that the redox indicators in solution have promise as indicators of redox conditions for environmental samples, problems arose when solids were added to the reactor.

The adsorption of positively-charged redox indicators to the surface of solid particles necessitated the isolation of the indicators from the solid phase. Two indicators, thionine and phenosafranine, were successfully immobilized on

an affinity chromatography gel. The gel bead are then isolated from the solids in the reactor by confining them to a flow cell and pumping the filtered reactor solution through the cell. These immobilized indicators are characterized in terms of spectrochemical (absorbance) and electrochemical (formal potential) characteristics.

The reactor and immobilized thionine were then used to study redox transformations in several soil samples as presented in Chapter 6. The soil solutions were deaerated to remove dissolved O_2 and were allowed to achieve reducing conditions through microbiological activity. Transformations of the immobilized thionine in contact with the soil solution were followed by measuring the absorbance of its oxidized form. Parameters monitored included the E_H, DO, and concentrations of dissolved Fe(II), Mn(II) and PO_4^{3-}. The E_H was then increased and maintained at various potentials by addition of H_2O_2 or O_2 while the above mentioned parameters were monitored. Correlations between the measured E_H, the concentration of Fe(II), the concentration of PO_4^{3-}, and the indicator speciation were investigated.

References

1. Ross, D. S.; Sjogren, R. E.; Bartlett, R. J. *J. Environ. Qual.*, **1981**, *10*, 145.

2. Knight, B. C. J. G. *Biochem. J.*, (London), **1930**, *24*, 1075.

3. Patrick, William H. *Nature*, **1966**, *212*, 1278.

4. Patrick, W. H. Jr.; Williams, B. G.; Moraghan, J. T.; *Soil Sci. Soc. Amer. Proc.*, **1973**, *37*, 332.

5. Masscheleyn, Patrick H.; Pardue, John H.; Delaune, Ronald D.; Patrick, William H. Jr. *Environ. Sci. Technol.*, **1992**, *26*, 1217.

6. Patrick, W. H. Jr.; Jugsujinda, A. *Soil Sci. Soc. Am. J.*, **1992**, *56*, 1071.

7. Frevert, Tönnies *Schweiz. Z. Hydrol.*, **1984**, *42(2)*, 269.

8. Jee, Hae Sung; Mano, Tarumi; Nishio, Naomichi; Nagai, Shiro *J. Ferment. Technol.*, **1988**, *66*, 123.

9. Jee, Hae Sung; Nishio, Naomichi; Nagai, Shiro *J. Gen. Microbiol.*, ***1987***, *33*, 401.

10. Fetzer S.; Conrad R. *Arch. Microbiol.*, **1993**, *160*, 108.

11. Jacob, H. E. In *Methods in Microbiology, Vol 2*; Norris, J. R.; Ribbons, D. W., Eds., Academic Press, Inc.: New York, 1970.

12. Walden, W. C.; Hentges, D. J. *Appl. Microbiol.*, **1975**, *30*, 782.

13. McBride *Environmental Chemistry of Soils*, Oxford Press: New York, 1994.

Chapter 2
Historical

Oxidation and reduction reactions can be described several ways. Oxidation sometimes includes the addition of oxygen, but can also be interpreted as a loss of hydrogen. More generally, an oxidation reaction involves the loss of electrons:

$$\text{reduced form (red)} \rightarrow \text{oxidized form (ox)} + \text{electrons} \qquad (2.1)$$

In some cases, reduction can be interpreted as a gain of hydrogen or a loss of oxygen, but more generally includes the gain of electrons:

$$\text{oxidized form (ox)} + \text{electrons} \rightarrow \text{reduced form (red)} \qquad (2.2)$$

The oxidation (loss of electrons) of one substance in a system is always coupled to the reduction (gain of electrons) of another substance. The overall reduction/oxidation (redox) equation is then:

$$ox_1 + red_2 \rightleftharpoons red_1 + ox_2 \qquad (2.3)$$

The component that becomes reduced (ox_1) is an oxidizing agent or an electron acceptor because it accepts electrons from a species that becomes oxidized (red_2) in the reaction. The component that donates the electrons (red_2) is the reducing agent or electron donor.

There is a potential associated with any redox half reaction. This potential (E) is determined from the Nernst equation:

$$E = E^{o} - \frac{RT}{nF}\ln\frac{a_{red}}{a_{ox}} \qquad (2.4)$$

where E° is the standard reduction potential of the redox couple (V), R is the molar gas constant (J/mol K), T is the temperature (K), n is the number of electrons, F is the faraday constant (C/eq), a_{red} is the equilibrium activity of the reduced species, and a_{ox} is the equilibrium activity of the oxidized species. Often, a formal potential based on concentrations rather than activities is employed.

Redox chemistry is very important in many different fields including aquatic chemistry, soil chemistry, environmental chemistry and microbiology. The redox state of soils affects the speciation of many components. Inorganic components that can exist in more than one oxidation state in soils include oxygen (O_2, H_2O_2, H_2O), nitrogen (NO_3^-, NO_2^-, N_2, NH_4^+), sulfur (SO_4^{2-}, SO_3^{2-}, S^0, H_2S), iron (Fe^{2+}, Fe(II)- and Fe(III)-minerals), and manganese (Mn^{2+}, Mn(IV)-minerals). Many trace elements in soils are also redox-active such as Cr, As, Se, Ag, Cu, Hg, Sb and Tl. The oxidation state of carbon can vary significantly with changing redox conditions (alkanes, alcohols, sugars, carboxylic acids, carbon dioxide). A thorough review of oxidation and reduction reactions important in water and soil chemistry can be found in several books (1, 2, 3) and journal articles (4, 5, 6).

Microbiological activity in soils leads to the oxidation of organic carbon, which must be accompanied by the reduction of an electron acceptor. The most important electron acceptor is O_2 due to its ease of reduction, availability and diffusivity in soils (7). When the flux of O_2 into the soil decreases due to flooding, aerobic activity exhausts the residual O_2 that is soluble in water. At this

time, the biological activity becomes anaerobic, and organisms capable of utilizing inorganic electron acceptors become active. After reduction of O_2, the following electron acceptors are reduced sequentially; NO_3^-, Mn(IV) compounds, Fe(III) compounds, SO_4^{2-}, and CO_2 (7). If the soil dries out and becomes aerated, the reactions occur in the reverse direction as conditions become more oxidizing.

There are currently four primary methods employed to determine the redox state of soil or water samples. These methods are: (i) potential measurement with an inert electrode; (ii) direct measurement of the concentrations of all significant redox-active species; (iii) evaluation of redox indicator speciation; and (iv) determination of dissolved H_2 concentration.

The most common method of determining the redox status of a sample is to measure the oxidation-reduction (redox) potential with a Pt electrode (E_H). The platinum electrode is said to be "poised" when the measure potential is "stable" on whatever time scale and voltage scale is under consideration (8). Thus, the definition of poised is completely operational. One reaction or many reactions may participate in poising the electrode, and the reactions may or may not be at equilibrium. For example, a Pt electrode may be poised by Fe(II)/Fe(III) at a potential that is consistent with equilibrium thermodynamics; or, an actively corroding iron electrode might be poised by oxygen reduction and iron oxidation at a potential that is determined by the kinetics of both processes and cannot be related to equilibrium thermodynamics.

Platinum electrodes have been used for over a century. The first redox potential measurements were made by Bancroft in 1892 (2). However, there are many problems with this approach. First, many environmental redox reactions are slow to reach equilibrium. Because species associated with many redox couples are present, and these species often do not couple with one another, it is possible to have different apparent redox potentials in the same solution. These conditions can lead to a measured potential which is actually a mixed potential, and does not indicate the speciation of any one couple. Many redox couples do not react in a reversible manner at the electrode surface (1) or the concentrations are low and result in a low exchange current (3). The exchange current density must be at least 10^{-7} A/cm^2 for reliable potentiometric measurements (3). Finally, the Pt electrode may develop an oxide or sulfide coating which affects the measured potential. For these reasons, the E_H cannot normally be used in thermodynamic equations to determine the solution speciation of redox-active components. However, the measure E_H is often useful as a qualitative evaluation of the redox level and component speciation.

A combination of measured E_H and component speciation is the method used by Patrick and co-workers (7, 9 - 16). They have conducted many studies to determine where transformations of NO_3^- (measure [NO_3^-] and [NH_4^+]), Mn(IV) compounds (measure [Mn(II)]), Fe(III) compounds (measure [Fe(II)]), SO_4^{2-} (measure [SO_4^{2-}]), and several redox-active elements (i.e., Cr, Se, As) begin to occur relative to the measured E_H.

To study redox transformations in the laboratory under specific E_H and pH conditions, a reactor system is necessary. Because most of the important redox reactions also involve H^+, the reactions are affected by pH as well as E_H. Therefore, the pH and also E_H must be carefully controlled throughout each experiment. The development of reactor systems used to study redox transformations are reviewed in Chapters 3 and 4.

A redox indicator (In) is a compound (usually organic) that undergoes oxidation and reduction chemistry with an accompanying change in absorbance or fluorescence characteristics. This change in absorbance or fluorescence of one or both species in the couple allows the amount of oxidized and reduced forms to be monitored, and the redox potential of the system to be calculated from the Nernst equation and the formal potential of the indicator. The use of redox indicators to recognize a reductive process was first described by Helmholtz in 1883 (17). However, redox indicators have not been used extensively to evaluate the E_H of environmental systems. A more complete discussion of redox indicators is found in Chapter 5.

More recently, Lovely (18, 19) has found a correlation between the concentration of dissolved H_2 and the redox reactions occurring in anaerobic groundwaters. Their results indicate that the H_2 concentration can be used to determine whether the terminal electron accepting process is Mn(IV)- and/or nitrate-reduction ([H_2] below the 0.05 nM detection limit), Fe(III) reduction ([H_2] < 1 nM). sulfate reduction ([H_2] between 1 - 2 nM), and methanogenesis ([H_2] > 5 nM).

References

1. McBride, Murray B. *Environmental Chemistry of Soils*; Oxford University Press: New York, 1994.

2. Hesse, P. R. *A Textbook of Soil Chemical Analysis*; Chemical Publishing Co., Inc.: New York, 1971.

3. Stumm, W., Morgan, J. J. *Aquatic Chemistry*, Wiley-Interscience: New York, 1981.

4. Hostettler, John D. *American Journal of Science*, **1984**, *284*, 734.

5. Frevert, Tönnies; *Arch. Hydrobiol.*, **1979**, *11*, 278.

6. Frevert, Tönnies; *Schweiz. Z. Hydrol.*, **1984**, *46/2*, 269.

7. Patrick, W. H. Jr.; Jugsijunda, A. *Soil Sci. Soc. Am. J.*, **1992**, *56*, 1071.

8. Westall, J. C.; Private communication; Oregon State University, 1995.

9. Patrick W. H. Jr.; Gotoh, S. *Soil Sci. Soc. Amer. Proc.*, **1972**, *36*, 738.

10. Gotoh, S; Patrick, W. H. Jr. *Soil Sci. Soc. Amer. Proc.*, **1974**, *38*, 66.

11. Patrick, W. H. Jr.; Henderson, R. E. *Soil Sci. Soc. Am. J.*, **1981**, *45*, 855.

12. Charoenchamratcheep, C.; Smith, C. J.; Satawathananont, S.; Patrick, W. H. Jr. *Soil Sci. Soc. Am. J.*, **1987**, *51*, 630.

13. Masscheleyn, Patrick H.; Delaune, Ronald D.; Patrick, W. H. Jr. *Environ. Sci. Technol.*, **1990**, *24*, 91.

14. Masscheleyn, P. H.; Delaune, R. D.; Patrick, W. H. Jr. *J. Environ. Qual.*, **1991**, *20*, 522.

15. Masscheleyn, Patrick, H.; Delaune, Ronald D., Patrick, William H. Jr. *Environ. Sci. Technol.*, **1991**, *25*, 1414.

16. Masscheleyn, Patrick H.; Pardue, John H.; Delaune, Ronald D.; Patrick, W. H. Jr. *Environ. Sci. Technol.*, **1992**, *26*, 1217.

17. Jacob, H. E. *Methods in Microbiology*, Norris, J. R.; Ribbons, D. W., Eds., Academic Press, Inc.: New York, 1970.

18. Lovley, Derek R. *Geochimica et Cosmochimica Acta*, **1988**, *52*, 2993.

19. Lovley, Derek, R.; Chapelle, Francis H.; Woodward, Joan C. *Environ. Sci. Technol.*, **1994**, *28*, 1205.

Chapter 3
Reactor System for Study of Reductive Dechlorination in Anaerobic Cultures

Teresa L. Lemmon and James D. Ingle Jr.*

Department of Chemistry
Oregon State University
Corvallis, OR 97331

3.1 Introduction

Theoretically, in soil and aquifer systems, the distribution of the species involved in redox couples reflects the reduction/oxidation (redox) potential of the system if all species are in equilibrium. Because the kinetics of many redox reactions are slow, oxidized species may be observed in environments with very low apparent redox potentials (measured with the Pt electrode). This slow approach to equilibrium and the dependence of biodegradation kinetics on environmental conditions make it difficult to interpret observed biodegradation rates in complex systems.

One approach taken to evaluate such a complex system is to study the kinetics of one process in a dynamic medium in which other parameters are maintained approximately constant (e.g., in a laboratory reactor system). The tendency of the redox potential to decrease to a relatively low constant value in anaerobic cultures makes study of reactions at any other potential difficult. To investigate reactions at higher potentials, an oxidant must be added at a controlled rate to counteract the reducing effect of the medium. Oxygen is often chosen because it is a natural oxidant, it is directly or indirectly reduced to water, and because it does not increase the solution volume. As the redox potential decreases, the level of oxygen in the reactor medium decreases and a lower level of oxygen must be maintained. The system becomes more sensitive to the addition of oxygen, and so the oxygen content of the gas bubbled into the solution must also decrease.

One of the first researchers to devise a method to control redox potentials utilizing oxygen was Knight (1). His method involved constant addition of oxygen to prevent the apparent potential as measured with a Pt electrode from decreasing below a desired point. The oxygen content in the gas stream was controlled by varying the percentage of unpurified nitrogen allowed to mix with the purified nitrogen bubbling through the media. This percentage was manually adjusted until the desired E_H was obtained. The potential remained constant without further adjustment of the gases only if there was no microbiological activity. Other researchers (2, 3) have used electrolysis to control the E_H. Reduction of the E_H through H_2 production is proposed (3).

Patrick and co-workers (4, 5) were among the first researchers to take an automated approach to redox control. They have extensively studied the redox transformations of inorganic components in soils over a wide range of controlled pH and redox potential conditions (6 - 11). To control the addition of oxygen, an electronic comparator circuit compares the platinum electrode potential to a user set potential and activates either a solenoid valve or an air pump. However, their studies required several gas mixtures ranging from 0.002 to 21% O_2 in N_2 (7) to achieve the desired range of redox potentials without a surge in potential when the solenoid valve was opened. Frevert also conducted experiments in which the pH/E_H was controlled in a feedback loop by adding N_2/air and CO_2/N_2 (12).

The automated systems described above all maintained the redox condition by adding gas with a varying percentage of oxygen. When the

potential decreased below the set point, the valve was opened and oxygen was added to the system. The gas was added continuously to the system until the potential reached the set value and the valve was closed.

Some workers have employed peristaltic pumps as dispensers to add liquid redox reagents, including potassium ferricyanide, titanium(III) citrate, dithionite, thioglycolate, ascorbic acid, dithiothreitol or FAD, to change the measured E_H (13 - 17). However, it appears that no attempt was made to quantify the redox buffer capacity or monitor the amount or rate of gas or reagent addition. The capacity information could indicate how well the electrode is poised, and the addition rate would provide information about the kinetics of the reactions.

There are also pH/E_H controllers that are commercially available. These controllers function similarly to the systems described above. When the measured pH (E_H) value is outside a selected range, power is supplied to an AC outlet on the control unit. This outlet can be used to drive pumps, valves or other equipment.

Described here is a sophisticated reactor system that has been developed to study the kinetics of pentachlorophenol (PCP) reductive dechlorination reactions under specified environmental conditions. It allows measurement of biodegradation rate constants while maintaining constant conditions such as pH, acetate concentrations and apparent E_H. This approach is advantageous since fully dynamic systems are hard to interpret due to the covariation of several parameters such as pH and E_H (4,5).

An advantage the apparatus described here has over commercially available pH/E_H control systems is the wealth of information provided. In addition to maintaining the selected pH and redox experimental conditions, there is a record of the amount of reagents added with each individual addition, the total amount of reagent added for the duration of the experiment and a continual tracking of capacity values of the system -- both pH buffer capacity and "redox" buffer capacity. Another unique aspect of this reactor system is the ability to control not only pH and E_H conditions, but also the concentration of a primary nutrient.

3.2 Experimental

The culture studied consists of an acetate and pentachlorophenol (PCP) degrading anaerobic consortium originally obtained from a municipal anaerobic digester (Corvallis, OR). Reactor feed was modeled after anaerobic media developed by Owen et. al. (18), with acetate as the primary carbon source.

The reactor system (shown in Figure 3.1) consists of a reaction vessel, and pumps and electrodes interfaced to a personal computer (PC). The components of the reactor system are used to perform two separate functions, monitoring parameters and controlling or changing conditions, both of which are managed through interfacing with a PC. The hardware components and software capabilities of the reactor system are described below.

3.2.1 Instrumentation

The reactor vessel is a 2.5-L Kimex beaded process pipe. Stainless steel and Teflon-lined flange fittings secure 1/2" aluminum plates for the reactor's top and bottom. The bottom plate is lined with 1/16" Teflon sheet to prevent contact of the culture liquid with aluminum. The top plate includes the following fittings: five electrode ports (Cole Parmer in-line electrode housing); 1/8" Swagelok inlet port with a shut off valve (influent port); septum port (for withdrawing samples with a syringe); gas outlet port with a Swagelok, one-way pressure release valve; eight standard 1/4"-28 ports for inlet/outlet of liquids and inlet of gases. The tubing used throughout the system is either stainless steel or PEEK

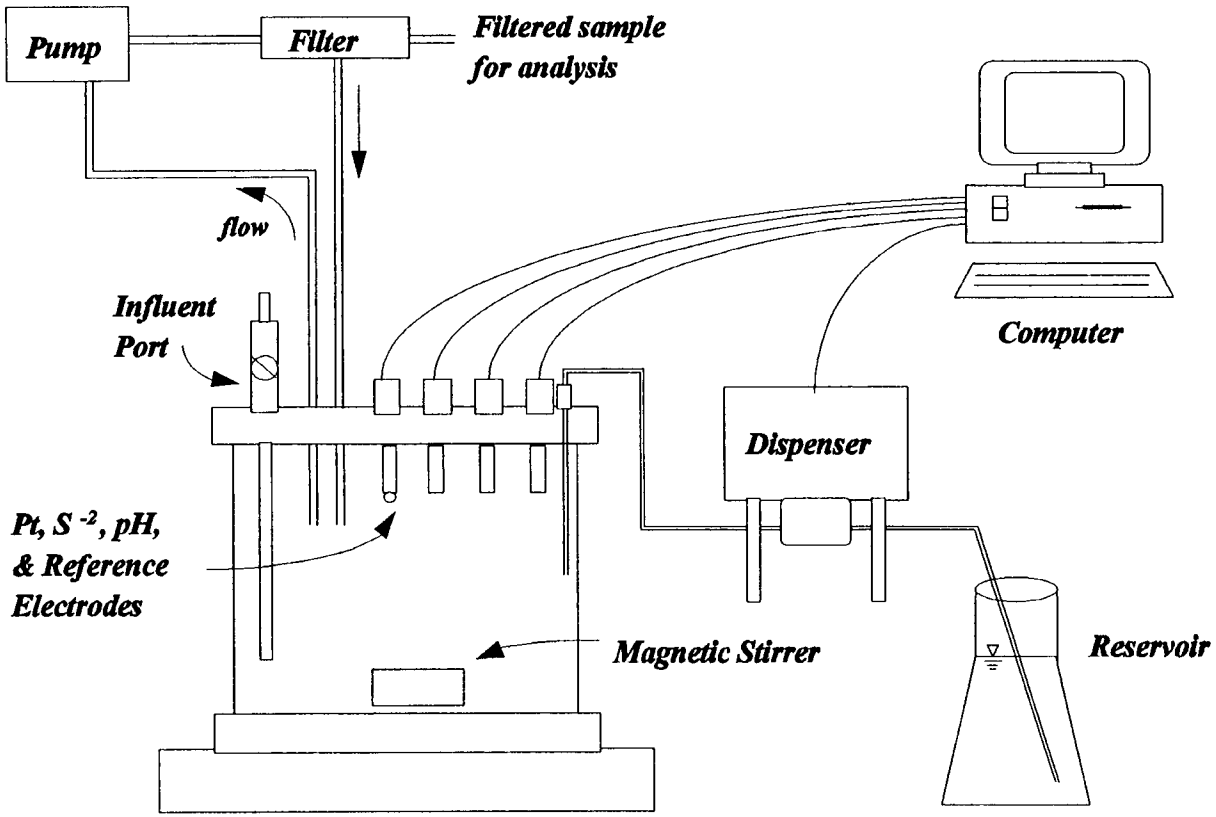

Figure 3.1 Schematic of reactor system.

(polyetheretherketone, selected for low oxygen permeability). A stainless steel sparging stone is attached to the end of the gas inlet tubing for efficient gas transfer. A commercial crossflow filter (Applikon A-SEP) is included in a flow loop. The culture is pumped from the reactor, through the filter module, and back to the reactor. Inert silver membrane filters (Poretics Corp., 0.8 μm, 53150) are used to prevent adsorption of PCP. This configuration allow filtered samples to be obtained without exposing the culture media to atmospheric oxygen. Hollow fiber systems are another method used to obtain filtered samples without exposure to oxygen (19).

Electrodes fitted in the lid of the reactor are used for on-line monitoring of the following parameters: pH, utilizing a glass electrode (Orion Ross pH half cell 8101BN); potential at a silver/silver sulfide ion selective electrode (Orion 9416BN); apparent E_H at either one or two Pt electrodes (several kinds have been employed including: Photovolt Corp. 0410401, Cole Parmer 05994-21, Orion 977800, Analytical Sensors Inc. OR100031). The same Ag/AgCl reference electrode (Orion double junction 900200) is used for all the indicator electrodes to eliminate problems that can arise when two or more reference electrodes are present in the same solution. When two Pt electrodes are included, one is designated the control electrode for E_H adjustments. The sulfide electrode is calibrated by automated multiple standard additions of Na_2S at the end of data collection.

During an experiment, several additional parameters are monitored externally. These include acetate concentrations using an ion chromatograph

(Dionex 4000i with conductivity detector), headspace composition (CO_2, O_2, CH_4, N_2) with a Fisher gas partitioner (model 25 V), and pentachlorophenol and degradation products with a gas chromatograph (Hewlett Packard 5890 with electron capture detector).

The reactor system is located in an environmental room maintained at 31 (±1) °C to ensure constant temperature. The biomass is continuously stirred with a magnetic stirrer. A Tylan RO-28 readout and control box in conjunction with three Tylan FC280 mass flow controllers provide a selected composition of methane, carbon dioxide and either hydrogen sulfide or hydrogen. The reactor vessel is flushed with a mixture of methane and carbon dioxide to remove oxygen prior to transferring the biomass at the start of an experiment. Often, no gas is bubbled during the experiment because the medium produces CO_2 and CH_4 creating a positive pressure in the reactor. Sometimes a mixture of $CO_2/CH_4/H_2$ is added during data collection to observe the effect of H_2 on the measured E_H.

Precision liquid dispensing pumps (Fluid Metering Inc., Micro ∏-Petter) are used to add small amounts of concentrated solutions to minimize the volume added during long-term experiments. Solutions are added to control system parameters such as pH, E_H and acetate concentration, or to make standard additions of sodium sulfide to calibrate the sulfide electrode. The pump volume adjusts from 2 to 50 µL per stroke and is typically set to deliver 10-25 µL. The delivery rate is limited by the programming to dispense once every two seconds. For good precision and accuracy, concentrations and volumes are selected such

that four to five dispensing cycles are made per addition. The dispensing pumps were modified for digital control with two solid state relays (Grayhill 140 VAC, 3 A) (See Appendix A).

3.2.2 Interfacing

The reactor components are interfaced to a 286 PC equipped with a multiplexed 12-bit ADC and I/O board (Computer Boards Inc., CIO-AD08-PGA). The computer board includes eight differential ADC channels with programmable gain (used for potentiometric measurements) and four digital output (DO) ports (used for dispensing pump control). The board is connected to a single component box which allows signal transfer by means of BNC or banana connectors. The pH electrode is connected to a pH meter (Orion 407A) with the recorder output connected to an ADC channel. Details about connections are given in Appendix A.

3.2.3 Software

The computer program which provides computer control of reagent addition and synchronized data acquisition was developed in QuickBASIC 4.5. The function of the software can again be divided into monitoring and controlling tasks similar to that for the hardware instrumentation. Electrode measurements are typically obtained every 15 min. When the pH is maintained at a set point, reagent addition is immediately prior to electrode data acquisition. Initially, there

are many adjustable parameters that must be entered by the user. These include pH calibration information, the volume of the biomass, the calibrated delivery volume of the dispensing pumps, the concentration of solutions added with the dispensing pumps, and the time between electrode measurements. In addition, the user can select the initial level of control (i.e., no pH adjustment, add acetic acid at constant rate, or pH-stat with acetic acid solution).

Figure 3.2 shows the menu options and the data displayed on the computer monitor during program execution. The electrode measurements (Pt, S^{2-} and pH in Figure 3.2) are the average of 200 consequent ADC readings taken over about 200 ms. This averaging is needed to reduce the effect of 60-Hz noise and obtain a reproducibility of about 0.5 mV. The displayed potentials for the Pt and S^{2-} electrodes have been corrected for the reference electrode so they are versus a standard hydrogen electrode. Also displayed are the rates of change of the electrode potentials which serve to indicate when the system has reached a steady-state condition (e.g., when the equilibration portion of the experiment discussed below is over).

The program is interactive and responds to keystrokes (Menu keys in Figure 3.2). Menu option 4 allows an extra set of electrode readings to be obtained without disturbing the timed measurements. This is useful when sampling the electrode potentials infrequently. Options 6 and 7 allow the selected level of pH and E_H control to be changed. This permits the pH stat to be activated after the initial equilibration period, and allows data collection at several redox levels consecutively. When the E_H-stat mode is selected, the user

MENU: PRESS THE KEY OF YOUR CHOICE

1) Withdraw sample for analysis
2) Enter acetate concentration from chromatograph (mM)
3) Enter sulfate concentration from chromatograph (mM)
4) Take electrode readings
5) Manual adj (rate, setpoint: pH/Ac/SO4, tolerance, volume, NaAc conc, time btwn)
6) Switch to adding Hac at constant rate (CURRENTLY, pH RESPONSE)
7) Start E_H stat by addition of oxidant or reductant
8) Make an addition of acetic acid
9) Standard addition of Sulfide
0) STOP DATA COLLECTION - go to sulfide standard addition

Time	Pt	S	pH	effRate HacADD mM/hr: 0.36			BufCap mM/pH
10:15	-0.2517	-0.2609	7.047				@ last 3 Hac
10:30	-0.2513	-0.2611	7.051	pH Stat value 7.05			additions
10:45	-0.2520	-0.2621	7.049				
11:00	-0.2507	-0.2613	7.053	Change/hr: based on last 3 data			12.38
11:15	-0.2519	-0.2625	7.046	Pt(V/hr)	S(V/hr)	pH(pH/hr)	20.03
11:30	-0.2523	-0.2637	7.049	-0.0002	-0.0003	-0.0005	15.20

Current Status: ---
OK to enter number of your selection.

Figure 3.2 Computer screen display during experiment.

enters the stroke volume of the pump, the concentration of the solution, the potential set point, and time between additions.

The manual adjustment option (5) allows many parameters to be changed during a given experiment. The time between acquisition of electrode potentials is selected initially, but can be adjusted. This allows infrequent data collection during equilibration, or more frequent data collection during redox or pH shifts. The entered concentration of added reagents can also be changed when the solution concentrations are adjusted.

When a sample is withdrawn for external analysis, the user enters the sample volume (1) and measured concentration (2). This allows the program to record the sampling time and track the total solution volume, accounting for both sample withdrawal and reagent addition. The program also manages continual tracking of total amount (moles) of pH adjustment solution added (acid, base, buffer) and total amount of oxidant (reductant) added. The options to monitor and control sulfate were developed parallel to those for acetate, but the sulfate control has not been implemented at this time.

There are three automated modes of adding reagents from the dispensing pumps: single dose in response to a user-entered value (e.g. to bring the concentration of acetate to a specified level), continual addition at a constant, predetermined rate (nutrient or substrate addition), or feedback loop in response to a continually monitored parameter (E_H- or pH-stat).

The first two methods of addition are straightforward, while the third is more complicated. A schematic of the pH-stat approach is shown in Figure 3.3.

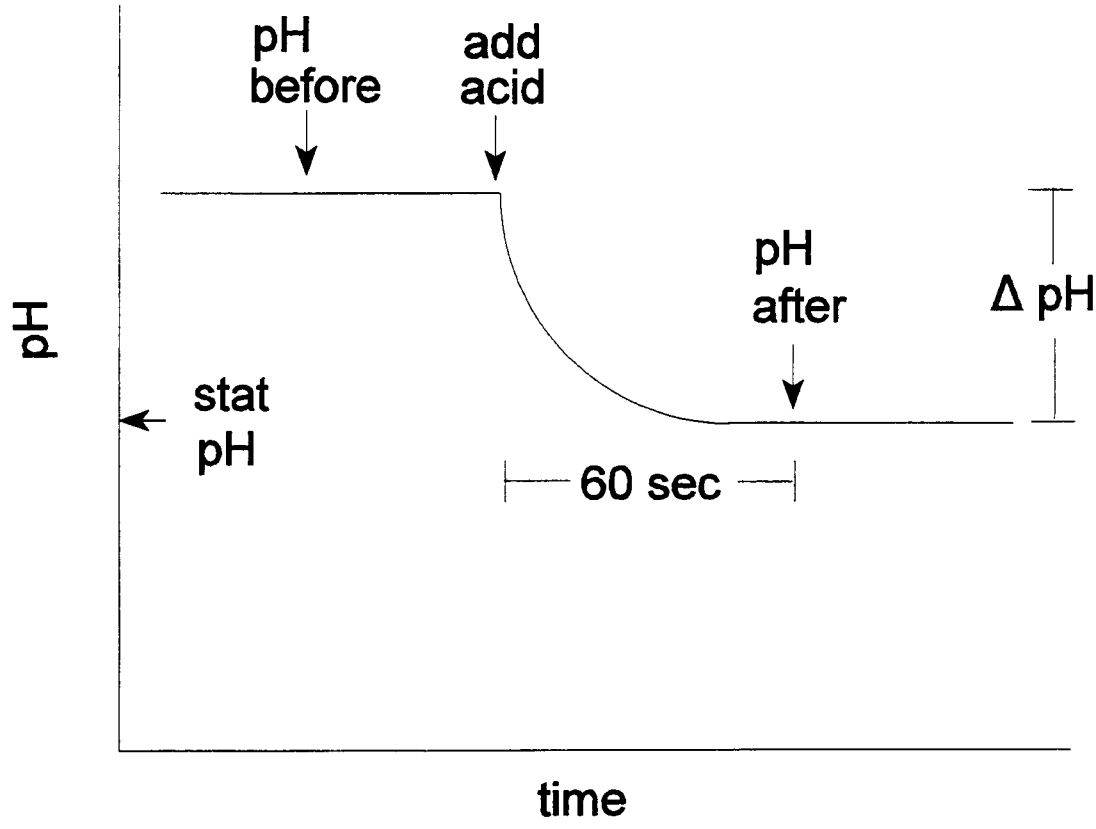

Figure 3.3 Schematic of pH-stat approach.

The user enters the desired pH set or stat point. The pH is maintained at the set point as follows:

a) The current pH is monitored (pH before);

b) Based on an average of six previous capacity values, the change in acid (base) molarity in the reactor (Δ[acid]) necessary to return the system to the set-point is calculated from

$$\Delta[acid] = pH\ Buffer\ Capacity \times (pH\ before - pH\ setpoint) \quad (3.1)$$

The program then calculates the volume of solution to add via the dispensing pumps based on the reactor solution volume and the concentration of the pH adjustment solution.

c) The actual buffer capacity of the system is calculated from

$$pH\ Buffer\ Capacity = \frac{\Delta\ [acid]}{\Delta\ pH} \quad (3.2)$$

where ΔpH = pH before - pH after.

The pH is adjusted (if necessary) every time a pH reading is made (typcially every 15 min). The capacity value used in equation 3.1 is a running average of the last six calculated capacities to prevent one outlying value from significantly affecting the amount added. The values are normally collected before the pH-stat option is selected or values can be entered based on previous experiments. The one-minute time period between the before and after pH readings (Figure 3.3) allows thorough mixing.

A similar approach is employed to hold the system at a selected E_H other than the natural E_H of the biomass. The redox capacity is calculated from

$$Redox\ Buffer\ Capacity = \frac{\Delta[oxidant\ (reductant)]}{|\Delta E|} \qquad (3.3)$$

where ΔE is the difference in the potential measured at the platinum electrode before and one minute after the addition. However, before the system is held at a different redox condition, it must first be changed to the new condition. This is accomplished in two steps. In the first step the redox buffer capacity is evaluated by adding a specific amount of redox reagent (typically five aliquots or 50 μL), monitoring the potential difference at the platinum electrode, and calculating the redox buffer capacity from equation 3.3. This step is repeated several times to create an array of capacity values. During the second step the E_H is changed to the selected set point in 30 mV increments. This incremental approach is taken to prevent exceeding the desired E_H set point. Often the redox buffering capacity changes with redox potential.

The program checks measured and calculated values to prevent erroneous data from being used for control purposes. For example, AC line transients or operator manipulations around portions of the reactor can cause an occasional spurious pH (E_H) reading. If two adjacent pH reading differ by 0.1 or greater (> 0.2 V for E_H), the previous value is stored. If the calculated buffer capacity is greater than four times the average of the last six capacities, a value four times the average is included in the array. This prevents an erroneously large value from affecting the amount added for the next six additions (until it is replaced in the array), but still allows the values to change if the actual capacity is changing. If no addition is made (condition is within the tolerance range, or less than one stroke volume is needed), no buffer capacity is calculated. This

prevents the array from filling with zeros and thereby causing reagent addition to cease. Continual tracking allows variations in pH and redox buffer capacities to be correlated to changes in other variables such as system E_H or PCP concentration.

All the data are written to three separate files that are easily imported to a spreadsheet. The main data file contains a list of the parameters initially selected, the time of electrode readings, the measured pH, and potential at the platinum and sulfide electrode. The other two files are used to record the pH- and E_H- stat information: the time of additions, the electrode readings before and after addition, the volume of solution added and the calculated capacities. If the redox potential is being adjusted frequently, the user can select how much of the information is written to the file (i.e., every fourth time) to limit the file to a manageable size.

3.2.4 Procedure

There are two phases within an experiment, the equilibration phase and acetic acid addition phase. The goal of the equilibration phase is to allow the system to equilibrate, as indicated by constant platinum and sulfide electrode readings, and to allow the initiation of acetate degradation. Then the pH stat is begun to maintain constant pH and acetate concentrations while the degradation of PCP is monitored at various E_H conditions.

Prior to biomass transfer, the sealed reactor with the Pt (one or two) and sulfide electrodes installed (the other electrode ports are plugged) is flushed with a 1:1, CO_2:CH_4 mixture for 6-24 hr until O_2 is barely detectable in the headspace (as measured with a gas partitioner). The pH and reference electrodes are inserted into the electrode ports in the reactor vessel and the gas purge is continued for at least one hour. Then, about 2.3 L of the anaerobic inoculum is siphoned from the "mother reactor" into the batch reactor and sodium acetate is added immediately (typically to a concentration of about 20 mM). The system is allowed to equilibrate until a constant E_H is achieved (usually one day). The "natural" E_H of the culture is observed to be -250 to -260 mV. Throughout the equilibration period, the E_H, pH and potential at the sulfide electrode are monitored automatically and the pH-stat is not activated. As the acetate is consumed, the pH increases. Head space samples are analyzed for CO_2, N_2, O_2 and CH_4 during the equilibration period and throughout the experiment.

When the E_H has stabilized, an addition of acetic acid is made to bring the acetate concentration up to 10 - 20 mM and the pH down to about 7. Alternatively, the pH-stat mode can be set to begin when a certain pH value is reached. The pH-stat mode is activated utilizing a mixture of sodium acetate and acetic acid to maintain the acetate concentration and the pH simultaneously. The concentration of acetic acid is 0.87 M while the sodium acetate concentration varies (0.1 - 0.8 M) but is typically 0.3 M. Next, the PCP is added and the reductive dechlorination rates are measured. In some experiments, the

E_H is then changed to and maintained at a more oxidizing condition by adding hydrogen peroxide or potassium ferricyanide, or a more reducing condition by adding Ti(III) citrate or H_2 and the reductive dechlorination rates are measured again.

After the end of data collection, the sulfide electrode is calibrated *in-situ* by multiple standard addition potentiometry (20). This method allows the sulfide concentration to be determined without exposure to oxygen and subsequent oxidation. Several additions of 0.04 M Na_2S are made (typically 100-200 µL) and the potential at the sulfide electrode is measured after each addition. The user enters the concentration of Na_2S, the pump stroke volume and the desired increase in sulfide concentration in the reactor. The program then calculates and delivers the appropriate amount of Na_2S. The initial concentration is calculated as follows:

1) With a spreadsheet, a graph of Z versus the concentration sulfide added (concentration in the reactor) is prepared where Z is Antilog(sulfide voltage / 0.0302), and the theoretical Nernstian slope RT/nF (0.0302) at 31°C is used.
2) The slope of the line is used to determine the x-intercept.

The x-intercept is the initial concentration of sulfide in the reactor.

This technique involves several assumptions in addition to a Nernstian response. Before and throughout the sulfide additions, the activity coefficient of the sulfide ion and the liquid junction potential are assumed to remain constant, as is the fraction of total sulfide present as free sulfide ions (S^{2-}). Typical sulfide

concentrations in the reactor determined with this method range from 10-100 μM.

3.3 Results and Discussion

The described reactor system has been used to study PCP degradation kinetics at well-controlled pH, acetate and redox potential conditions. The results regarding the PCP dechlorination and rate constants will be presented elsewhere; here we confine our discussion to control of experimental conditions by the reactor system.

Initially, the pH and acetate concentrations were controlled separately by dispensing a solution of acetic acid at a constant rate selected by the user (the previously measured consumption rate). The measured acetate degradation rate varies between experiments and even during a given experiment which resulted in the need to manually enter a new addition rate at frequent intervals. In a subsequent program option, the necessary addition rate to maintain the acetate concentration was automatically calculated based on user-entered measured concentrations of acetate. This again required frequent manual determination of acetate to prevent the concentration from varying widely and therefore was inconvenient and ineffective.

The pH-stat feedback loop was developed to add acetic acid as necessary to maintain a constant pH. Although this method controlled the pH very well, the acetate concentration slowly decreased. This behavior may be due to the conversion of acetate to CO_2 followed by loss of some CO_2 due to precipitation or microbial conversion to CH_4 or biomass. Gas analysis indicates that the percentage of CO_2 in the head space increases during an experiment. A

mixture of acetic acid and sodium acetate was found to effectively maintain the acetate concentration as well as the pH. Slight adjustments in the sodium acetate concentration are necessary throughout the experiment, but typically once every few days is sufficient to maintain the acetate concentration within 2-3 mM as shown in Figure 3.4. Using this method, the operator need only determine the acetate concentration every few days. The pH is adjusted every 15 min which limits the pH variation to 0.05, as also shown in the figure. An example of the continual tracking of acetate added is shown in Figure 3.5. The change in acetate addition rate corresponds to changes in the controlled redox potential. The potential was first increased, and then allowed to return to the "natural" potential of the system (about -250 mV versus SHE). While the redox potential was held at an elevated level, acetate consumption and its corresponding addition stopped. This tracking of acetate addition enables variations in metabolism rates to be observed.

For the E_H control, the time allowed for mixing before acquiring the value of E_H-after and the time interval between corrections are critical. The redox processes are typically slower to reach steady-state values than acid/base processes. However, when forcing the system to an E_H different from the "natural" E_H, the measured potential can change significantly during one minute. If a significant fraction of the added oxidant is consumed during the one minute allowed for mixing and equilibration, the value of ΔE in equation 3.3 is erroneously low, and the calculated redox buffer capacity is erroneously large.

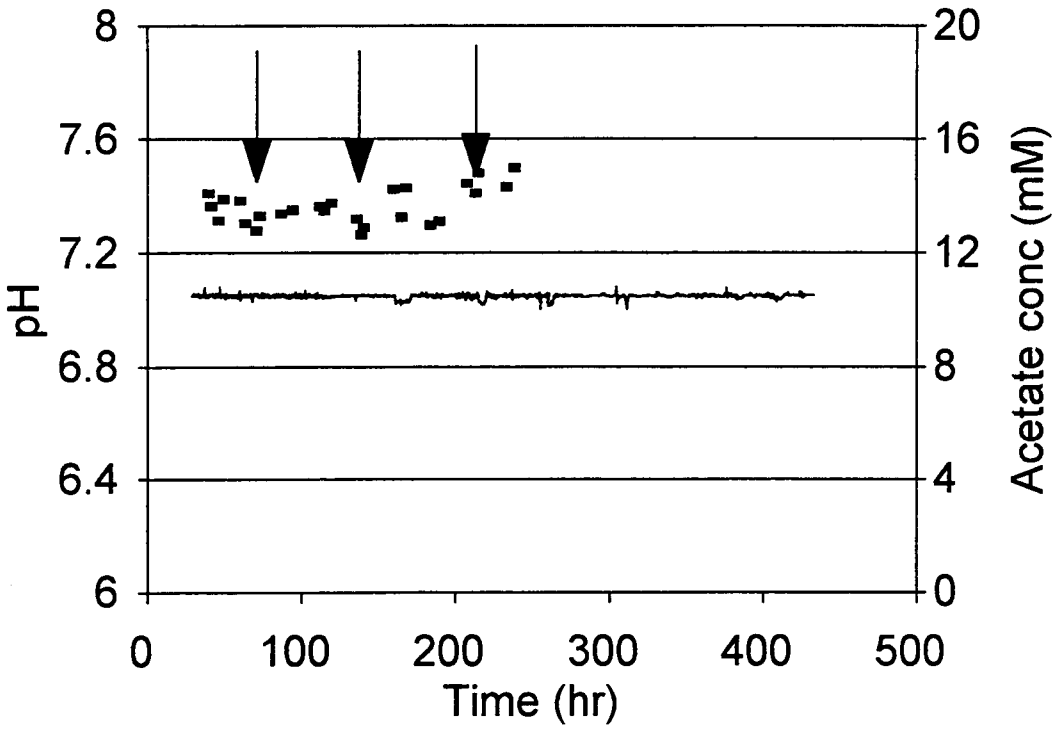

Figure 3.4 Variation of pH (-) and acetate concentrations (▬)during an experiment of about 2 weeks. The arrows indicate the time where the ratio of acetic acid to sodium acetate was adjusted.

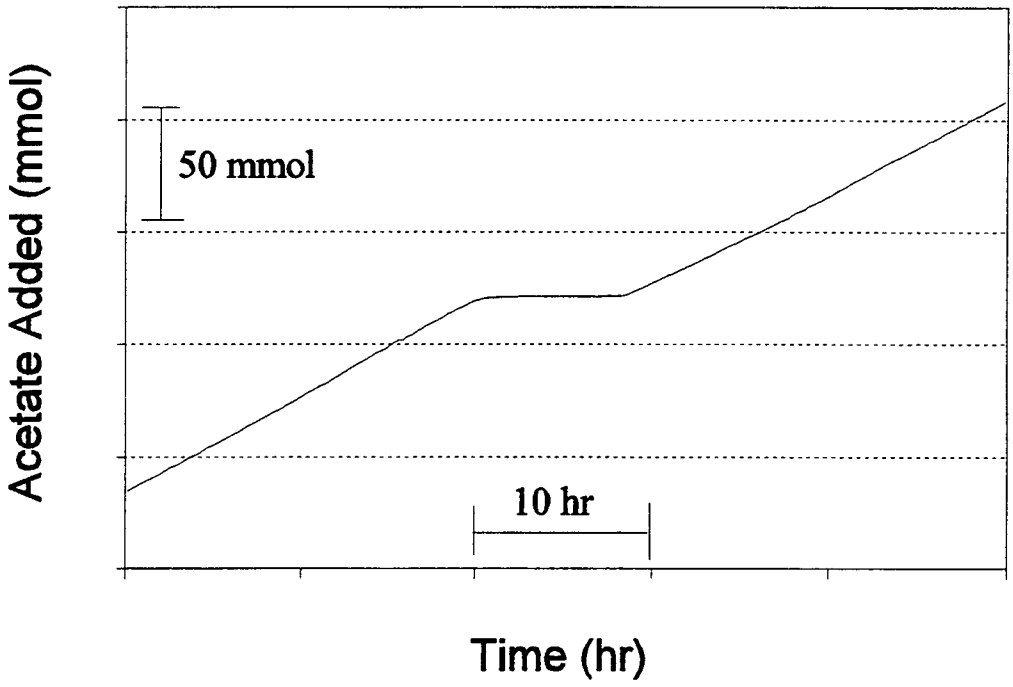

Figure 3.5 Total amount of acetate added during a portion of an experiment. Change in rate of addition corresponds to changing E_H; acetate addition stopped when the potential was increased with H_2O_2 and resumed when the potential was allowed to return to a "natural" condition.

Such large capacity values will cause a large amount of oxidant to be added the next time, and the measured potential will increase dramatically. This results in large fluctuations in the measured potential as shown in Figure 3.6, rather than tightly controlled redox conditions.

To maintain a steady potential, the equilibration time is user-adjustable. Typically, one-minute mixing is acceptable when the controlled potential is within 100 mV of the "natural" potential. For larger shifts in potential, 30 s is more appropriate because the E_H changes more rapidly. Another user-adjustable parameter is the time between additions of redox reagent. To change rapidly to the new potential, additions can be made every minute. The addition time is usually changed to every five minutes when the new potential has been reached.

Figure 3.7 is a composite of two separate experiments illustrating the ability of the system to add a reductant to maintain a lower redox potential, and an oxidant to maintain a higher redox potential than the natural potential of the biomass. The figure shows that the further the potential is shifted from the natural potential, the more difficult the redox condition is to maintain. This larger variation in the measured E_H around the set-point is due to the system being held further away from steady-state conditions. Although the redox reagent is added at a faster rate, the consumption rate of the reagent is fast relative to the time between additions. For this reason, the time between redox reagent additions can be decreased by the user when the potential shift increases. The potential can be controlled very tightly (± 5 mV) if changed less than 50 mV.

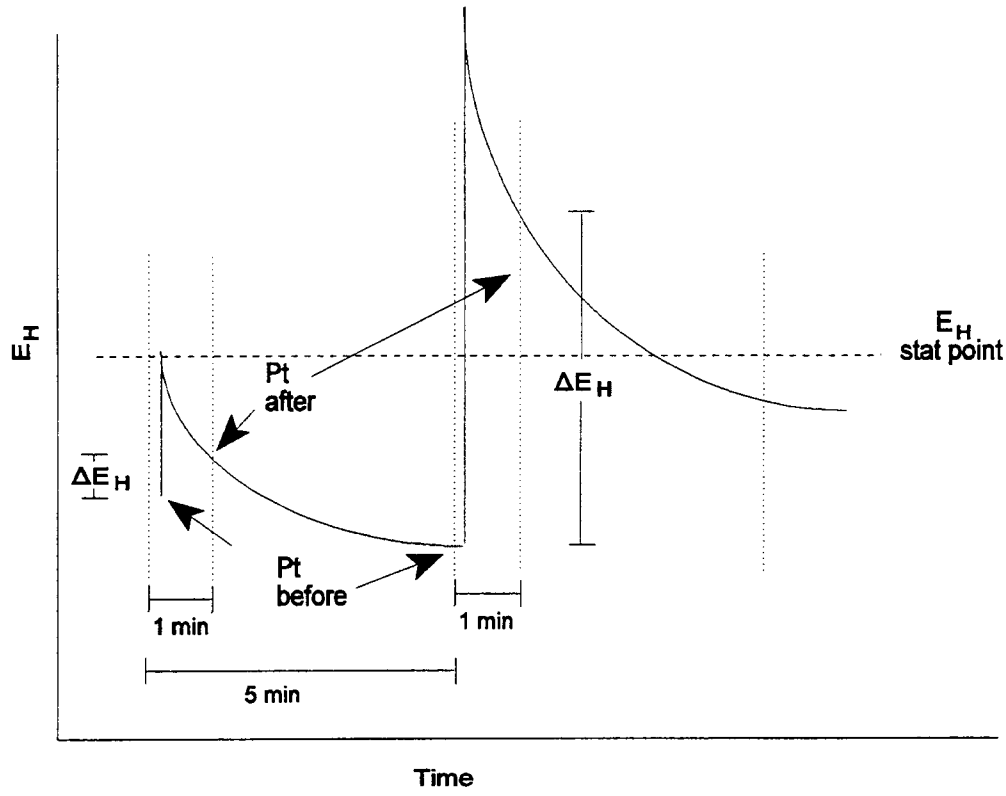

Figure 3.6 Example of wide fluctuations in measured potential when a significant amount of oxidant is consumed in the one minute between reagent addition and measurement of Pt after. The value of ΔE_H (Pt after - Pt before) is erroneously low, the calculated redox buffer capacity is erroneously high, and too much oxidant is added in the next addition period.

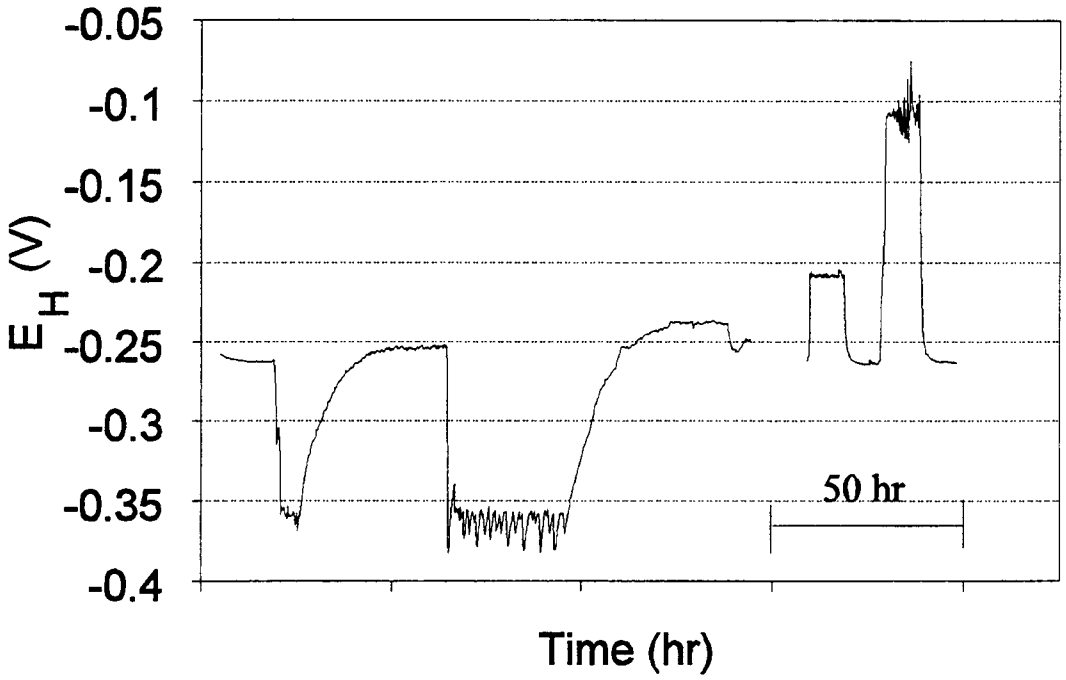

Figure 3.7 Example of changing redox condition during two experiments. The potential is decreased to -0.36 V by adding Ti(III) citrate, and increased to -0.21 and -0.11 V by adding H_2O_2

3.4 Conclusions

We have developed a laboratory reactor with feedback control or "redox/pH-stat", which allows studies of reductive dechlorination rates to be conducted over a large range of environmental redox levels under well controlled, quasi steady-state conditions. The reactor system is capable of achieving and maintaining a selected E_H both above and below the "natural" E_H of the biological system. It is also able to maintain a constant pH and acetate concentration for periods as long as three weeks. It manages continual tracking of cumulative nutrient, acid, base or redox reagent added to monitor metabolism rates and stoichiometry. Both the system pH buffer capacity and redox buffer capacity are monitored throughout the experiment. Finally, all the data are written to three separate files that are easily imported to a spreadsheet to allow changes in various parameters to be correlated.

Innovations include the in-situ standardization of the sulfide electrode and the control of acetate concentration. The in-situ determination of sulfide by standard addition could be extended to other oxygen sensitive species that can be determined potentiometrically.

The concept of using a pH-stat to also maintain a nutrient concentration could be extended to other systems where the nutrient consumption rate is a constant fraction of the acid (or base) consumption. The system would then be controlled with a mixture of a strong acid or base and a nutrient solution of

appropriate concentration. This would be very beneficial in systems where it is difficult to conduct on-line measurements of nutrient concentrations.

3.5 References

1. Knight, B. C. J. G. *Biochem. J.*, (London), **1930**, *24*, 1075.

2. Hanke, M. E.; Katz, Y. J. *Arch. Biochem.*, **1943**, *2*, 183.

3. Vainshtein, M. B.; Gogotova, G. I. *Microbiology,* **1987**, *56*, 23.

4. Patrick, William H. *Nature*, **1966**, *212*, 1278.

5. Patrick, W. H. Jr.; Williams, B. G.; Moraghan, J. T.; *Soil Sci. Soc. Amer. Proc.*, **1973**, *37*, 332.

6. Patrick, W. H. Jr.; Gotoh, S. *Soil Sci. Soc. Amer. Proc.*, **1972**, *36*, 738.

7. Gotoh, S.; Patrick, W. H. Jr. *Soil Sci. Soc. Amer. Proc.*, **1974**, *38*, 66.

8. Patrick, W. H. Jr.; Henderson, R. E.; *Soil Sci. Soc. Am. J.*, **1981**, *45*, 856.

9. Masscheleyn, Patrick H.; Delaune, Ronald D.; Patrick, William H. Jr. *Environ. Sci. Technol.*, **1990**, *24*, 91.

10. Masscheleyn, Patrick H.; Pardue, John H.; Delaune, Ronald D.; Patrick, William H. Jr. *Environ. Sci. Technol.*, **1992**, *26*, 1217.

11. Patrick, W. H. Jr.; Jugsujinda, A. *Soil Sci. Soc. Am. J.*, **1992**, *56*, 1071.

12. Frevert, Tönnies *Schweiz. Z. Hydrol.*, **1984**, *42(2)*, 269.

13. Jee, Hae Sung; Mano, Tarumi; Nishio, Naomichi; Nagai, Shiro *J. Ferment. Technol.*, **1988**, *66*, 123.

14. Jee, Hae Sung; Nishio, Naomichi; Nagai, Shiro *J. Gen. Microbiol.*, ***1987,*** *33*, 401.

15. Fetzer S.; Conrad R. *Arch. Microbiol.*, **1993**, *160*, 108.

16. Jacob, H. E. In *Methods in Microbiology, Vol 2*; Norris, J. R.; Ribbons, D. W., Eds., Academic Press, Inc.: New York, 1970.

17. Walden, W. C.; Hentges, D. J. *Appl. Microbiol.*, **1975**, *30*, 782.

18. Owen, W. F.; Stuckey, D. C.; Healy, J. B. Jr.; Young, L. Y.; McCarty, P. L. *Water Research*, **1979**, *13*, 485.

19. Ljungdahl, Lars G.; Wiegel, Juergen *Manual of Industrial Microbiology and Biotechnology*, A. L. Deamin and N. A. Solomen Eds.; American Society for Microbiology: Washington D. C., 1986.

20. Smith, Michael J.; Manahan, Stanley, E. *Analytical Chemistry*, **1973**, *45*, 836.

Chapter 4
Reactor System for Study of Redox Transformations in Controlled Environmental Conditions

Teresa L. Lemmon and James D. Ingle Jr.*

Department of Chemistry
Oregon State University
Corvallis, OR 97331

4.1 Introduction

A clear understanding of the redox state and speciation of chemicals is required in virtually all aspects of hazardous waste management: (i) evaluation of disposal options, (ii) risk assessments of contaminated sites, and (iii) evaluation of clean-up options for contaminated sites. Specifically, the redox state of an inorganic or organic pollutant affects its speciation and thereby its transport, fate and biological effects.

The distribution of species in redox couples reflects the oxidation/ reduction (redox) potential of the system if all components in the system are in equilibrium. Because the kinetics of many redox reactions are slow, oxidized species may be observed in environments with very low apparent redox potentials (measured with the Pt electrode). This slow approach to equilibrium and the slow rates of mineral dissolution and biological activity make complex systems difficult to interpret.

One approach taken to evaluate such a complex system is to study the kinetics of one process in a dynamic medium in which other parameters values are maintained at approximately constant values (e.g., in a laboratory reactor system). The tendency of the redox potential to decrease to a relatively low constant value in anaerobic cultures makes study of reactions at any other potential difficult. To investigate reactions at higher potentials, an oxidant must be added at a controlled rate to counteract the reducing effect of the medium. Oxygen is often chosen because it is a natural oxidant, it is directly or indirectly

reduced to water, and because it does not increase the solution volume. As the redox potential decreases, the level of oxygen in the reactor medium decreases and a lower level of oxygen must be maintained. The system becomes more sensitive to the addition of oxygen, and so the oxygen content of the gas bubbled into the solution must also decrease.

One of the first researchers to devise a method to control redox potentials utilizing oxygen was Knight (1). His method involved constant addition of oxygen to prevent the apparent potential as measured with a Pt electrode from decreasing below a desired point. The oxygen content in the gas stream was controlled by varying the percentage of unpurified nitrogen allowed to mix with the purified nitrogen bubbling through the media. This percentage was manually adjusted until the desired E_H was obtained. The potential remained constant without further adjustment of the gases only if there was no microbiological activity. Other researchers (2, 3) have used electrolysis to control the E_H. Reduction of the E_H through H_2 production is proposed (3).

Patrick and co-workers (4, 5) were among the first researchers to take an automated approach to redox control. They have extensively studied the redox transformations of inorganic components in soils over a wide range of controlled pH and redox potential conditions (6 - 11). The couples studied include Fe(II)/Fe(III), Cr(VI)/Cr(III), Mn(IV)/Mn(II) and As(III)/As(V). To control the addition of oxygen, an electronic comparator circuit compares the platinum electrode potential to a user set potential and activates either a solenoid valve or an air pump. However, even their studies required several gas mixtures ranging

from 0.002 to 21% O_2 in N_2 (7) to achieve the desired range of redox potentials without a resulting surge in potential when the solenoid valve was opened. Frevert also conducted experiments in which the pH/E_H was controlled in a feedback loop utilizing N_2/air and CO_2/N_2 (12).

All of the automated systems described above maintained the redox condition by added gas with a varying percentage of oxygen. When the potential decreased below the set point, the valve was opened and oxygen was added to the system. The gas was added continuously to the system until the potential reached the set value and the valve was closed.

Some workers have employed peristaltic pumps as dispensers to add liquid redox reagents, including potassium ferricyanide, titanium(III) citrate, dithionite, thioglycolate, ascorbic acid, dithiothreitol, or FAD, to change the measured E_H (13 - 17). However, it appears that no attempt was made to quantify the redox buffer capacity or monitor the amount or rate of gas or reagent addition. The capacity information could indicate how well the electrode is poised, and the addition rate would provide information about the kinetics of the reactions.

There are also pH/E_H controllers that are commercially available. These controllers function similarly to the systems described above. When the measured pH (E_H) value is outside a selected range, power is supplied to an AC outlet on the control unit. This outlet can be used to drive pumps, valves or other equipment.

This chapter describes a sophisticated reactor system that has been developed to study the redox transformations of environmentally relevant couples (e.g., Fe(II)/Fe(III), Mn(II)/Mn(IV), Cr(III)/Cr(VI)). This system supports pseudo-steady-state conditions which allow the kinetics of one process to be studied in a dynamic medium in which other parameters are maintained at approximately constant values. This approach is selected over fully dynamic systems (non-steady-state) that are difficult to interpret due to covariation of several parameters (3, 4) and are less tractable mathematically.

The reactor system described has some unique characteristics relative to previously discussed research systems and commercially available pH/E_H control apparatus. In addition to maintaining the selected pH and E_H conditions, a record is created which provides the following information: the amount of reagents added (pH and redox adjustments) for the duration of the experiment and continual tracking of system capacity values -- both pH buffer and "redox" buffer capacity.

There are two basic questions to be answered regarding redox transformations: (i) what is the redox state of redox active components in the system; (ii) will a particular component undergo a redox transformation under these conditions. Characterizing the redox state of a system is not a simple problem like measuring the pH of a system. Many redox reactions are slow so total redox equilibrium is not reached. One specific potential cannot describe the speciation of all redox couples present in a complex system

Several approaches can be taken to evaluate the redox status of an environmental sample: measure the potential at a platinum electrode; determine the concentrations of major redox-active species (i.e., O_2, Mn(II), NO_3^-, NH_4^+, Fe(II), SO_4^{2-}, HS^-, CH_4) (18); monitor the concentration of dissolved hydrogen (19, 20) or measure the redox state of added redox indicators (21, 22). With the reactor system presented here, we can maintain the potential measured at the Pt electrode to a selected value, measure the concentrations of redox-active species and observe the state of redox indicators. The second question can then be posed "can the state of a redox indicator be used to determine when redox transformations will occur". In many respects, monitoring the speciation of redox indicators is a simpler analytical problem than measuring the concentration of H_2.

The reactor has been used to study transformations of indicators in a variety of systems. They include: simple solutions of dissolved redox-active species such as Fe(II), Ti(III), and Cr(VI); minerals including siderite ($FeCO_3$), birnessite (δ-MnO_2), and pyrolusite (β-MnO_2); and biologically-active soil samples (Aloha and Bashaw).

4.2 Experimental

The reactor system used in this study is shown in Figure 4.1. It consists of a reaction vessel, electrodes and dispensing pumps interfaced to a PC, a dual flow loop to provide on-line filtered samples, and a spectrophotometer. The components of the reactor system are used to perform two separate functions, monitoring parameters and controlling or changing conditions, both of which are managed by a personal computer (PC). The hardware components and software capabilities of the reactor system are described below.

4.2.1 Instrumentation

The basic reactor vessel is a commercial 2-L glass bioreactor (Applikon). Several of the original components of the commercial system (stirrer, propeller, filter module and reactor lid) are made of stainless steel, which is unsuitable for study of trace metal chemistry. These parts were replaced with plastic parts (made in-house if not available) or coated with Teflon to minimize potential metal contamination. The stirrer shaft was covered with Teflon heat shrink, and the propeller replaced with a similarly shaped plastic propeller.

A Delrin lid was constructed with air-tight fittings, including eight inlet/outlet ports with 1/4"-28 threads for liquid and gas tubing connectors, five electrode ports, a stirrer shaft port, and a thermometer port (for more detail, see Appendix A). One electrode port is currently fitted with a Chemi-inert septum

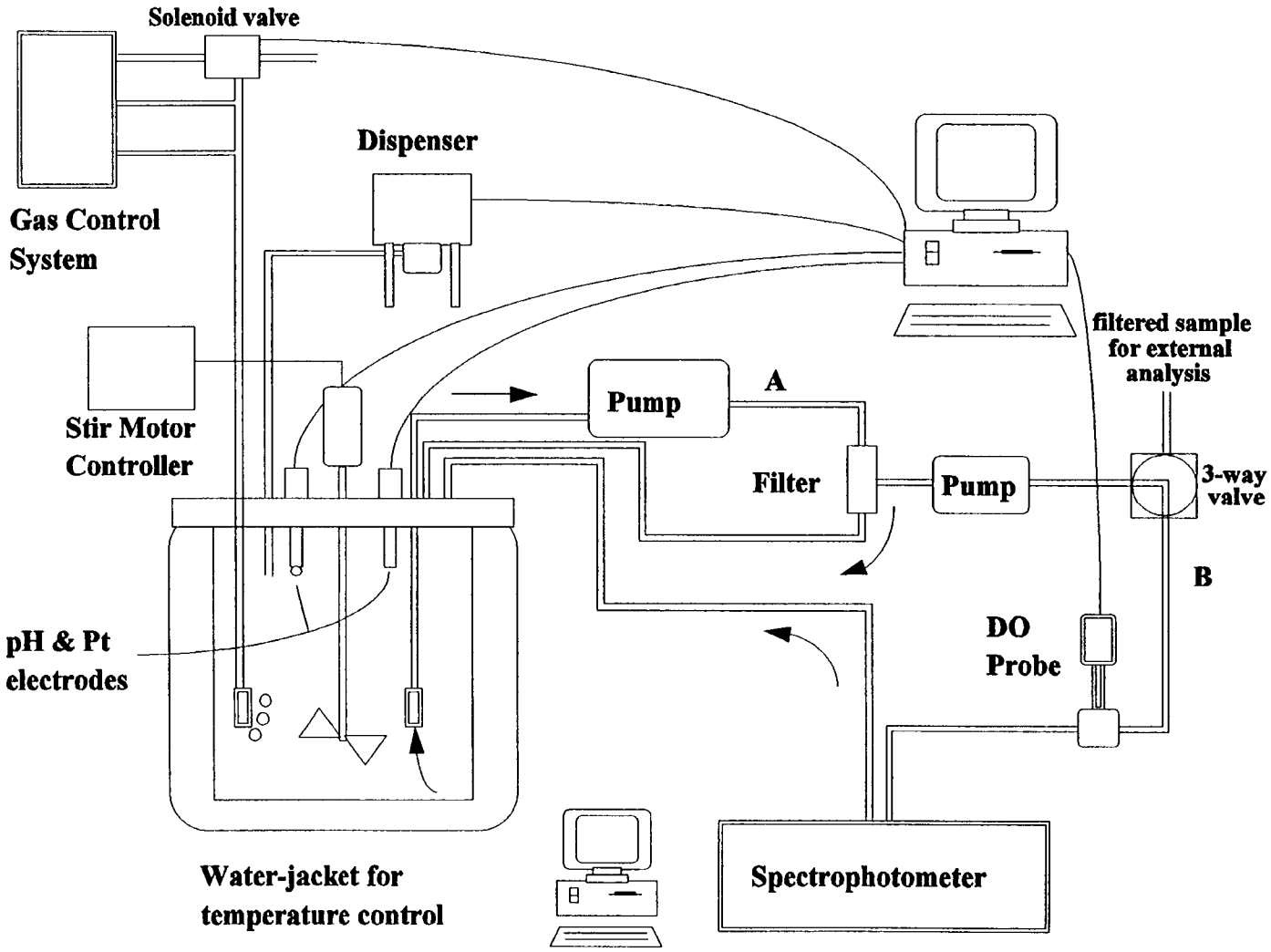

Figure 4.1 Schematic of reactor system. Arrows indicate flow direction in the primary loop (A) and secondary loop (B)

cap for adding or withdrawing air-sensitive solutions with Hamilton gas-tight syringes. Attached to the end of the gas inlet tube is a 10-μm filter (Upchurch Scientific UHMWPE solvent filter, A•426) used as a sparger for gas transfer. The tubing used throughout the system (with one exception detailed below) is either 1/16" or 1/8" - OD PEEK (polyetheretherketone) selected for low oxygen permeability.

A dual-flow loop configuration is included to provide a continuously filtered sample for on-line spectrophotometric measurements without interference due to scattering by solid matrix components or exposure to atmospheric oxygen. The primary loop (A) consists of a peristaltic pump (Masterflex speed controller, Easy load pump head 7518-50, Tygon tubing, size 14, 20-30 ml/min) and a cross-flow filter apparatus. All tubing in the primary loop is PEEK (1/8" - OD, 0.08" - ID) except for a short (approximately 10") section of Tygon tubing at the pump head. Attached to the filter inlet tubing in the reactor is a plastic mesh filter (a particulate filter for a lawn sprinkler with 0.1-0.2 mm openings) to exclude large particles. The filter outlet tube returns to the reactor.

The original cross-flow filter apparatus (Applikon A-SEP filter module) was constructed of stainless steel, so a Delrin replicate was built. The filter module was intended for use with culture media instead of soil solutions containing clay, so it was very difficult to achieve on-line filtering of soil samples without plugging the flow path in the filter module. The final result was combination of modifications. The channel in the bottom plate of the filter module was enlarged as were the inlet and outlet holes to a cross sectional

diameter of 3/32". This enlargement helps minimize solid accumulation in the channels which blocks the flow. The Durapore filter (Millipore, 0.65 μm) was sandwiched between two mesh filters (Spectra-Mesh fluorocarbon, 70 μm). Thin film Teflon rings ((PTFE, 0.005" thick) between the mesh filter and the Delrin minimize leaking around the edges of the filter module (see Appendix A for details). Finally, the module is placed in an ultrasonic bath (Bransonic 52), which is turned on for approximately 15 min every hour.

The secondary loop consists of an FMI Micro Π-Petter pump (0.5 - 1 ml/min), a right angle flow switching 3-way valve (Upchurch Scientific), a spectrophotometer flow cell (HP 0100-1224, 1-cm path length or Hellma 170.700, 1-mm path length), and an electrode flow cell holder containing a dissolved oxygen probe. The outlet of the secondary loop also returns to the reactor. The switching valve allows collection of filtered samples for external analysis (spectrophotometric, atomic absorption spectrophotometry, ion chromatography etc.).

The reactor lid is fitted with a glass electrode (Orion 9101BN) for pH monitoring, a Pt electrode (Orion 967800) for E_H measurements, and a single reference electrode (Orion double junction 900200) that is used for both indicator electrodes. Included in the external sample loop described previously, is a Clark polarographic electrode (Orion 970800) for determination of dissolved oxygen concentration. There are two reasons for including the DO probe in the secondary loop: its bulky construction prevents it from being included in the reactor lid and a filtered sample minimizes membrane fouling.

During an experiment, the absorption spectra over the 190 to 820 nm range are obtained using an Hewlett Packard 8452A diode array spectrophotometer. This on-line spectrophotometric monitoring of components is used to follow changes in concentrations of pollutants, redox indicators or immobilized redox indicators as described in Chapter 5. In addition, several parameters were monitored externally on withdrawn samples. These include Mn determined by atomic absorption spectrophotometry (Buck Scientific), Fe determined colorimetrically (1,10-phenantholine method and HP 8452A Diode array spectrophotometer) and major ions such as Na^+, NH_4^+, K^+, Mg^{2+}, Ca^{2+},and acetate with ion chromatography.

The glass bioreactor is equipped with a water jacket. The temperature in the jacket is maintained at 25°C (Haake FJ temperature controller water bath circulator). For continuous stirring, a high-quality stirring motor (Applikon P100) and controller (Applikon ADI 1012) are included in the reactor system. The stirring motor rate is typically set at 500 rpm.

The gas control portion of the apparatus consists of a Tylan RO-28 readout and control box and three Tylan FC280 mass flow controllers for CO_2, pre-purified N_2 and O_2. Included in the nitrogen line, between the gas cylinder and the flow controller, is an oxygen trap (Alltech Oxy-Trap 4001) and an indicating oxygen trap (Alltech 4004). A computer controlled 3-way solenoid valve (Appendix A) is located between the O_2 flow controller and the Swagelok cross where the gas flows are combined before entering the reactor. This allows

computer controlled addition of O_2 to the reactor for E_H control as described below.

Precision liquid dispensing pumps (Fluid Metering Inc. Micro ∏-Petter) are used to add small amount of concentrated solutions to minimize the volume added during long-term experiments. Solutions can be added to control system parameters such as pH and E_H or to titrate the system. The pump volume adjusts from 2 to 50 µL per stroke, and is typically set to 25 µL. The delivery rate is limited by the programming to dispense once every two seconds. For good precision and accuracy, concentrations and volumes are selected such that four to five dispensing cycles are made per addition. The dispensing pumps were modified for digital control with two solid state relays (Grayhill 140 VAC, 3 A) (See Appendix A).

4.2.2 Interfacing

The system is interfaced to a 286 PC equipped with a multiplexed ADC and I/O board (Computer Boards Inc., CIO-AD08-PGA). The computer board includes eight differential A/D channels with programmable gain (used for potentiometric measurements) and four digital output ports (used for dispensing pump control). Each digital output line controls a separate pump: acid, base, redox reagent and other reagent (manual addition described below). The board is connected to a single component box which allows signal transfer by means of BNC or banana connectors. The pH electrode is connected to a pH meter

(Chemtrix Type 60A) with the recorder output connected to an ADC channel. Details about connections are givein in Appendix A.

4.2.3 Software

The computer program which provides computer control of reagent addition and synchronized data acquisition was developed in QuickBASIC 4.5 (a copy of the program or file is available upon request). The function of the software can again be divided into monitoring and controlling tasks similar to the hardware instrumentation. Electrode measurements are typically obtained every 15 min. When the pH is maintained at a set point, a different time can be selected between pH adjustments and data acquisition. However, if the same time is selected, reagent addition is immediately prior to electrode data acquisition. Initially, there are many adjustable parameters that must be input by the user. These include pH and DO calibration information, the volume of the solution in the reactor, the calibrated delivery volume of the dispensing pumps, the concentration of solutions added with the dispensing pumps, the time between electrode measurements, the tolerance level for pH statting (adjust when differs from the set point by more than the selected amount), and an initial estimate of the buffer capacity. In addition, the user can select the initial level of control (i.e., monitor pH/E_H without adjustment or maintain a selected set point).

Figure 4.2 shows the menu options and the data displayed on the computer monitor during program execution. The electrode measurements (Pt,

MENU: PRESS THE KEY OF YOUR CHOICE

1) Withdraw sample for analysis. Time is recorded
2) Add solution X with dispense pump. (pump connected to DO3)
3) Enter new gas flow parameters (change manually), print to data file.
4) Take electrode readings
5) Change the pH of the solution to a selected pH
6) Stop pH stat (currently pH stat is on)
7) Manual change of parameters: time between readings, acid/base conc, tolerance etc
8) Stop adding liquid oxidant/reductant to stat the Eh

Time	Pt(vs SHE)	DO	pH	pH stat	Rcap uM/V	BufCap mM/pH
10:15	0.2517	0.019	6.025	6.00	1310	1.69
10:30	0.2513	0.021	6.027	Eh Stat (mV)	1520	2.43
10:45	0.2520	0.020	6.026	250	1032	1.61
11:00	0.2507	0.017	6.027		Change/hr: based on last 3 data	
11:15	0.2519	0.019	6.029		Pt(V/hr)	DO(ppm/hr) pH(pH/hr)
11:30	0.2523	0.022	6.030		-0.0002	-0.0003 -0.0005

Current Status: ---
OK to enter number of your selection.

Figure 4.2 Computer screen display during experiment.

DO and pH in Figure 4.2) are the average of 200 ADC readings taken over about 200 ms. Signal averaging is included to reduce the effect of 60-Hz noise and obtain a reproducibility of about 0.5 mV. The displayed potentials for the Pt electrode have been corrected for the reference electrode so they are versus a standard hydrogen electrode. Also displayed are the rates of change of the electrodes which can be used to indicate when steady-state conditions have been achieved or when the system has been purged of oxygen. The concentration of oxygen in the system after the initial purge is usually below the detection limit of the DO probe (about 0.1 ppm). Hence, the probe is useful for monitoring the disappearance of oxygen at the beginning of the experiment and for detecting an oxygen leak in the system.

The program is interactive and responds to keystrokes (Menu keys in Figure 4.2). The current status message changes as appropriate (e.g., adding reagent, please wait to enter you selection). Menu option 4 allows an extra set of electrode readings to be obtained without disturbing the timed measurements. This is useful when infrequently sampling the electrode potentials. Option 2 is selected to add a single shot of a reagent with a dispensing pump connected to DO3. This method of addition is explained below.

Options 5, 6 and 8 allow the selected level of pH and E_H control to be changed. This permits the pH to be changed to a selected level, the pH-stat to be activated after an initial equilibration period, and data to be collected at several redox levels consecutively. When the E_H-stat mode is selected, the user has the option of adding a liquid or gas reagent by connecting either a

dispensing pump or solenoid valve to the digital output line (DO4). The user enters the needed information: the volume of the pump stroke, the concentration of the solution, the potential set point, the tolerance level, and the time between adjustments for solution addition; and the type of gas used, the duty cycle and the tolerance level for gas addition.

The manual adjustment option 7 allows many parameters to be changed during a given experiment. The time between acquisition of electrode potentials is selected initially, but can be adjusted to allow infrequent data collection during the approach to the natural E_H, or more frequent data collection during redox or pH shifts. The concentration of added reagents can also be adjusted as needed.

When a sample is withdrawn for external analysis, the user enters the sample volume (option 1). This allows the program to record the sampling time and track the total solution volume, accounting for both sample withdrawal and reagent addition. The program also manages continual tracking of total amount (moles) of pH adjustment solution added (acid, base, buffer) and total amount of oxidant (reductant) added.

There are three automated modes of computer activated liquid reagent addition utilizing the dispensing pumps; single dose in response to a user-entered value (manual titration); feedback loop in response to a continually monitored parameter (E_H- or pH-stat); feedback loop in response to a user entered value (E_H- or pH-shift).

The first method of addition is straightforward, while the next two are more complicated, but similar. Figure 4.3 shows the conceptual approach to E_H and

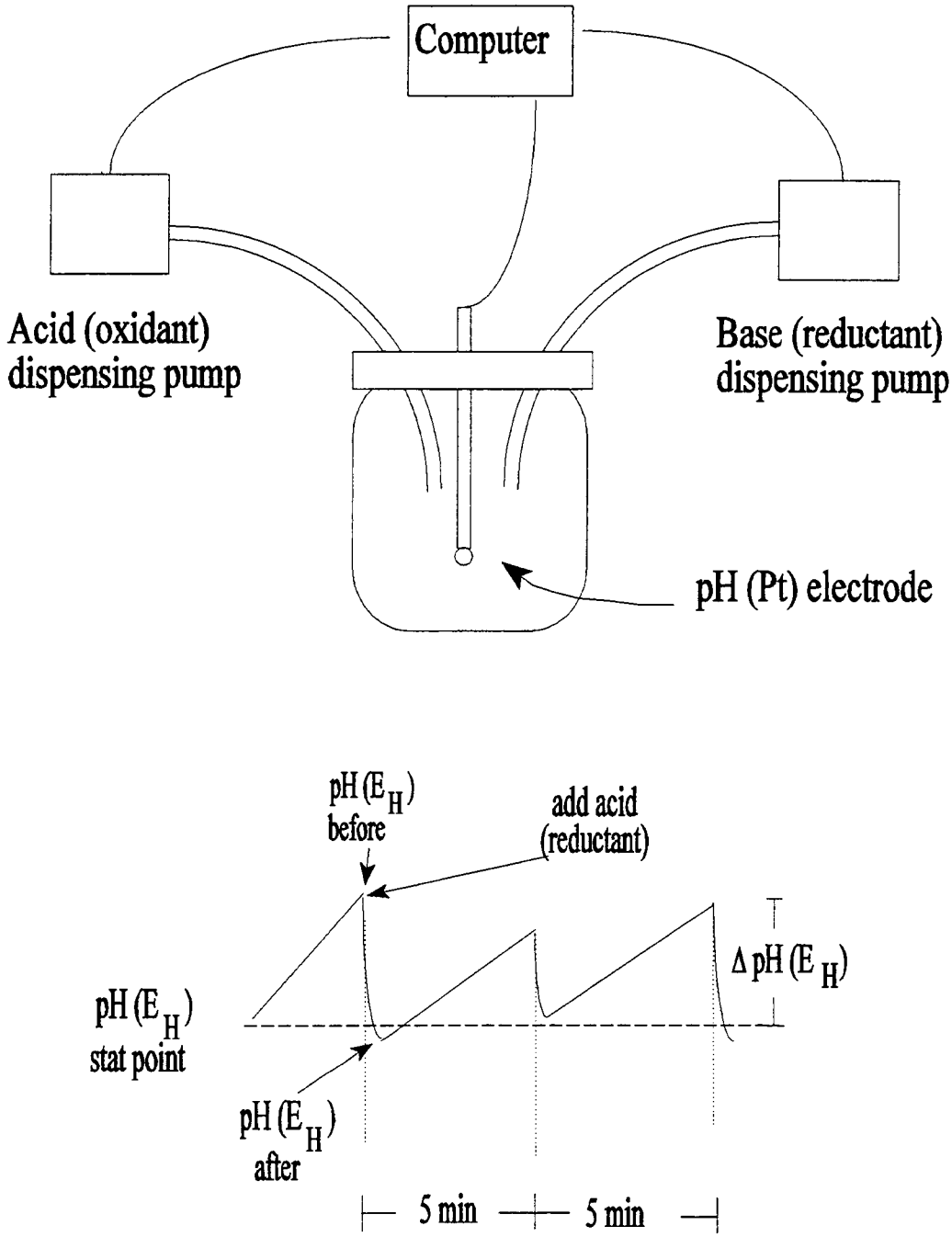

Figure 4.3 Conceptual approach to E_H- and pH-stat with a liquid

pH statting using a solution of acid, base, oxidant or reductant and computer controlled dispensing pumps. For the E_H-stat, the user enters the desired set point. When the pH-stat is initiated, the current pH is the set point. (The pH set point can be changed as described below.) The user also selects a tolerance level; no reagent is added until the measured value differs from the set point by more than the selected tolerance level. This approach is different from the reactor system described in Chapter 3 which did not include a similar comparison of pH before adjustment. The pH and E_H changes are much slower in the soil solutions studied in this research relative to the changes in the highly active biological media used in Chapter 3. Therefore, adjustments are not necessary every time interval. The tolerance level is needed so that small additions (one pump stroke volume) are not made due to small random variations in the E_H or pH. Typical tolerances are 0.05 for pH and 5 mV for E_H.

The pH is maintained at the set point as follows:

a) The current pH condition is monitored (pH before);

b) Based on previous measured pH buffer capacity values, the change in acid (base) molarity in the reactor necessary to return the system to the set-point is calculated from

$$\Delta[acid(base)] = BufferCapacity \times |(pH\,before - pH\,setpoint)| \qquad (4.1)$$

The program then calculates the volume of solution to add via the dispensing pumps based on the reactor solution volume and the concentration of the pH adjustment solution. The required number of

additions is calculated and truncated to an integer number. If the volume calculated is less than the stroke volume, no addition is made.

c) The actual buffer capacity of the system is determined from

$$Buffer\ Capacity = \frac{\Delta\ [acid\ (base)]}{|\Delta\ pH|} \qquad (4.2)$$

where ΔpH = pH before - pH after. The time interval between these measurements is typically one minute to allow for mixing.

The capacity value used by the program to calculate Δ[acid(base)] with equation 4.1 is a running average of the last six calculated capacities. A similar approach is employed to hold the system at a selected E_H. The redox capacity is calculated from

$$Redox\ Capacity = \frac{\Delta\ [oxidant\ (reductant)]}{|\ \Delta\ E\ |} \qquad (4.3)$$

where ΔE is the difference in the potential measured at the platinum electrode.

The third mode of reagent addition is to change the pH or E_H to a new, user-entered condition. In both cases it is recognized that the system buffer capacity can vary significantly with the parameter value (e.g., buffer capacity can be quite different at pH 5 and 7). Because the capacity values are used to determine the amount of reagent to add, these values must also be allowed to shift. This is accomplished slightly differently for the two parameters.

To change the pH, only a percentage of the calculated amount of acid is added dependent on how different the selected pH is from the current pH (e.g., if current pH and set point differ by more than 1, 20% of the calculated amount is added). As the current pH approaches the selected pH, the percentage increases (e.g., if current pH and set point differ between 0.2 and 0.5, 60% of

the calculated amount is added). This allows the buffer capacity values to change and prevents excessive over correction of the pH when changing from a highly buffered pH region to a less buffered pH. A similar incremental approach is used to change to a new redox potential. However in this case, each step consists of adding redox reagent to result in a 20 mV change in potential until the change required is less than 20 mV. This again allows the capacity values to change along with the redox condition.

Error checking is included to ensure the pH/E_H changes a reasonable amount in the expected direction. Spurious variations in E_H or pH can occur due to AC line transients or operator manipulations around the reactor. When controlling the pH or E_H at a given value, if the "before" value is not within 0.3 pH or 0.2 V of the set point, it is disregarded as an error. In this case, the amount of reagent added is the same as that for the previous time. The "after" values are also checked and must be within 0.5 pH or 0.2 V of the "before" value before a buffer capacity is calculated (redox or pH). If the calculated capacity is greater than four times the average of the last six capacities, a value four times the average is included in the array. This prevents an erroneously large value from affecting the amount added for the next six additions, but still allows the values to change if the actual capacity is changing. An erroneous buffer capacity value could also be calculated if less reagent is added than desired. This can occur due to dilution of reagent in the dispensing tube and is another reason for adding more than one stroke volume each time. If no addition is made (condition is within the tolerance range, or less than one addition volume was

needed), no buffer capacity is calculated. If zero values were calculated, the array could fill with zeros and no more additions would be made. Continual tracking of the two system capacities allows comparison between experiments to see if the capacities are dependent on the type of soil, the redox condition, or the redox history of the system.

Another option of controlling the measured E_H is to use a gas oxidant or reductant instead of a liquid reagent. The gas addition described here is similar to methods used by others (4-12) but somewhat more sophisticated. The digital I/O line normally used to control a dispensing pump, is used instead to control a solenoid valve. A three-way valve is used instead of an on/off valve because the flow meter sensor can overheat if no gas is allowed to flow. As shown in Figure 4.4, when the E_H decreases below an acceptable tolerance level (typically user set to 5 mV), the valve switches so oxygen is mixed with the N_2. The potential is monitored continuously. When the intermediate level is reached (half-way between the set point and the tolerance point), the addition of oxygen to the system is stopped. The use of an intermediate level reduces the overshoot past the E_H set point caused by the time delay between closing the valve and the response of the Pt electrode to the added O_2. The separation of the tolerance level (valve on) and the intermediate level (valve off) prevents the valve from "chattering" at the selected set point. Because the oxygen flow controller is 10 sccm full scale, oxygen can be delivered down to 0.2 sccm or 0.4% (N_2 flow of 50 sccm).

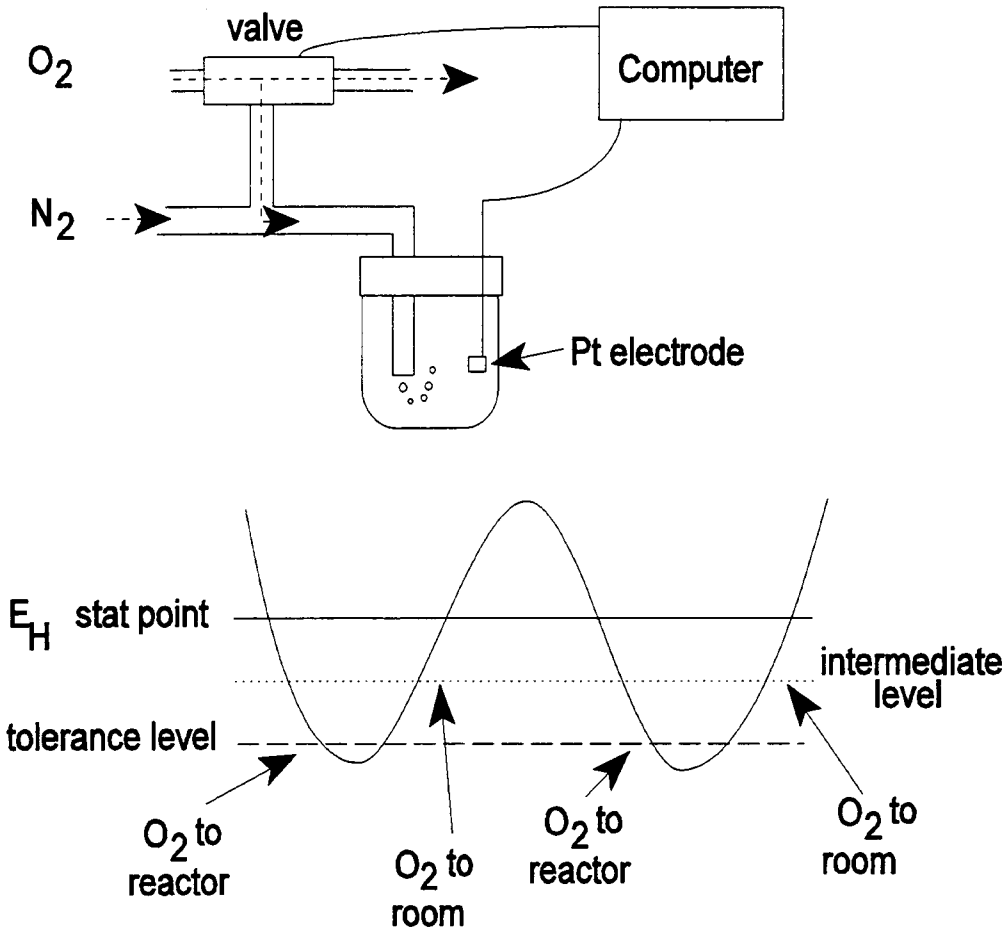

Figure 4.4 Conceptual approach to E_H-stat with O_2 gas.

Another option available is the use of a "duty cycle" when low redox potentials are desired. The duty cycle limits the time the valve is open during a 10-s interval, even when the potential is below the set point. The duty cycle is selected by the user from 100% (continuous addition until the intermediate level is reached as described above) to 1%. For instance, 10% "duty cycle" means oxygen is added to the system one second out of every ten until the intermediate level is reached. Overall, the adjustment of the O_2 flow rate, the N_2 flow rate, and the duty cycle allow the percent O_2 to be varied from 100% down to about 0.002%. This is the same dynamic range achieved by others (6), but without changing gas cylinders. When the potential is controlled with a gas, no capacity values are calculated since the exact gas transfer efficiency is not known. Parallel code exists to add a reducing gas (hydrogen) to decrease the E_H.

All the data are written to three separate files that are easily imported to a spreadsheet. The main data file contains a list of the parameters initially selected, the time of electrode readings, the measured pH, the potential at the platinum and the DO concentration. The other two files are used to record the pH- and E_H- stat information: the time of additions, the electrode readings before and after addition, the volume of solution added, the calculated capacities, and whether adding acid or base for pH-adjustment.

4.2.4 Procedure

The setup procedure varies depending on the experiment and the system studied (i.e., solutions only, mineral, soil, immobilized indicator). A detailed setup procedure is included in Appendix C and specifics are discussed in Chapters 5 and 6. A general procedure is presented here.

The initial components are placed in the reactor vessel. The pH and DO electrodes are calibrated. The reactor system is then assembled as follows: 1) reactor lid - sealed; 2) electrodes - placed in ports, connections made to meters and interface box; 3) gas flow - nitrogen flow (50 sccm) started; 4) dual flow loop - tubing connected and filter assembled; 5) dispensing pumps - calibrated, tubing flushed, connected to interface box; 6) program started.

4.3 Results and Discussion

The reactor system described here has been utilized to study redox transformations in progressively complex systems from simple solutions to minerals to soils. The results of these experiments are presented in subsequent chapters. The discussion here is limited to some critical aspects in the development of the software and the capability of the reactor system.

The modular QuickBASIC program for the system has developed and expanded as necessary. It currently consists of 33 procedures, A modular approach was used so a function can be called from several procedures (i.e., dispensing pump control and analog-to-digital conversion). A program flow chart is shown in Figure 4.5.

The main body of the program is a continuous loop that calls procedures and subroutines as needed to add reagents, read electrode voltages, or respond to user input. As mentioned above, the program is interactive and responds to keystrokes. There is a limited time for the user to continue entering information after a key is pressed. This allows the program execution to resume if a key is inadvertently pressed, rather than stalling on an input statement.

Adding reagents to maintain a set point has priority over sampling electrode potentials; electrode potentials cannot be read during reagent addition to prevent spurious readings from electrodes responding to unmixed solutions or electrical noise from the dispensing pump cycle or solenoid activation. Depending on the amount of reagent added, the electrode readings

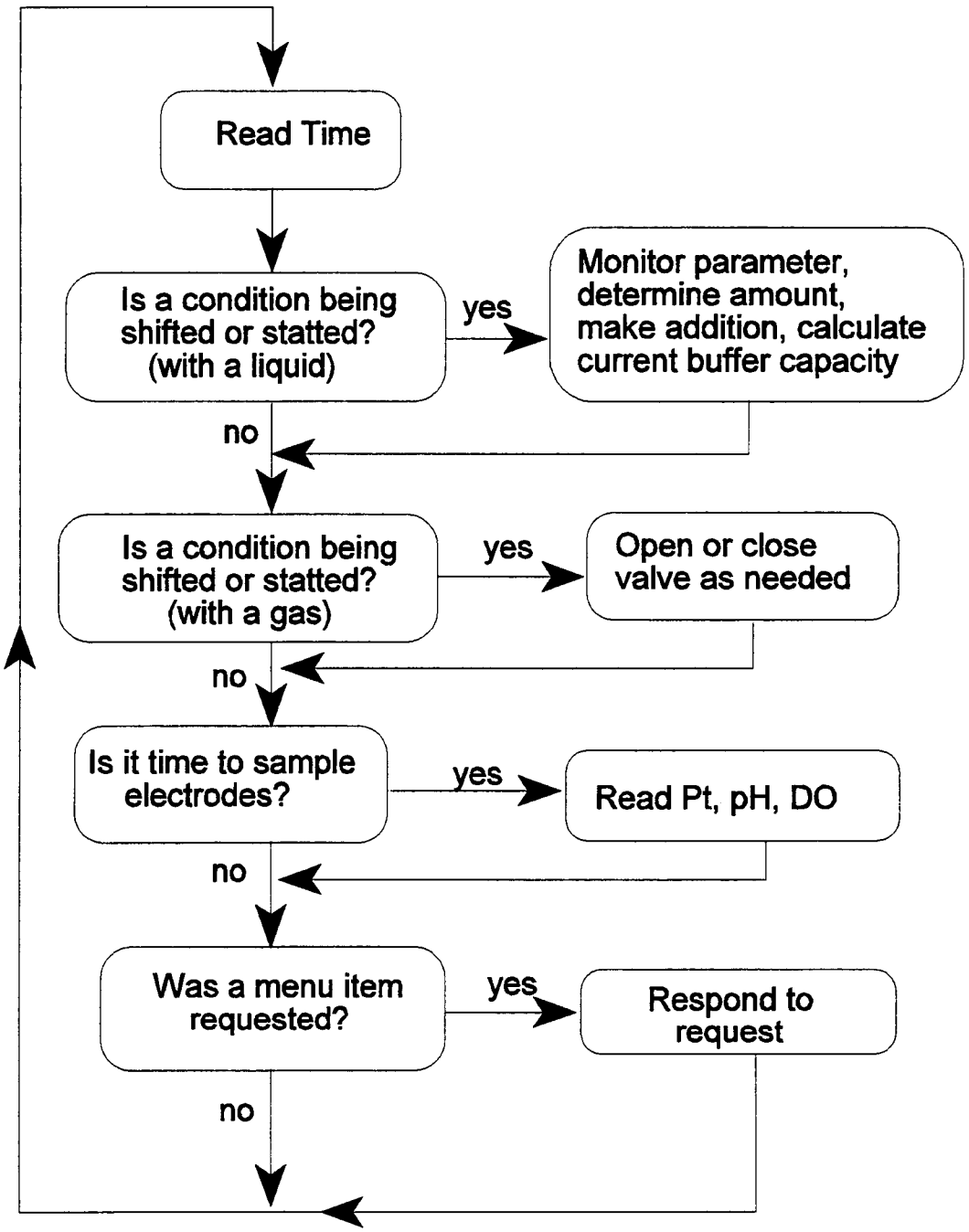

Figure 4.5 Program flow chart.

may be delayed (each pump stroke requires two seconds). This delay is typically less than one minute and so is insignificant in terms of week long experiments.

The biological culture studied in the previously described reactor system (Chapter 3) was much more active than the soils studied here. Because the biological activity was high, the pH (and E_H) always changed during the interval between reagent additions (15 min). However, pH (E_H) changes in the soil systems were much slower as mentioned previously. To prevent the dispensing pumps from adding one stroke volume as needed, a tolerance level was included. A pH (E_H) adjustment is made only when the condition differs from the set point by a specified amount (typically 5 mV or 0.05 pH).

Figure 4.6 shows the system ability to control the pH by adding acid or base as necessary. The pH is held with the tolerance of 0.05 specified. The system is also capable of maintaining the measured redox potential within several millivolts of the selected potential with either hydrogen peroxide (Figure 4.7) or oxygen.

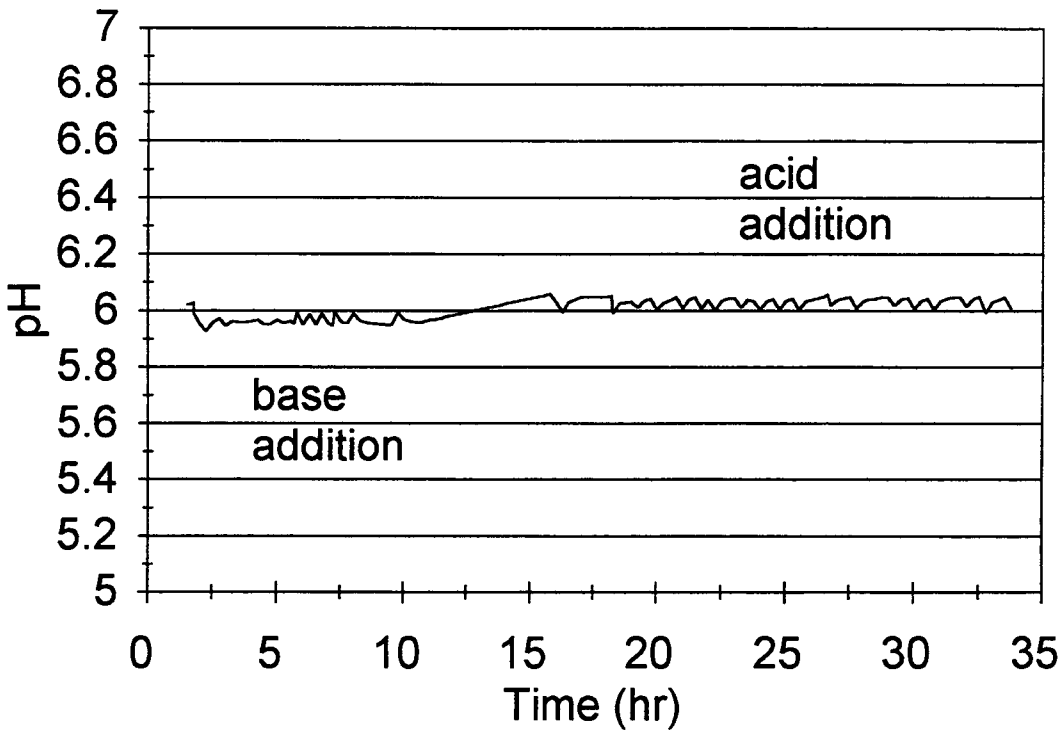

Figure 4.6 Example of pH-stat at pH 6 utilizing acid (1 M) and base (1 M). The reactor solution is Bashaw A1 soil with an natural pH below 6, so base was added to overcome the soil buffering the first ten hours. After 10 hr, the E_H started to decrease witha resultant consumption of H^+ and the program switched to acid addition.

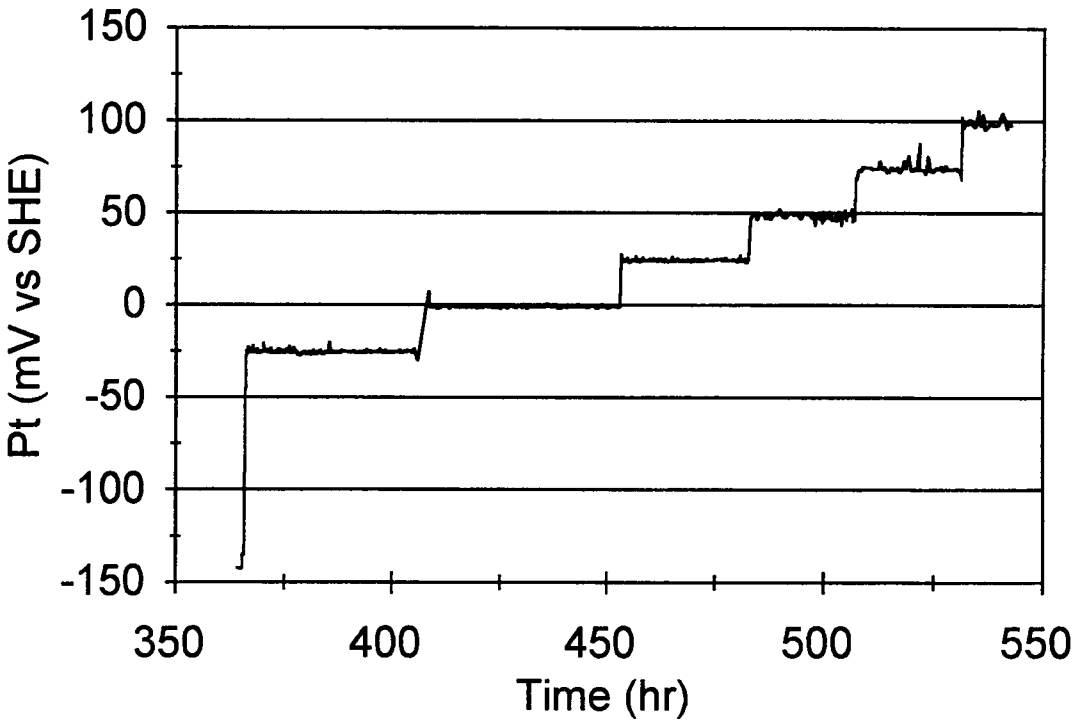

Figure 4.7 Example of E_H-stat utilizing H_2O_2 to maintain various redox potentials. The reactor solution is a Bashaw A1 soil maintained at pH 6 (same solution as Figure 4.6).

4.4 Conclusions

We have developed a laboratory reactor with feedback control or "redox/pH-stat", which allows studies of redox transformations of inorganic matrix components, inorganic and organic pollutants and organic redox indicators to be conducted at any environmental redox level under well controlled, quasi steady-state conditions. The reactor system is capable of achieving and maintaining a selected E_H by adding a redox reagent as either a gas or a liquid. The concentration of O_2 in the N_2 purge gas can be varied over about five orders of magnitude without changing gas cylinders. A constant pH is maintained by addition of acid or base as necessary. The program manages continual tracking of solution volume, and cumulative acid, base or redox reagent added. Both the system pH buffer capacity and redox buffer capacity are monitored throughout the experiment. Finally, all the data are written three separate files that are easily imported to a spreadsheet to allow changes in various parameters to be correlated.

The most unique aspect of this reactor system compared to previously developed soil reactor systems is the dual-flow loop which allows on-line measurements of a filtered sample. This is critical for spectrophotometric measurements and allows other sensors to be added to the system.

4.5 References

1. Knight, B. C. J. G. *Biochem. J.*, (London), **1930**, *24*, 1075.
2. Hanke, M. E.; Katz, Y. J. *Arch. Biochem.*, **1943**, *2*, 183.
3. Vainshtein, M. B.; Gogotava, G. I. *Microbiology*, **1987**, *56*, 23.
4. Patrick, William H. *Nature*, **1966**, *212*, 1278.
5. Patrick, W. H. Jr.; Williams, B. G.; Moraghan, J. T.; *Soil Sci. Soc. Amer. Proc.*, **1973**, *37*, 332.
6. Patrick. W. H. Jr.; Gotoh, S. *Soil Sci. Soc. Amer. Proc.*, **1972**, *36*, 738.
7. Gotoh, S.; Patrick, W. H. Jr. *Soil Sci. Soc. Amer. Proc.*, **1974**, *38*, 66.
8. Patrick, W. H. Jr.; Henderson, R. E.; *Soil Sci. Soc. Am. J.*, **1981**, *45*, 856.
9. Masscheleyn, Patrick H.; Delaune, Ronald D.; Patrick, William H. Jr. *Environ. Sci. Technol.*, **1990**, *24*, 91.
10. Masscheleyn, Patrick H.; Pardue, John H.; Delaune, Ronald D.; Patrick, William H. Jr. *Environ. Sci. Technol.*, **1992**, *26*, 1217.
11. Patrick, W. H. Jr.; Jugsujinda, A. *Soil Sci. Soc. Am. J.*, **1992**, *56*, 1071.
12. Frevert, Tönnies *Schweiz. Z. Hydrol.*, **1984**, *42(2)*, 269.
13. Jee, Hae Sung; Mano, Tarumi; Nishio, Naomichi; Nagai, Shiro *J. Ferment. Technol.*, **1988**, *66*, 123.
14. Jee, Hae Sung; Nishio, Naomichi; Nagai, Shiro *J. Gen. Microbiol.*, ***1987***, *33*, 401.
15. Fetzer, S.; Conrad, R. *Arch. Microbiol.*, **1993**, *160*, 108.
16. Jacob, H. E. In *Methods in Microbiology, Vol 2*; Norris, J. R.; Ribbons, D. W., Eds., Academic Press, Inc.: New York, 1970.
17. Walden, W. C.; Hentges, D. J. *Appl. Microbiol*, **1975**, *30*, 782.
18. Stumm, W. *Schweiz. Z. Hydrol,*. **1984**, *46*, 291.
19. Lovley, D. R.; Goodwin, S. *Science*, **1988**, *52*, 2993.

20. Lovley, D. H.; Chapelle, F. H.; Woodward, J. C. *Environ. Sci. Technol.*, **1994**, 1205.

21. ZoBell, Claude E. *Bull. Am. Assoc. Petroleum. Geol.*, **1946**, *30*, 477.

22. Tratnyek, Paul G.; Wolfe, N. Lee, *Environ, Toxicol. Chem.*, **1990**, *9*, 289.

Chapter 5
Characterization and Immobilization of Redox Indicators

Teresa L. Lemmon and James D. Ingle Jr.*

Department of Chemistry
Oregon State University
Corvallis, OR 97331

5.1 Introduction

A redox indicator (In) is a compound that undergoes oxidation and reduction chemistry with an accompanying change in absorbance or fluorescence characteristics. This change in absorbance or fluorescence of one or both species in the reaction

$$In_{ox} + ne^- \rightleftarrows In_{red} \qquad (5.1)$$

allows the amount of oxidized and reduced forms to be monitored. The reduction potential (E_H) relative to the standard hydrogen electrode (SHE) is then determined by

$$E_H = E^{o'} - \frac{RT}{nF} \ln \frac{[In_{red}]}{[In_{ox}]} \qquad (5.2)$$

where $E^{o'}$ is the formal potential of the redox indicator which is dependent on solution composition (e.g., pH, ionic strength). In this manner, the absorbance of a redox indicator can be used to estimate the redox potential of a well poised redox solution.

Compounds with these properties were developed primarily as end point indicators for redox titrations. Since titration methods have often been replaced by instrumental methods of determination, much of the literature on this topic is three or more decades old. Clark (1) and Bishop (2) have reviewed and characterized a large number of redox indicators and thermodynamic constants.

ZoBell (3) did some early studies on the use of redox indicators to estimate the redox properties of complex systems (marine sediments). Redox indicators have been used in microbiological studies to characterize micro-

organisms and their metabolic efficiency (4) and as mediators of electron-transfer (5). However, they have not been applied extensively in environmental systems that include a solid phase. Possible reasons are the adsorption of these dyes on solids in environmental systems (5, 6) and the difficulty in separating the solution (and dissolved indicator) from the solid phase without disturbing the redox condition. It is necessary to separate the indicator from the solids to make quantitative spectrophotometric measurements. Due to these problems, Hesse (7) comments "On the whole, colorimetric procedures for determining the oxidation-reduction potential of soil are unsatisfactory and are not recommended". However, more recently McBride (6) notes that, although redox indicators have not yet been accepted as a satisfactory method for evaluating soil redox chemistry, "clever experimental designs might circumvent the known drawbacks".

Another possible reason why indicators are not used more is the dis-equilibrium among many redox species such that the indicator can not respond to all redox couples. This same concern is expressed in interpretation of the potential measured at a Pt electrode (8). However, redox indicators may couple with some common redox-active species in environmental systems that do not poise the Pt electrode.

Tratnyek and Wolfe (5) qualitatively evaluated the use of redox indicators to characterize the reducing properties of sediment slurries by selecting indicators with minimal adsorption to the sediments. They conclude that redox

indicators are useful for the investigation of reduction potential, measurement of reducing capacity, and study of redox reaction kinetics.

Previously in our laboratory, a number of redox indicators were characterized spectrochemically with a variety of oxidizing and reducing agents (often in great excess stoichiometrically) (9) and electrochemically by cyclic voltammetry (10). Aqueous solutions of the indicators were mixed with various reductants, including ascorbic acid, dithionite, sulfite, dithiothreitol, and Cr(II), and monitored in a spectrophotometric cell with N_2 purging. Oxidizing agents, such as Ce(IV), O_2, Cr(VI), Fe(III), and As(V), were then added to determine if the colorless reduced forms of the indicator could be re-oxidized. Absorption and fluorescence spectra of the reduced and oxidized form of most indicators were obtained.

Mobley (9) found that 14 of the indicators which are listed in Table 5.1 can be reduced and then re-oxidized, and both forms are stable in solution. For these indicators, the formal redox potential at pH 7 varies from -0.45 to 1.1 V. Nine of the indicators were reduced by dithionite and Cr(II) and were oxidized by Cr(VI), Fe(III), and O_2. These indicators were given a reversibility rating of "good" by Mobley. For about half of the indicators, quasi-reversible behavior was observed with cyclic voltammetry. The reversibility rating in the third column of Table 5.1 reflects the number of tested reductants and oxidants that reacted with the indicator as follows: (i) "good" - over 80% of the tested solutions coupled with the indicator; (ii) "bad" - less than two reactants coupled; (iii) "medium" - all other indicators.

Table 5.1 Summary of indicators, formal potentials and evaluations.

Indicator	E°' (V)[1]	Solution Reversibility[2]	Reactor Behavior	Immobilized Behavior
Ferroin	1.10	medium	---	---
Varamine blue	0.31	bad	no reduction observed	---
Phenol blue	0.224	bad	---	---
Dichloroindophenol	0.217	bad	good	---
Toluylene blue	0.123	---	not stable	not stable
Thionine	0.070	good	good	good, E°' = 0.053
Brilliant cresyl blue	0.047	good	---	---
Gallocynine	0.021	bad	---	---
Methylene blue	0.019	good	good	---
Indigo tetrasulfonic acid	-0.039	bad	slow response Pt electrode	---
Resorufin	-0.051	medium	---	---
Indigo trisulfonic acid	-0.081	bad	---	---
Nile blue	-0.113	good	adsorbs to components	good immobilization high pressure
Indigo carmine	-0.119	good	good	---
Phenosafranine	-0.244	---	good	good E°' = -0.286
Safranine O	-0.280	good	good	low coupling
Neutral red	-0.325	good	---	---
Benzyl viologen	-0.359	good	couldn't reduce second time	---
Methyl viologen	-0.446	good	good	---

[1]Formal potential at pH 7 from literature constants (2).
[2]From studies by Jim Mobley (9).

In this thesis the goal was to investigate more thoroughly and quantitatively the feasibility of utilizing redox indicators to develop a spectrochemical redox sensor. Such a sensor could be used to indicate when conditions exist for redox transformations of pollutants to occur. The ideal indicator should have the following properties: (i) the indicator reaction is reversible and rapid; (ii) the formal potential is near (±50 mV) the formal potential of the redox couple of the species (matrix or contaminant) of interest; (iii) the adsorption on the test matrix solids is insignificant; (iv) the absorption or fluorescence occurs in wavelength regions where the matrix or pollutant does not significantly absorb; (v) both forms of the indicator are stable; (vi) the indicator is readily available commercially.

Reactions of selected indicators with several reducing agents, oxidizing agents and a selected pollutant, Cr(VI), were studied in a sophisticated reactor system. The absorbance of the indicators and Cr(VI) were measured in a closed loop flow cell to determine the speciation of the indicator and chromium. These speciation measurements were then compared to the apparent redox potential (E_H). These studies were conducted to indicate which indicators are coupled with which matrix components (oxidants and reductants) and to determine if the redox transformations of chromium can be evaluated through the reactivity of the indicator.

Most of the indicators used in this study, as well as many identified in the literature, are positively charged and adsorb strongly to negatively-charged surfaces prevalent in minerals and soils. The surfaces of weathered soils are

generally negatively-charged (6, 11) at or near neutral pH and adsorption of the positively-charged dyes to these surfaces is generally strong. Hydrophobic interactions due to adsorbed organic manner are also possible.

To continue studies with solid matrix components, it was deemed necessary to immobilize the indicators to a "sensor" surface to prevent their adsorption on "geochemical matrix" surfaces. To be successful, this modification must be accomplished in a manner that meets the following criteria: (i) the coupling involves a stable and covalent bond; (ii) the indicators retain their redox activity and interactions with the dissolved matrix components; (iii) the absorbance characteristics of the reduced and oxidized forms are different; (iv) the background absorbance of the immobilization media must not be too great and (v) the colored form has an absorbance of 0.2 - 2 A.U. above the background. The last three criteria are necessary for the indicator speciation to still be monitored spectrophotometrically.

Several immobilization techniques were studied with one technique resulting in the successful immobilization of two of the indicators. The successful and unsuccessful reaction schemes are presented and the properties and redox behavior of the immobilized indicators are evaluated.

5.2 Experimental

5.2.1 Chemicals

Based on a literature review (1, 2) and previous studies in our laboratory (9), twelve indicators were selected for study because of their stability, reversibility and range of redox potentials. These indicators are listed in Table 5.2 along with the wavelength of maximum absorbance. Toluylene blue and phenosafranine were added to the list of indicators studied by Mobley to cover the range of redox potentials.

All indicators were received in the oxidized form except for ferroin. The oxidized form of all the indicators studied is colored in solution except for benzyl viologen and methyl viologen. The absorbance of the colored form is monitored to determine the speciation during an experiment.

A 2 mM stock solution of each indicator was prepared in DI water. Potassium dichromate ($K_2Cr_2O_7$, EM Science) was used to make a 1000 mg/L Cr(VI) solution. The bulk siderite ($FeCO_3$) was obtained from Wards Natural Science Establishment Inc. (5 g, crushed and sieved to < 53 μm), while the birnessite (δ-MnO_2, 5 g) was synthesized following the procedure given by McKenzie (12). The phosphate buffer was prepared at 1 M total phosphate from $NaH_2PO_4 \cdot H_2O$ (Mallinckrodt) and Na_2HPO_4 (Mallinckrodt). A 50 mM Fe(II) solution in 0.1 M acid was prepared with $Fe(ClO_4) \cdot 6H_2O$ and concentrated $HClO_4$. A solution of Ti(III) citrate (~250 mM) in Tris buffer (0.66 M) was

Table 5.2 Indicators studied.

Indicator (abbv.)	Source	λ_{max} (nm)
Varamine blue (VB)	Sigma	270
Dichloroindophenol (DCIP)	Baker	602
Toluylene blue (TB)	TCI	524
Thionine (Thi)	Aldrich	598
Methylene blue (MB)	Aldrich	662
Indigo tetrasulfonic acid (ITESA)	Aldrich	592
Nile blue (NB)	Aldrich	634
Indigo carmine (IC)	Aldrich	610
Phenosafranine (Psaf)	Aldrich	520
Safranine O (SafO)	Aldrich	520
Benzyl viologen (BV)	Aldrich	598
Methyl viologen (MV)	Aldrich	604

prepared from ultra pure Tris (tris (hydroxymethyl) aminomethane, BRL Life Technologies, Inc.), sodium citrate ($Na_3C_6H_5O_7 \cdot 2H_2O$, Mallinckrodt), and titanium (III) chloride ($TiCl_3$, 13% in 20% HCl, Fluka Chemika) as described by Zehnder (13). All reagents were used as received.

5.2.2 Characterization of Redox Indicators

Measurements were made in an air-tight reactor system (see Figure 5.1) consisting of a 2-L glass bioreactor, pH glass electrode, reference electrode, Pt electrode, dispensing pumps, gas control system, and a PC. There is an external flow loop which includes a pump, a dissolved oxygen (DO) probe and a spectrophotometer flow cell. A spectrophotometer (HP8452A diode array) is included to monitor absorbance spectra. The electrodes, which are used to monitor the experimental conditions, and pumps are interfaced to the PC. The dispensing pumps accurately add small volumes of reagent (oxidant or reductant) in a controlled manner to perform, in effect, a redox titration of the solution (indicator and Cr(VI)). The reactor system can also maintain pH or E_H (measured at the Pt electrode) utilizing the dispensing pumps.

The reactor system employed for these studies is identical to that described in detail in Chapter 4 except for the nature of the external flow loop. The inlet tubing to the pump is connected to an inlet filter in the reactor (Upchurch 10-μm UHMWPE (polyethylene) solvent filter, A•426). This arrangement worked well in initial solution studies, but when solids were present

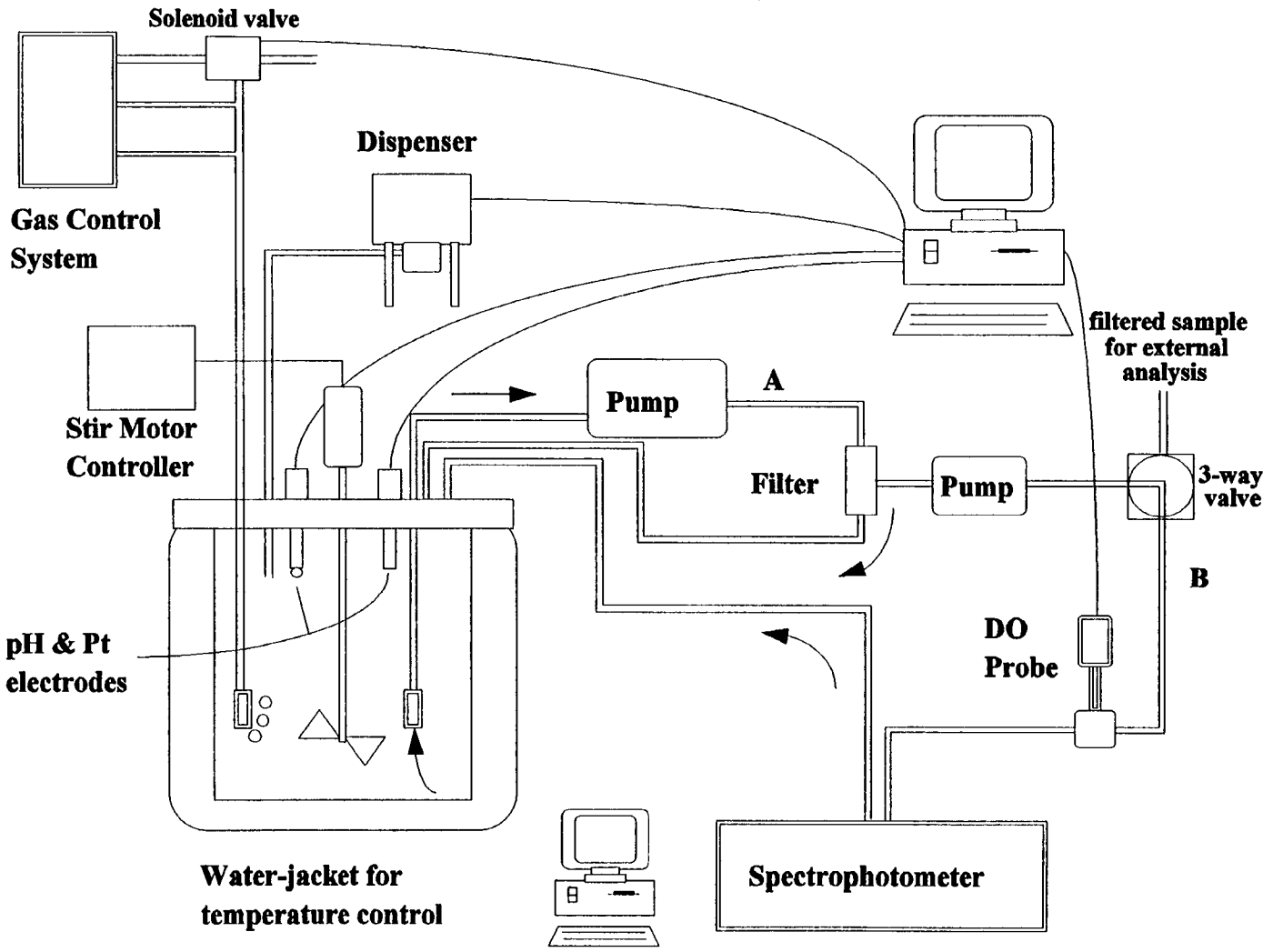

Figure 5.1 Schematic of reactor system. Arrows indicate direction of flow.

(either from the formation of Fe(III) minerals as the Fe(II) was oxidized, or as added minerals), the filter became plugged. This caused some oxygen to be drawn into the flow loop through fitting connections.

In a few initial studies, Cr(VI) was determined colorimetrically with s-diphenylcarbazide (14) (see Appendix B for details). Most Cr(VI) concentrations were determined by monitoring the chromate absorbance at 372 nm in a 1-cm pathlength flow cell. Either DI water or phosphate buffer was used as the blank; phosphate buffer being used for solution studies carried out in phosphate buffer. The absorbance at 790 nm was subtracted from all absorbance measurements to adjust for variations in the lamp intensity during long experiments.

The experiments conducted are outlined in Table 5.3. The general procedure for characterizing the indicators was as follows. The first step was to add reactants (indicator, or indicator and 10 mL of Cr(VI) stock solution), 40 mL of phosphate buffer and DI water to the reactor for a total volume of 1220 mL. The amount of indicator varied from 3 - 20 mL depending on the molar absorptivity. The final test solutions in the reactor contained 33 mM phosphate buffer, 158 μM Cr(VI), and 5-16 μM indicator. In the experiments with only indicator initially present, first a reducing agent solution and later a Cr(VI) solution were added to verify coupling and stoichiometry of the indicator with both the reductant and Cr(VI). For studies with both the indicator and Cr(VI) initially present, the reducing agent was added in steps to study the order of reactivity.

Table 5.3 Experiments conducted in the reactor system.

exp#	solution/matrix	titrant	exp#	solution/matrix	titrant
1	Cr(VI)	Fe(II)	15	benzyl viologen	Ti(III)
2	methylene blue	Fe(II) Cr(VI)	16	benzyl viologen Cr(VI)	Ti(III)
3	methylene blue Cr(VI)	Fe(II)	17	methyl viologen	Ti(III) Cr(VI)
4	thionine	Fe(II) Cr(VI)	18	methyl viologen Cr(VI)	Ti(III)
5	thionine Cr(VI)	Fe(II)	19	dichloroindophenol	Fe(II) Cr(VI)
6	safranine O	Ti(III) Cr(VI)	20	dichloroindophenol Cr(VI)	Fe(II)
7	safranine O Cr(VI)	Ti(III)	21	varamine blue	Fe(II) Cr(VI)
8	Cr(VI) thionine β-MnO_2	Fe(II)	22	indigo tetrasulfonic acid	Ti(III) Cr(VI)
9	thionine β-MnO_2	Fe(II)	23	indigo tetrasulfonic acid Cr(VI)	Ti(III)
10	thionine $FeCO_3$		24	toluylene blue	Fe(II) Cr(VI)
11	thionine δ-MnO_2	Fe(II)	25	toluylene blue Cr(VI)	Fe(II)
12	indigo carmine	Ti(III) Cr(VI)	26	phenosafranine	Ti(III) Cr(VI)
13	indigo carmine Cr(VI)	Ti(III)	27	phenosafranine Cr(VI)	Ti(III)
14	nile blue	Ti(III) Cr(VI)			

Due to the rapid oxidation of Ti(III) by oxygen, this reducing agent was added from a septum vial with a gas-tight syringe. The reductant was typically added in steps equivalent to 20% of the stoichiometric amount necessary for reduction of the Cr(VI) and the indicator. In four experiments a mineral was added as well.

After all components were in the reactor, the solution was purged with N_2 (100 cm^3/min) throughout the experiment. When the dissolved oxygen content decreased below the detection limit of the oxygen probe (about 0.1 ppm), an initial optical absorption spectrum was obtained. The system was titrated with the reducing agent (50 mM Fe(II) or 250 mM Ti(III)) while monitoring the absorption bands of the indicator and chromate, pH, DO content, and potential at the platinum electrode. In the mineral experiments the pH was lowered to 4 and the monitoring was continued.

5.2.3 Immobilization of Indicators

In order to retain its redox chemistry, the immobilization of an indicator must involve a reactive substituent that does not participate in the redox reaction of the indicator. Five of the indicators studied have a reactive primary amine group that is unaffected by the oxidation/reduction chemistry (Figure 5.2). This fact led to a review of existing technology for immobilizing proteins. Several affinity chromatography gels designed to attach the primary amine groups of proteins are commercially available.

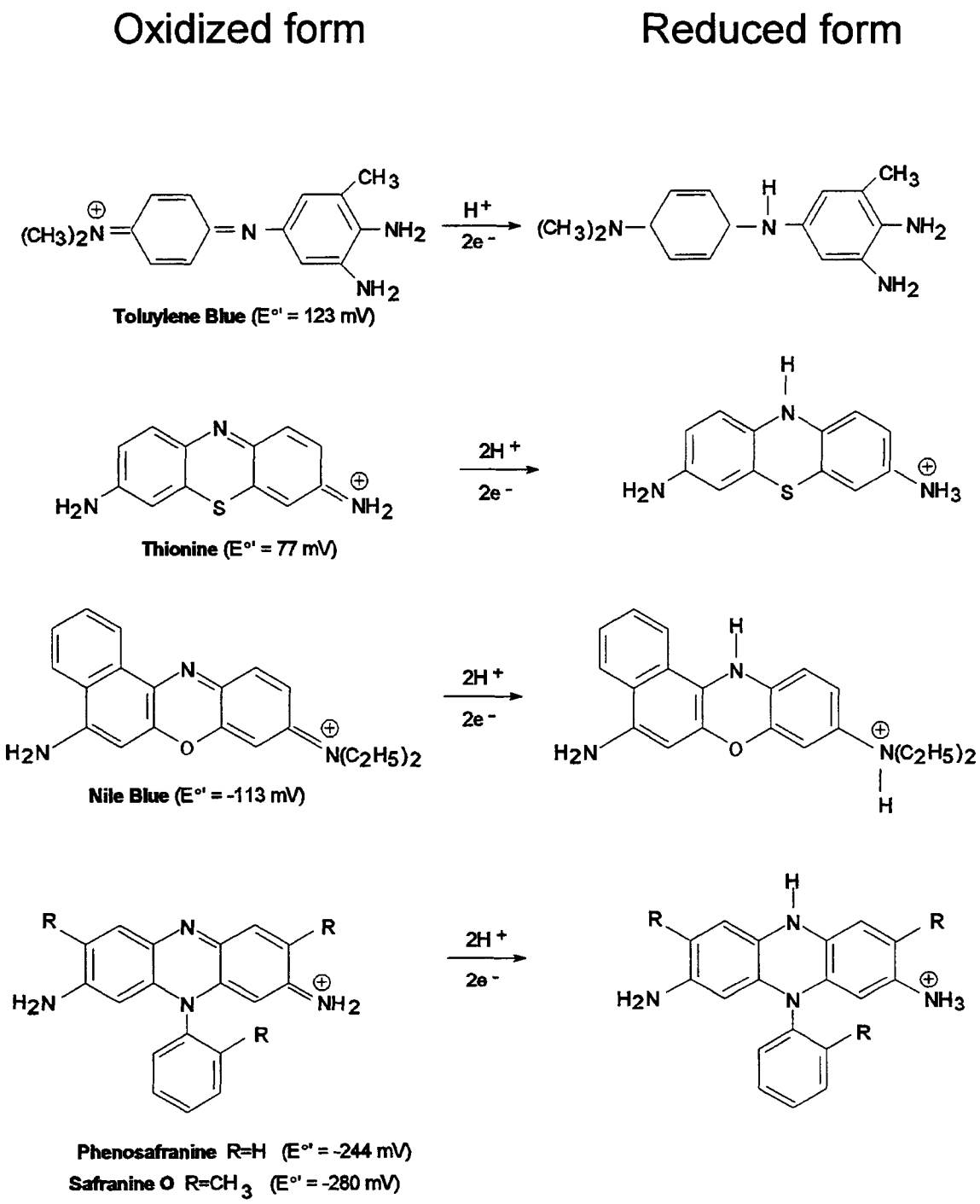

Figure 5.2 Indicators with amine groups not directly involved with the redox chemistry.

The indicators were immobilized on Spectra/Gel® MAS Beads Macroflow (Spectrum, 121508), which is a cross-linked agarose (4%) bead (40 - 60 μm diameter) with monoaldehyde surface groups attached to the matrix through a "5 atoms hydrophilic spacer arm". The concentration of the monoaldehyde binding group is 40-50 μmol/mL of gel. The macroflow beads can be utilized at pressures up to 100 psi without being crushed.

The chemistry involved in the coupling is reductive amination where the initial imine product, which is formed through the reaction of an aldehyde of the gel and the primary amine of the indicator, is subsequently reduced with the mild reducing agent $NaCNBH_3$ to a 2° amine (Figure 5.3). The immobilization procedure used was a slight modification of the procedure provided by the manufacturer (15). The indicators (toluylene blue, safranine O, phenosafranine and thionine) were prepared as 2 mM solutions in DI water. Several phosphate and acetate buffers were used with pH ranging from 3 to 7.

Approximately 0.5 mL of the gel was transferred to a fritted glass funnel (Pyrex® fritted disc funnel, medium (10-15 μm), 2 mL) and washed with three to four gel volumes of 0.1-M buffer solution. The gel was placed in a 3-mL vial along with 0.5 mL of buffer, 0.5 mL of indicator and 0.2-0.5 mL of sodium cyanoborohydride solution (1 M, prepared from Aldrich, $NaCNBH_3$, 95%), and then mixed for three to four hours on a rotator (Labquake Shaker, Labindustries, INC., C400-110). The $NaCNBH_3$ is a mild reducing agent which reduces the imine to a 2° amine (see Figure 5.3) without reducing any uncoupled aldehyde

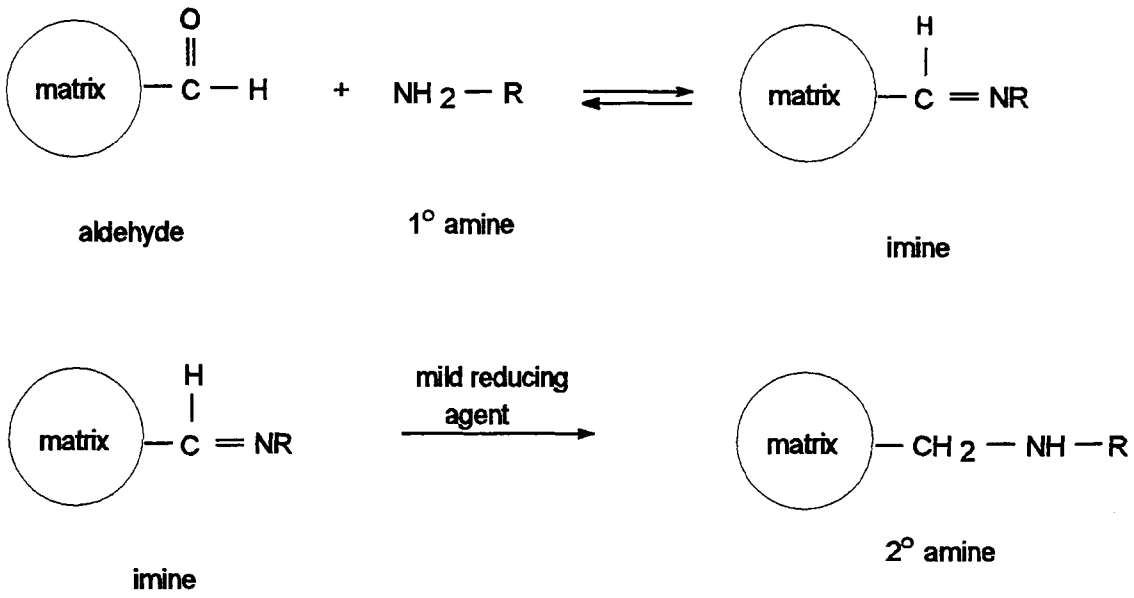

Figure 5.3 Reaction scheme for coupling indicators to Spectra/Gel® MAS (MonoAldehyde Surface) beads. Matrix = gel; 1° amine = indicator; mild reducing agent = $NaCNBH_3$.

groups. Next the gel was rinsed with at least 10 volumes of 0.5 M NaCl in the filtering funnel. It was then transferred back to the vial with 1 mL ethanolamine solution at a pH identical to that of the coupling buffer (0.1 M prepared from Aldrich, ethanolamine 99%). The ethanolamine replaces any indicator still coupled as an imine and not reduced to the stable amine bond. After rotating for another hour, the gel is rinsed first with NaCl and then with buffer until the filtrate is colorless.

To monitor the absorbance of the indicator immobilized on the gel beads, the beads must be contained in a flow cell placed in the sample compartment of a spectrophotometer. The sample cell is located in the external loop so the beads are constantly exposed to filtered solution from the reactor. Filtering of solid particles is required to prevent obstruction of solution flow in the sample cell.

The spectrophotometer cell used for the immobilized indicator was a 1-mm path length flow cell (Hellma, 170.700-QS, aperture dimensions 17.5 x 3.5 mm) with a chamber volume of 61 µL. The gel was confined in the cell by two Neoprene gaskets (1/32" thick, 1/16" ID, 3/16" OD) and a nylon mesh filter (Spectrum, 30 µm) in the outlet fitting as shown in Figure 5.4. Several filters were tried (e. g., Durapore, cellulose) but either the gel broke through the filter, or the pressure build up was too great and the beads were crushed. The nylon mesh filter openings are small enough to exclude the gel (40 - 60 µM), but large enough that the pressure created by the solution flow is acceptable. The

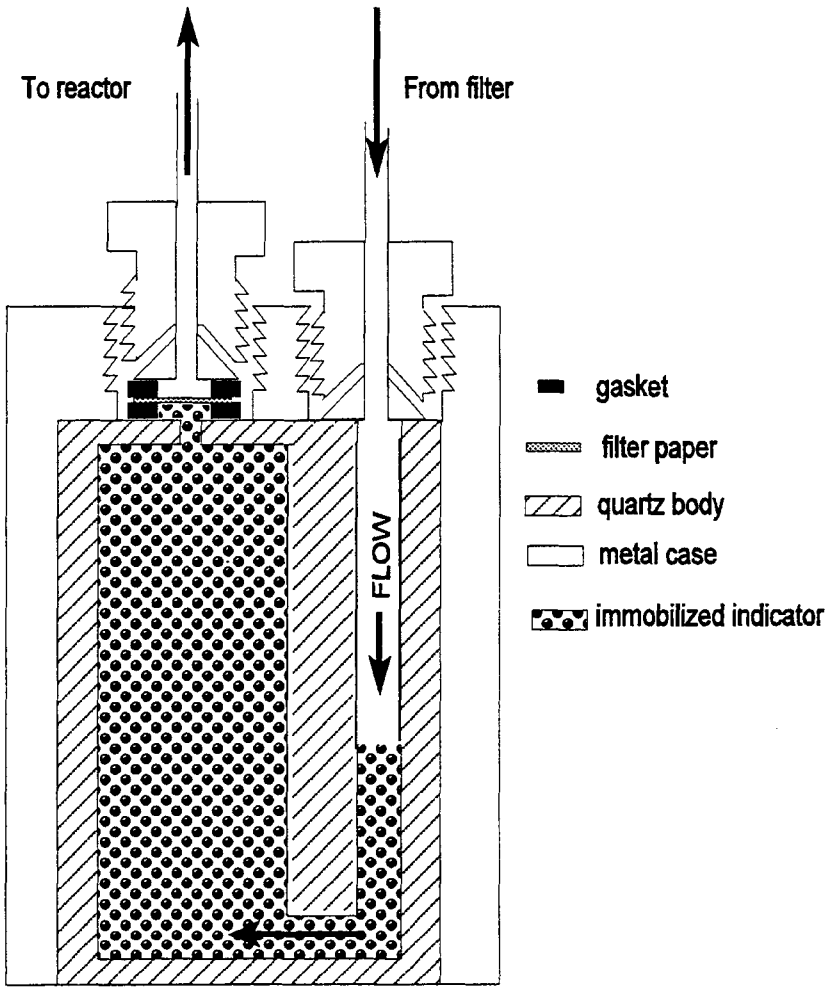

Figure 5.4 Flow cell packed with immobilized indicator

gaskets were necessary to achieve a sealed, leak-free fitting. Without the gaskets, the solution leaked around the mesh and out the joint between the quartz cell body and the metal cell case. The flow cell was "packed" with the immobilized indicator by employing a 5-mL syringe with a luer adapter on the outlet tubing to draw the gel into the cell.

The immobilized indicators were first evaluated in terms of absorbance of the indicator above the background scatter of the gel, the pressure created in the cell when solution was pumped through at a rate of 1- 1.5 mL/min, and redox activity. The pressure was monitored with the meter in a pulse dampener (FMI, PD-60-LF) between the three-way valve and the flow cell (see Figure 5.1) and was typically 10 - 45 psi depending on the indicator, the amount immobilized, the packing efficiency and the length of time of use. Reducing agents and oxidizing agents were then added to the reactor as described in the previous section to determine if the indicators were still redox active with an accompanying change in the absorbance spectrum. As with the solution experiments, the absorbance is always corrected by subtracting the absorbance at 790 nm. This correction was important since solution flowing through the cell caused the gel to become compressed and packed more tightly, which increased background absorbance due to the gel. A separate 1-mm path length cell with DI water was used to obtain the "blank scan".

A simplified schematic of the configuration used to evaluate the formal potential ($E^{o'}$) of the immobilized indicators is given in Figure 5.5. Some "free"

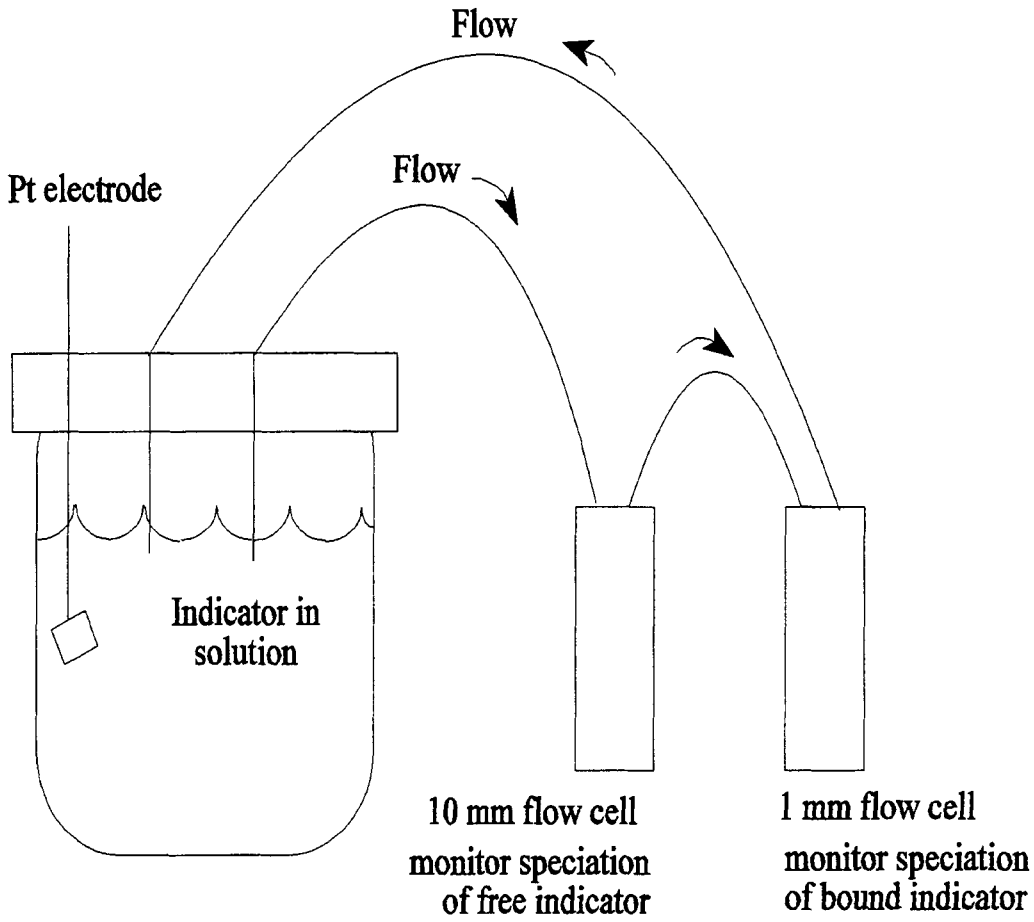

Figure 5.5 Flow loop to determine E°' for bound indicators.

(unbound) indicator is added to the reactor to poise the platinum electrode. The amount of indicator was adjusted to provide a peak absorbance with a 1-cm pathlength of 0.3 - 0.4 (5 mL of 2 mM phenosafranine solution or 5 mL of 2 mM of thionine). The speciation of the free indicator was monitored in a 1-cm pathlength flow cell (Helma, 176.730-QS) while the speciation of the immobilized indicator was monitored in the 1-mm pathlength flow cell.

Absorbance measurements were obtained by manually alternating the cells in the spectrophotometer sample compartment as the solution was titrated with a reducing agent. The error from the absorbance of free indicator in the 1-mm packed flow cell was calculated to be less than 2% and therefore neglected. This was determined from the higher concentration of the immobilized indicator (the effective concentration of the immobilized indicator was 30 - 40 times greater), the shorter path length, and the maximum volume of the cell not occupied by the gel (assuming a solution volume of 80% in packed porous particles).

Two other attempts were made to immobilize the indicators. The first was with Affi-Gel 10 (BIO-RAD, 153-6099), which is also an affinity chromatography gel that employs a different coupling chemistry. The gel is cross-linked agarose with an N-hydroxysuccinimide ester functional group for binding primary amines. The particle size is 75-300 μm, and the chemical capacity is 15 μmol/mL gel. This chromatography matrix had a significantly higher background absorbance compared to the Spectra/Gel®. Even in the 1-mm path length flow cell, the background absorbance of the gel (before coupling) was 1.6 - 1.7 above 300

nm. In addition, the indicator was not sufficiently immobilized. The most efficient coupling was with phenosafranine, which resulted in an indicator peak absorbance of only 0.1 above the background due to scattering by the gel. For these reasons, the Affi-Gel coupling was not pursued.

The last attempt at immobilization did not involve attaching the indicator to a chromatography gel, but rather to water-soluble polymer chains which would pass through the external loop and be present throughout the reactor. This scheme would allow the indicator to interact with the solid particles in the reactor rather than being confined to the flow cell and interacting only with the filtered solution from the reactor. Two poly(acrylic acid) polymers of different molecular weight (MW) were selected (Aldrich, MW 540,000 and 2,000) to immobilize the indicators. Two different coupling chemistries were employed (reaction schemes shown in Figure 5.6). The first involved the addition of $SOCl_2$ to the polymer (MW 450,000) to form an acyl halide, which was then combined with the indicator to form an amide (16, 17). The second utilized DCC (dicyclohexyl carbodiimide) as a coupling agent to form the amide bond (18, 19) between the polymer (MW 2,000) and the indicator. It was hoped that unreacted carboxylic acids would prevent the polymer from adsorbing to the negative matrix particles.

Neither of the reaction schemes for attaching the indicator to the poly(acrylic acid) was successful. When the reaction products were transferred to dialysis tubing to separate the polymer-indicator product from the free indicator, the solution remaining inside the dialysis membrane was not colored.

Scheme 1

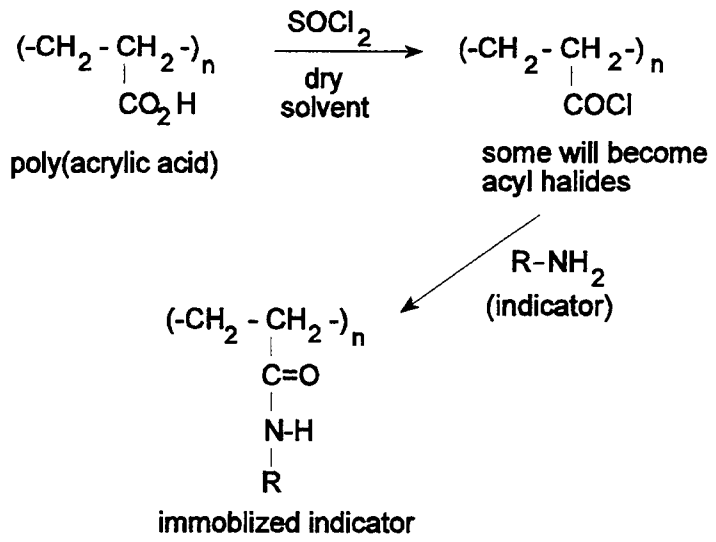

Scheme 2

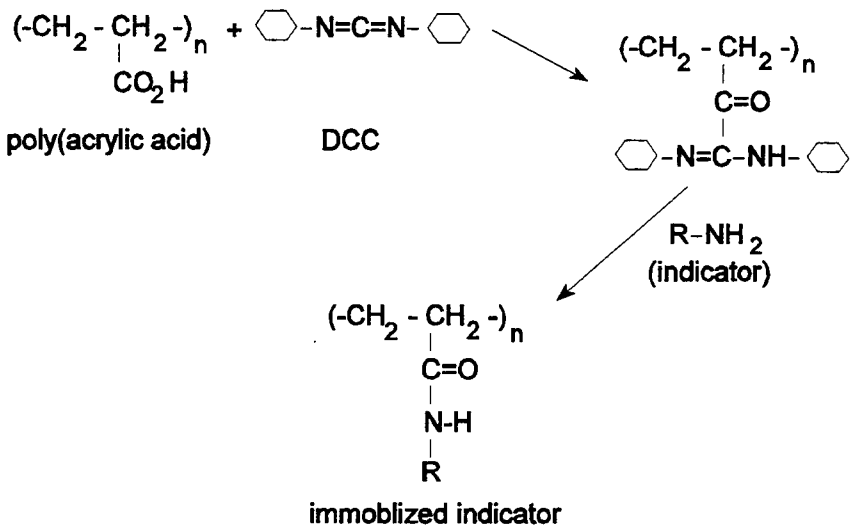

Figure 5.6 Two reaction schemes for attaching an indicator to a polymer.

Therefore, no indicator was covalently attached to the polymer and this immobilization technique was abandoned.

5.2.4 Characterization of Oxygen Response

Experiments were conducted to determine the response of sensors in the reactor to O_2. The reactor was filled with a solution of thionine similar to that used in the characterization of redox indicators (5 mL of 2 mM thionine, 40 mL of 1 M phosphate buffer, DI water to a total volume of 1220 mL). The reactor was purged with N_2 (100 sccm) to remove dissolved oxygen (DO < 0.2 ppm). Then, Ti(III) citrate was added (200 - 300 µL of 250 mM) to reduce the thionine. The gas E_H-stat (based on the computer-controlled solenoid valve, see Figure 5.1) was employed to increase the potential measured at the Pt electrode to various levels by the inclusion of O_2 in the purge gas. The oxygen volume flow rate (F) was adjusted to 0.495 mL/min (5% full scale) to yield a gas stream O_2 composition of 0.49%. The delivery rate of O_2 in mol/min (F') was determined to be 22 µmol/min from the ideal gas law:

$$F' = 10^{-3}\ P\ F\ /\ RT \qquad (5.3)$$

where P = 1 atm, F(mL/min) = 4.95, T = 298 K, and R = 0.08206 L atm/mol K.

During the addition of O_2, the oxidation of the indicator was monitored by the increase in absorbance of its oxidized form in the spectrophotometer flow cell and the increase in DO was measured.

5.3 Results and Discussion

5.3.1 Characterization of Redox Indicators

Representative results of solution experiments are given in Figures 5.7, 5.8 and 5.9. The absorption spectrum of the solution before titration with Fe(II) shows the absorption bands of chromate at 372 nm and thionine at 598 nm (Figure 5.7a). After titration with Fe(II), both absorption bands disappear (Figure 5.7b) exhibiting the reduction of Cr(VI) and the indicator by Fe(II). It is notable that the reduction of Cr(VI) is complete before the reduction of thionine begins (Figure 5.8a). Figure 5.8b illustrates that the platinum electrode potential is not stable until thionine reduction has started. Figure 5.9 shows that the dissolved oxygen concentration decreases as the system is purged with N_2, and reducing agent is not added until the measured DO reaches a constant value at about 150 min. The pH decreased with each addition of acidic Fe(II) solution because the pH-stat portion of the program was not utilized during this experiment. However, the overall pH change was less than 0.1 due to the buffering of the solution.

Similar results were obtained for most of the indicators studied (see Figures 5.10 - 5.13 and Table 5.1). The Cr(VI) was reduced before the indicator, and the indicator coupled with the platinum electrode to "poise" the redox potential as illustrated by the stability of the potential after indicator reduction commences. The indicators with a value of $E^{o'}$ above 0 V, dichloroindophenol, toluylene blue, thionine and methylene blue, were reduced with Fe(II) solution.

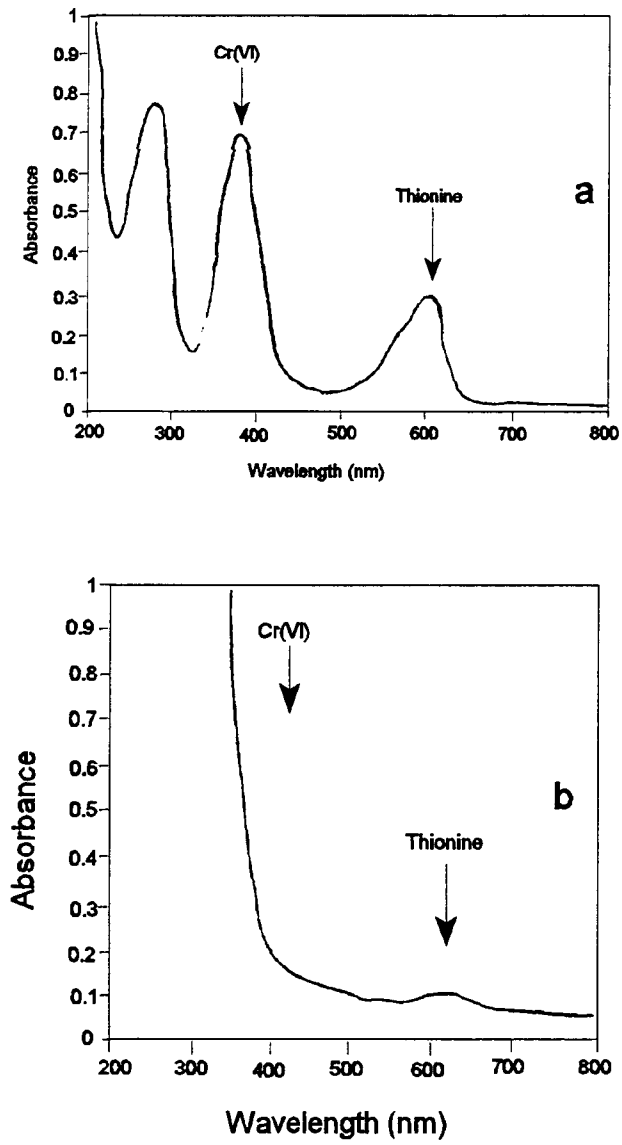

Figure 5.7 Absorption spectrum of Cr(VI) (157 μM) and thionine (5 μM) solution; (a) before and (b) after titration with Fe(II) (50 mM). The absorption bands of chromate at 372 nm and oxidized thionine at 598 nm both disappear upon reduction by added Fe(II).

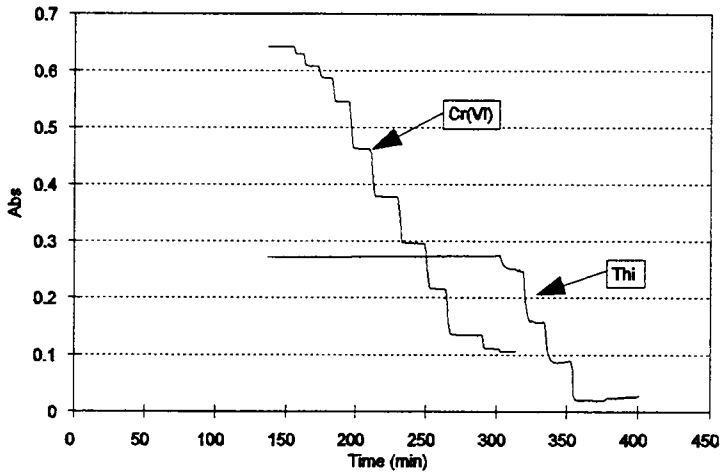

a

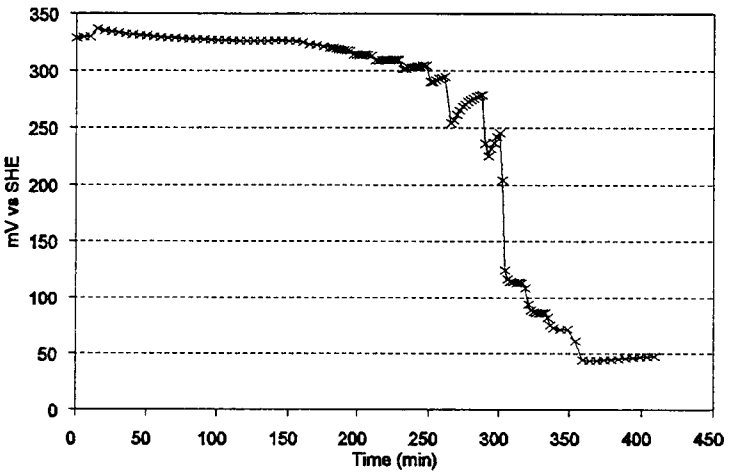

b

Figure 5.8 Titration of Cr(VI) and thionine (Thi) with Fe(II): (a) absorbance of chromate (372 nm) and Thi (598 nm); (b) potential at a platinum electrode. Note: chromate is reduced before thionine, and the potential is not stable until reduction of thionine begins.

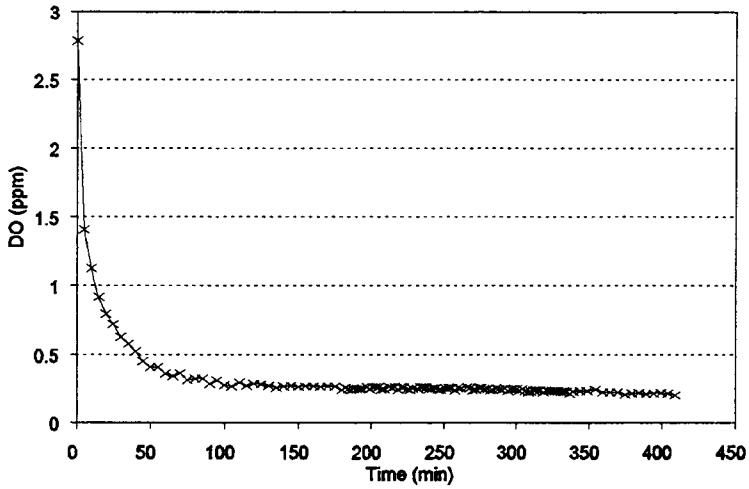

a

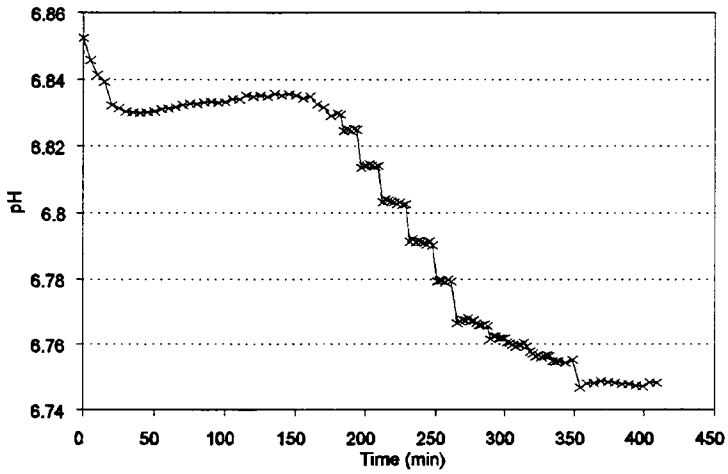

b

Figure 5.9 Additional electrode data obtained during titration of Cr(VI) and Thi experiment: (a) measured DO concentration; (b) pH.

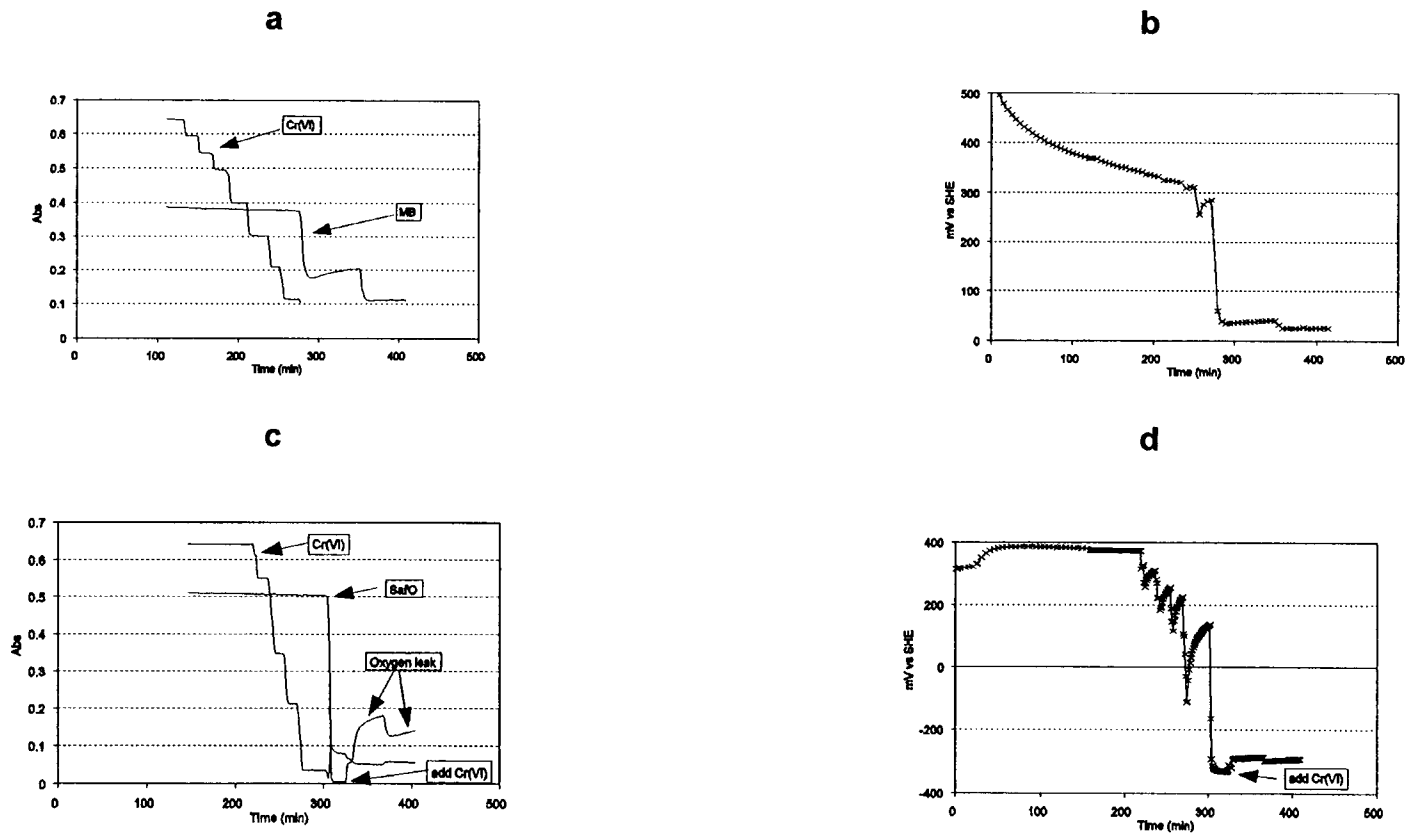

Figure 5.10 Titration of Cr(VI) and methylene blue (MB) with Fe(II) (a, b), and titration of Cr(VI) and safranine O (SafO) with Ti(III) (c, d): (a) abs of Cr(VI) (372 nm) and MB (664 nm); (b) potential at a platinum electrode; (c) abs of Cr(VI) (372 nm) and SafO (520 nm). There was a noticable O_2 leak that resulted in oxidation the the SafO (c).

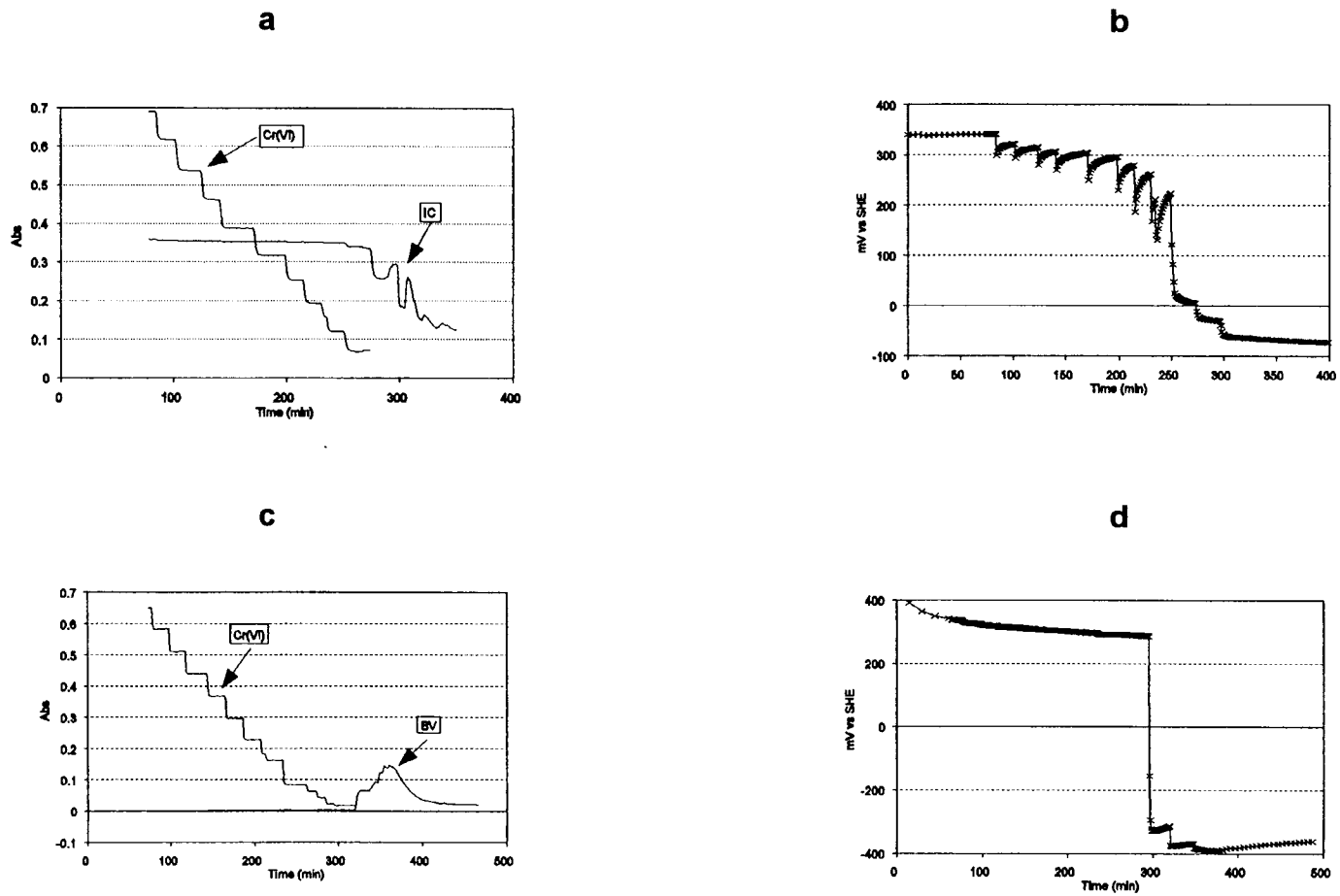

Figure 5.11 Titration of Cr(VI) and indicator (indigo carmine (IC) a and b, benzyl viologen (BV) c and d) with Ti(III): (a) abs of Cr(VI) (372 nm) and IC (610 nm); (b) potential at a platinum electrode; (c) abs of Cr(VI) (372 nm) and BV (598 nm). BV is colored in the reduced form and clear in the oxidized form..

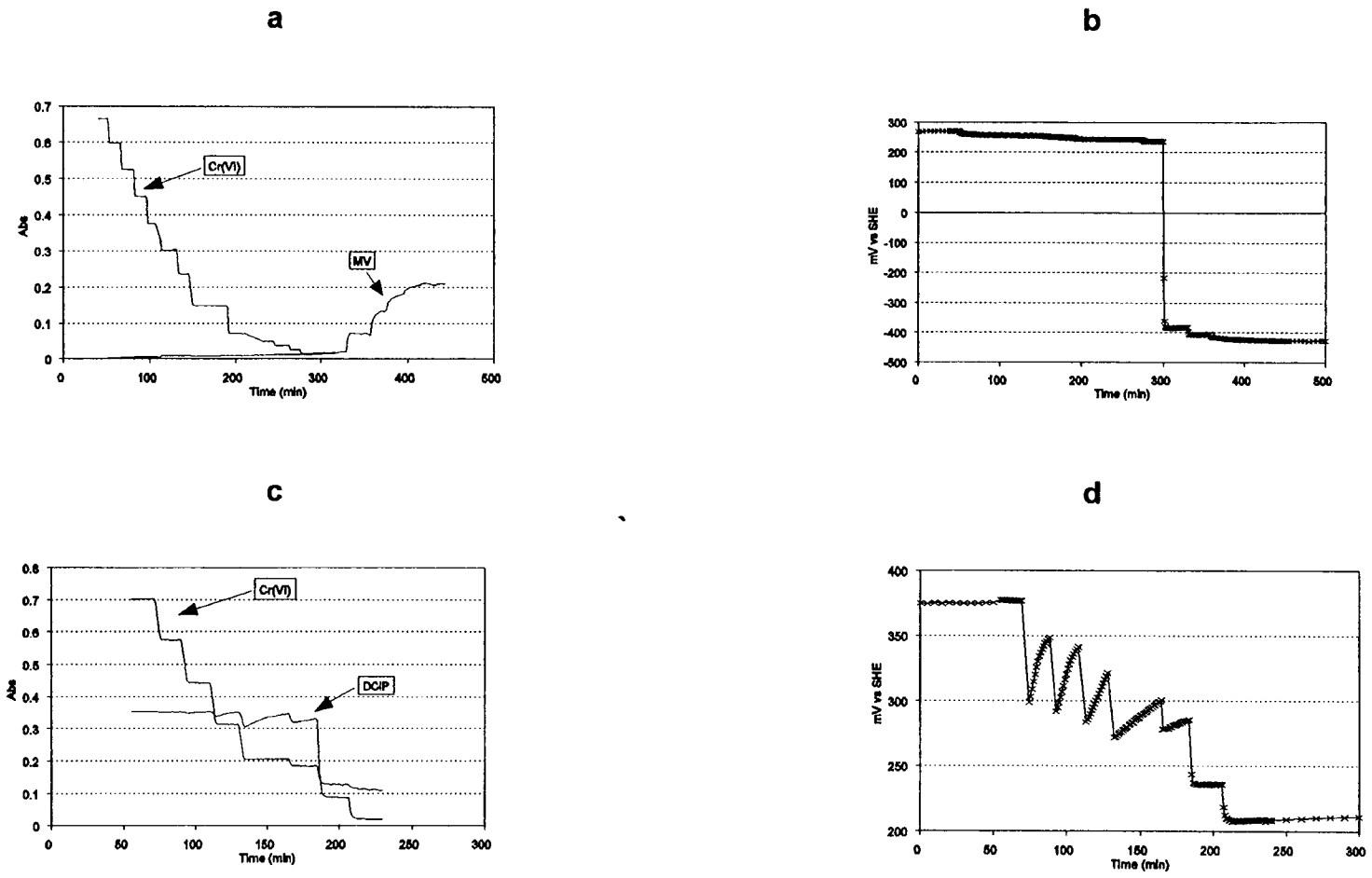

Figure 5.12 Titration of Cr(VI) and methyl viologen (MV) with Ti(III) (a, b), and titiration of dichloroindophenol (DCIP) (c, d) with Fe(II): (a) abs of Cr(VI) (372 nm) and MV (604 nm); (b) potential at a platinum electrode; (c) abs of Cr(VI) (372 nm) and DCIP (604 nm). MV is colored in the reduced form and clear in the oxidized form..

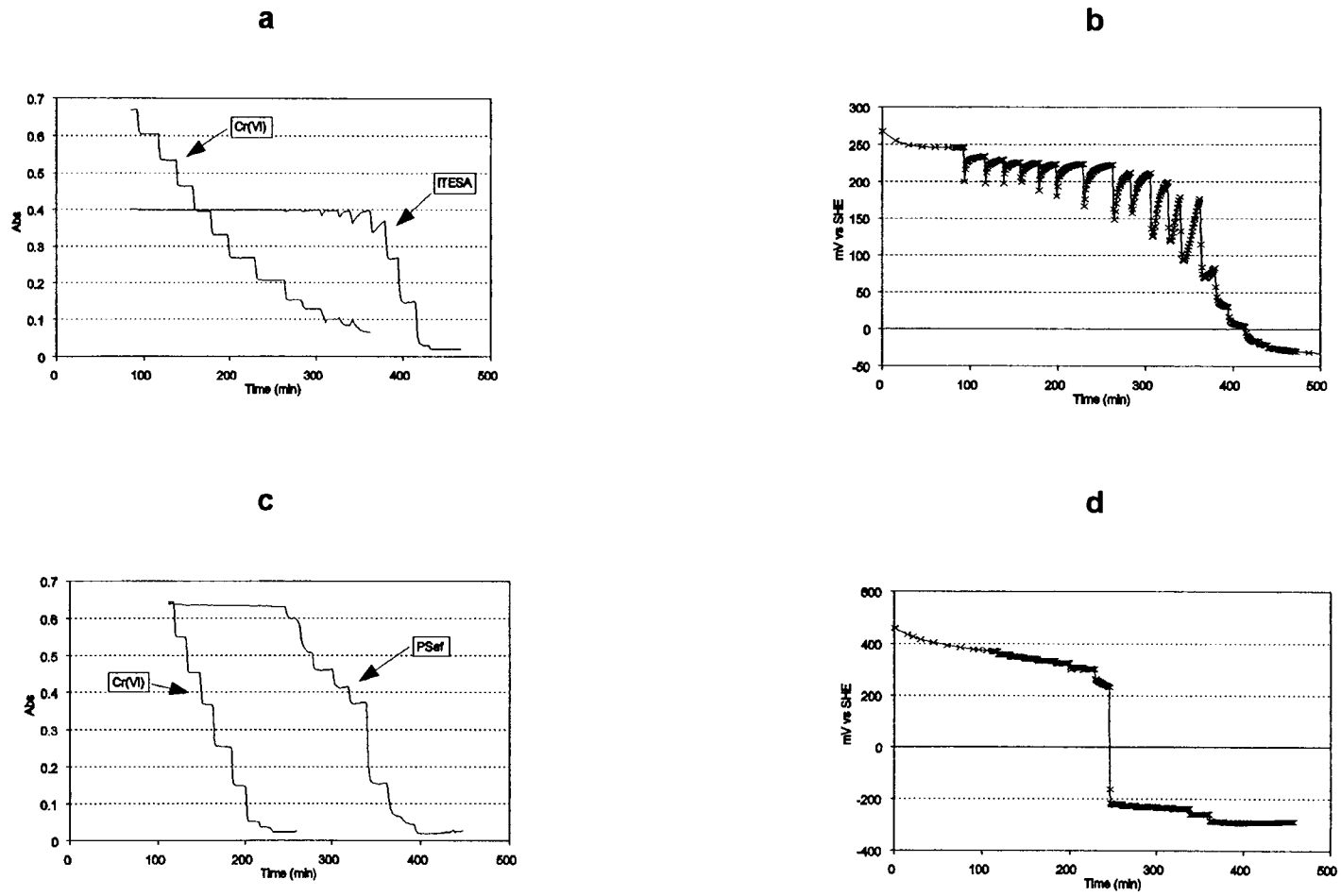

Figure 5.13 Titration of Cr(VI) and indicator (indigo tetrasulfonic acid (ITESA) a and b, phenosafranine (Psaf) c and d) with Ti(III): (a) abs of Cr(VI) (372 nm) and ITESA (590 nm); (b) potential at a platinum electrode; (c) abs of Cr(VI) (372 nm) and PSaf (520 nm).

The formal potential of methylene blue is very close to that of Fe(II), and an excess of Fe(II) was needed. For indicators with lower $E^{o'}$ values, a stronger reductant was required (Ti(III)). The indicator studies without Cr(VI) initially present, show that all reduced indicators are oxidized by Cr(VI) and O_2. Hence, it demonstrated that Cr(VI) and O_2 couple to these indicators but not to the Pt electrode. The behavior of four indicators require further discussion.

First, nile blue adsorbed very strongly to the reactor components (glass, Delrin, polyethylene filter, etc.) which made absorption measurements difficult. The oxidized indicator adsorbed to the filter continued to leach off after the solution indicator was fully reduced. This leaching of oxidized indicator into the flow loop resulted in absorbance measurements in the flow cell that did not reflect the redox state in the reactor.

Benzyl viologen was not reversible in terms of its ability to cycle between oxidized and reduced forms. It could not be reduced a second time, even after addition of a large excess of reducing agent.

Indigo tetrasulfonic acid did not couple well with the Pt electrode (see Figure 5.13a). During the experiment, the indicator was reduced and oxidized several times. It was noted that for a given speciation of the indicator (measured absorbance), the measured potential could vary as much as 30 mV. In addition, the kinetics of indicator reduction were slow. The decrease in absorbance upon addition of reducing agent was not sharp as with other indicators, but a gradual decrease over 10 - 15 min. The slow kinetics could be the cause of the

discrepancy in the measured potential as well. Indigo tetrasulfonic acid may be useful in long-term experiments when the kinetics are not limiting.

Toluylene blue was not stable in aqueous solution for more than a few days. The oxidized form degrades to a non-reducible compound with a different absorption spectrum. The degradation occurs gradually and during this time, the indicator is still redox active with an accompanying change in absorbance spectrum.

The E_H measured at a platinum electrode was compared with the E_H calculated from the indicator speciation. The calculated E_H was determined from literature $E^{o\prime}$ values, the measured pH and the absorbance of the oxidized form of the indicator as shown below for thionine:

1) The fraction of indicator present in the oxidized form (f_{ox}) is calculated by :
$$f_{ox} = \frac{A - A_{min}}{A_{max} - A_{min}} \qquad (5.4)$$
where A is the measured absorbance (at λ_{max}), A_{max} is the absorbance of fully oxidized indicator, and A_{min} is the absorbance of fully reduced indicator.

2) The formal potential at the measured pH (E_m) is calculated from:
$$E_m = E^{o\prime} + \frac{RT}{nF} \ln\left(\frac{[H^+]^4 + Kr_1[H^+]^3 + Kr_1Kr_2[H^+]^2}{[H^+] + Ko_1}\right) \qquad (5.5)$$
where $E^{o\prime}$ is the formal potential at pH 0, Kr_1 and Kr_2 are the acid dissociation constants of the reduced indicator, and Ko_1 is the acid dissociation constant of the oxidized indicator. The equation and constants used for each indicator were obtained from Bishop (2).

3) The calculated potential (E_H calc) is then determined from:

$$E_H = E_m - \frac{RT}{nF} \ln\left(\frac{(1-f_{ox})}{f_{ox}}\right) \quad (5.6)$$

Figure 5.14 illustrates that the calculated E_H value compares well with the E_H measured at a platinum electrode for nine redox indicators. As discussed previously, the agreement between indigo tetrasulfonic acid speciation and electrode potential is poor. The observed correlation contrasts the poor correlation between calculated and measured E_H values for the environmental couples compiled by Lindberg and Runnells (8). Many of the reactions in this other study are known not to be in equilibrium. Clearly, redox indicators have promise as indicators of redox conditions for environmental samples.

Figure 5.14 also illustrates that each indicator is effective over a limited potential range. For indicators reduced with a 2-electron transfer reaction, the potential range for the indicator to change from 99% oxidized to 99% reduced is 120 mV (4). Therefore, a combination of indicators must be used to obtain measurements over a wider range of potentials. The indicators studied encompass the potential range from -450 to 300 mV, except for a gap at -150 mV. During a second literature review of redox indicators (1, 2, 20), no commercially available indicators with a formal potential in that region were found. This second review did lead to the addition of phenosafranine to cover the potential range from -250 to -200 mV.

Redox cycling of chromium and indicators was studied with the reducing mineral siderite ($FeCO_3$) and the oxidizing minerals pyrolusite (β-MnO_2) and birnessite (δ-MnO_2) (experiments 8-11, Table 5.3). Previous studies on

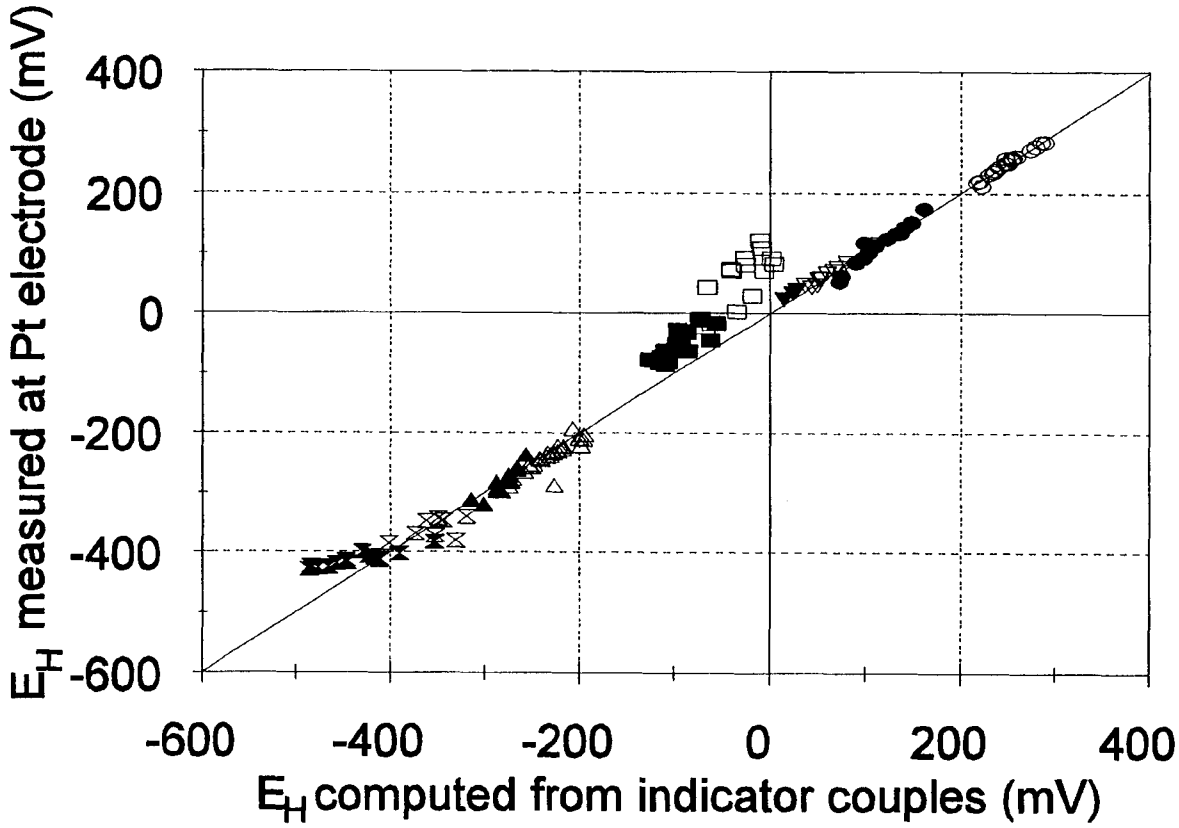

Figure 5.14 Comparison of observed E_H and computed E_H: ○=DCIP; ●=TB; ▽=THI; ▽=MB; □= ITESA; ■=IC; Δ=PSaf; ▲=SafO; ⧖=BV; ⧗=MV. The observed E_H is the potential measured at a Pt electrode. The computed E_H is determined by literature $E^{o'}$ values, the measured pH and the absorbance of the oxidized form of the indicator.

oxidation of Cr(III) by pyrolusite (21) showed that oxidation is very slow above pH 5; approximately 3 uM Cr(VI) produced in 400 hr. Birnessite has been shown to oxidize Cr(III) (22), although oxidation is not complete, even in the presence of excess birnessite. The reduction of Cr(VI) by siderite has not been previously investigated. To study reactions with oxidizing minerals, the Cr(VI) and thionine were initially reduced with Fe(II).

In the siderite study, no reduction of Cr(VI) or thionine was observed in the time of the experiment (44 hr), even when the pH was decreased to 4.5. The E_H decreased 40 mV from the initial potential of 350 mV during the first 2 hr. After that time, the E_H gradually increased to 375 mV over the next 42 hr and never appeared poised.

No re-oxidation of Cr(III) or thionine by β-MnO_2 was observed in the 20-hr experiment. The E_H decreased from 375 mV to 65 mV after addition of Fe(II) solution to reduce the Cr(VI) and the indicator. At this time, the Pt electrode was poised by the thionine couple. There was also no increase in E_H in the 20-hr experiment.

Birnessite did re-oxidize 39% of the Cr in 44 hr at an observed rate of 3 μM/hr. Oxidation continued after 44 hr, but at a much slower rate (0.5 μM/hr). The rate of oxidation did not increase when the pH was lowered to 4. The initial E_H was about 375 mV, similar to other experiments. However, the E_H increased to 525 mV during the first hour before addition of Fe(II). The potential decreased to 470 mV when Fe(II) solution was added and continued to decrease slowly (30 mV in 42 hr), even though the Cr(III) was being re-oxidized.

The formal potential of the birnessite couple (equation 5.7) is 630 mV at pH 7 (23).

$$\delta\text{-}MnO_2(s) + 4H^+ + 2e^- \rightleftharpoons Mn^{2+} + 2H_2O \qquad (5.7)$$

The observed potentials suggest that the measured potential is a mixed potential. The E_H is not high enough to be due to the birnessite couple alone, but it is higher than expected when poised by thionine ($E^{o'}$ = 70 mV), and higher than observed previously in mineral and solution experiments. In addition, the E_H decreased when birnessite was reduced (Cr re-oxidized). It appears that even though the birnessite couple does not poise the electrode alone, the observed potential is affected by the mineral.

The $Cr(OH)_3(s)$ oxidation half reaction is:

$$Cr(OH)_3(s) + 2H_2O \rightleftharpoons CrO_4^{2-} + 5H^+ + 3e^- \qquad (5.8)$$

Since more protons are being produced by the oxidation of $Cr(OH)_3$ than are consumed by the reduction of birnessite, the pH should decrease slightly. The pH did decrease from 6.7 to 6.5 during the re-oxidation of Cr. Although the solid phase present after the reduction of Cr(III) is probably a mixed solid, $(Fe,Cr)(OH)_3$ (24), the proton production would still occur. Overall, it is clear that kinetics of redox reactions with the minerals studied is quite slow and only with longer time studies might changes similar to those reported in the literature be observed.

During the birnessite experiment at pH 7, the indicator adsorbed on the surface of the mineral as expected (pH of zero point charge of 2.3 (22)) which

precluded spectrophotometric measurements of the indicator to determine speciation. This adsorption led to the immobilization of indicators on affinity chromatography gels discussed in the next section.

5.3.2 Immobilization of Indicators

The first question to be answered about the gel was whether or not the scatter of the solid particles would allow enough light to pass through to monitor the absorbance of the indicators. A background absorbance below 1 is desired to enable a significant absorbance due to the indicator (in general, spectrophotometric measurements should be made on solutions with an absorbance of 2 or lower (25)). The background absorbance (scatter) of the unreacted gel in a 1-mm path length cell is 0.5 - 0.8 over the wavelength range 375 - 820 nm (variation due to packing efficiency). (Below 300 nm the absorbance increases rapidly due to scattering.) This allows measurement of an indicator absorbance peak above the background. Clearly from Beer's law, cell path lengths greater than 1 mm cannot be used with the gel employed.

The amount of indicator immobilized must be controlled such that the absorbance of the indicator above the background is in a reasonable absorbance range. A net absorbance of at least 0.3 is desirable so that the absorbance can be measured with reasonable precision even when 90% of the indicator is reduced. The combined absorbance of the indicator and the gel should be below 2 to minimize nonlinearity.

In the coupling reaction (Figure 5.3), the formation of the imine is pH dependent with an optimum pH range of 3 - 4 (26). Because the pH of the coupling procedure can range from 3 to 10, the pH of the coupling buffer was varied to immobilize the amount of indicator necessary to achieve the desired absorbance. The optimum coupling pH for thionine (Thi) was found to be 5 - 6, resulting in a peak absorbance (above baseline) of typically 1 to 1.5 due to Thi (see Figure 5.15a). When the coupling pH was decreased below 5, too much indicator was immobilized (absorbance greater than 4). The optimum pH for phenosafranine (PSaf) coupling was 3 which resulted in a typical peak absorbance of about 1.5 due to the indicator (see Figure 5.15b). When PSaf was coupled at pH 7, the peak absorbance was only 0.1. Toluylene blue was immobilized in pH 7 buffer and had a peak absorbance of 0.4. Safranine O was not sufficiently immobilized in any of the buffers employed (no measurable peak at pH 7 and an absorbance less than 0.1 at pH 3). Further studies of immobilization of this indicator were not pursued.

Nile blue was found to be unsuitable for use in the packed cell. Although it coupled very well with the gel at pH 4, the pressure created by pumping aqueous solution through the packed cell was too great. Even with the amount of indicator immobilized decreased to give an absorbance of only 0.4, the pressure increased to 70 psi after 15 min. The macroflow beads will not crush until pressures over 100 psi are reached, but this pressure is too high for the pumps and the flow cell. One possible reason for this behavior is that the gel becomes more hydrophobic with immobilized nile blue compared to the other

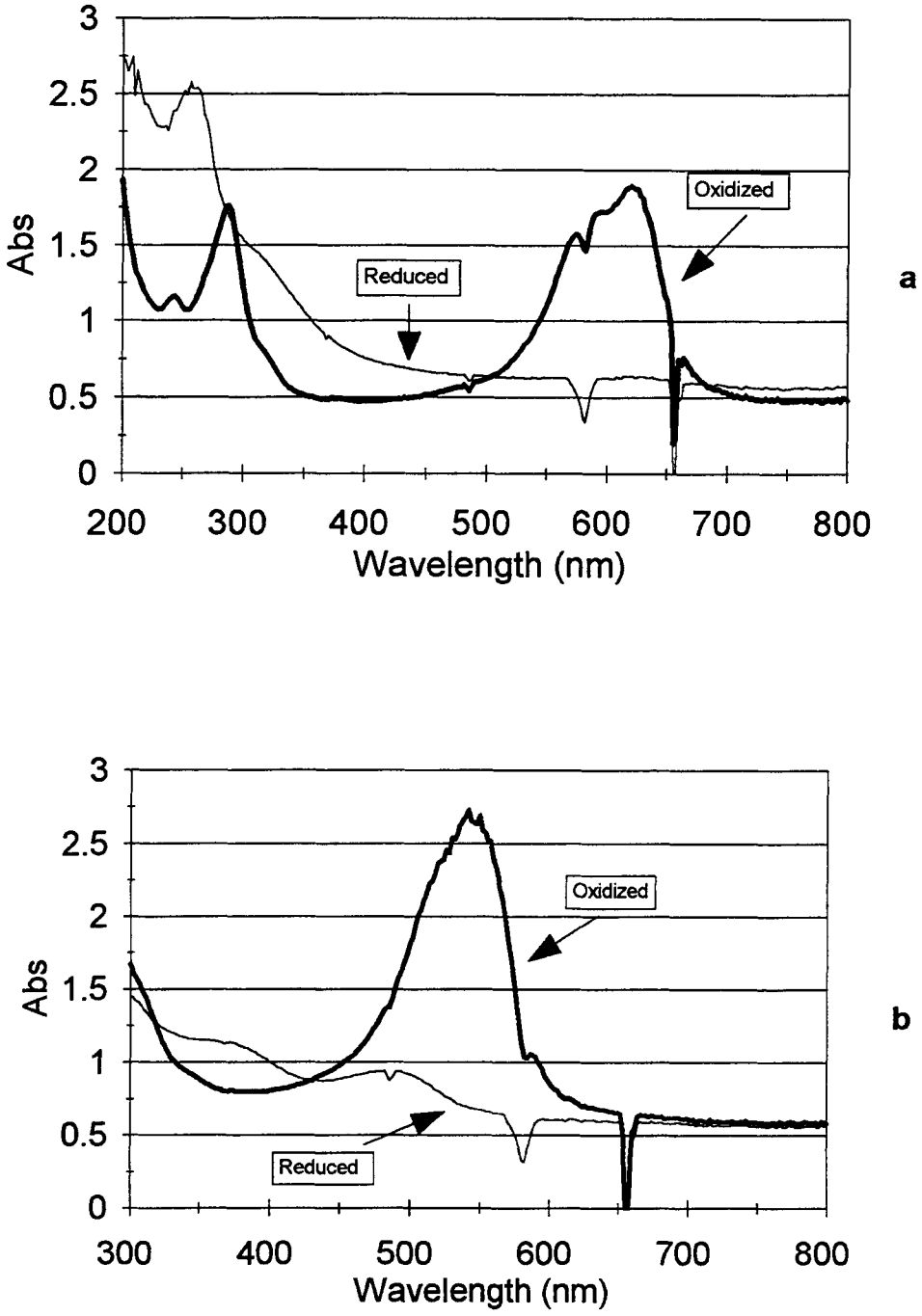

Figure 5.15 Absorption spectrum of immobilized indicators: (a) thionine; (b) phenosafranine

indicators, thus making it more difficult to push solution through the pores and interstitial channels. This difference is expected from the structure (see Figure 5.2). Compared to thionine and phenosafranine, nile blue has only one primary amine substituent; the second amine group is diethyl amine which is less hydrophilic than a primary amine. In addition, nile blue has four conjugated rings instead of three. A similar hydrophobic effect was observed in the solution studies; nile blue is the indicator that most strongly adsorbed to the reactor components of Delrin, glass and polyethylene.

Several attempts were made to decrease the high pressure. First, the immobilized gel was mixed 1:1 with unreacted gel, but the pressure was still above 60 psi. Methanol was pumped through the cell packed with immobilized nile blue to "wet" the gel prior to pumping water or buffer. The pressure with methanol remained below 10 psi but increased back to over 70 psi with buffer. A solution of the surfactant Triton X also had no effect on the pressure. Therefore, further experiments with immobilized nile blue were not considered.

Toluylene blue was found to be unstable both in solution and after immobilization. The oxidized form degrades to a non-reducible compound with a different absorption spectrum. Although toluylene blue is still redox active for several days in solution, it degrades to the non-reducible compound during the immobilization step and so is not useful.

The absorption spectra of the oxidized form of immobilized thionine and immobilized phenosafranine are shown in Figure 5.15. The absorption spectrum of the oxidized form of the immobilized indicators was shifted with respect to the

unbound indicators, however the spectra were very similar above 400 nm. Immobilization of Thi shifted the maximum absorbance from 598 to 640 nm, but the absorption peak shape was unchanged. Immobilization of PSaf resulted in a smaller change in the wavelength of maximum absorbance, from 520 to 544 nm, but the absorption peak was broader than the free PSaf. The small change in absorption spectra indicates that the electronic structure was only slightly changed.

The percentage of reactive sites on the gel that are "loaded" with the indicator was calculated for the immobilized Thi and PSaf. To estimate the effective concentration of indicator, it was assumed that the immobilized indicators had the same molar absorptivity as the free indicators. The concentration of immobilized indicator (c_i) was then calculated from

$$c_i = c_f \times \frac{A_i b_f}{A_f b_i} \tag{5.9}$$

where c_f is the concentration of free indicator in solution, A_f is the measured absorbance of free indicator in solution, A_i is the measured absorbance of the immobilized indicator in the packed cell, b_f is the path length of the solution cell (1 cm), and b_i is the path length of the packed cell (0.1 cm). The effective concentration of immobilized indicators was determined to be approximately 330 μM for PSaf and 170 μM for Thi. Because the concentration of monoaldehyde binding groups is reported to be 40-50 μmol/mL gel, PSaf and Thi are bound to less than 0.9% and 0.5% of the available immobilization sites, respectively.

The next experiments were conducted to verify the redox activity of the indicators that were successfully immobilized for use in the cell. Both

phenosafranine and thionine were still reversibly redox active after immobilization. The change in oxidation state was accompanied by a change in absorbance as seen in Figure 5.15.

Figure 5.16 illustrates the oxidation and reduction cycling of immobilized thionine. In this experiment, the oxidant (19.2 mM Cr(VI)) and reductant (~250 mM Ti(III)) were not added stoichiometrically. The volume of the second addition of Cr(VI) to the reactor was only one fourth the volume of the first addition. Since the oxidant concentration is less after the second addition, the oxidation of the indicator was slower and not complete as shown by the maximum absorbance reached (Figure 5.16). It took longer for a sufficient amount of oxidant to reach the indicator in the flow cell. The cycling in absorbance with redox cycling illustrates that the speciation of the indicator can be used to determine redox conditions for species that couple with the indicator.

Because immobilization of the indicators altered the structure, it was necessary to determine if the formal potential changed and if so, in which direction. As shown in Figure 5.8b, the Pt electrode was not poised until both forms of the free indicator were present. However, in the configuration used here (see Figure 5.5), the immobilized indicator is confined in the flow cell, completely isolated from the Pt electrode in the reactor. To solve this dilemma, free indicator was included in the system as well. The free indicator served to poise the Pt electrode and couple with the immobilized indicator. This arrangement allows the speciation of the immobilized indicator to be related to the measured potential.

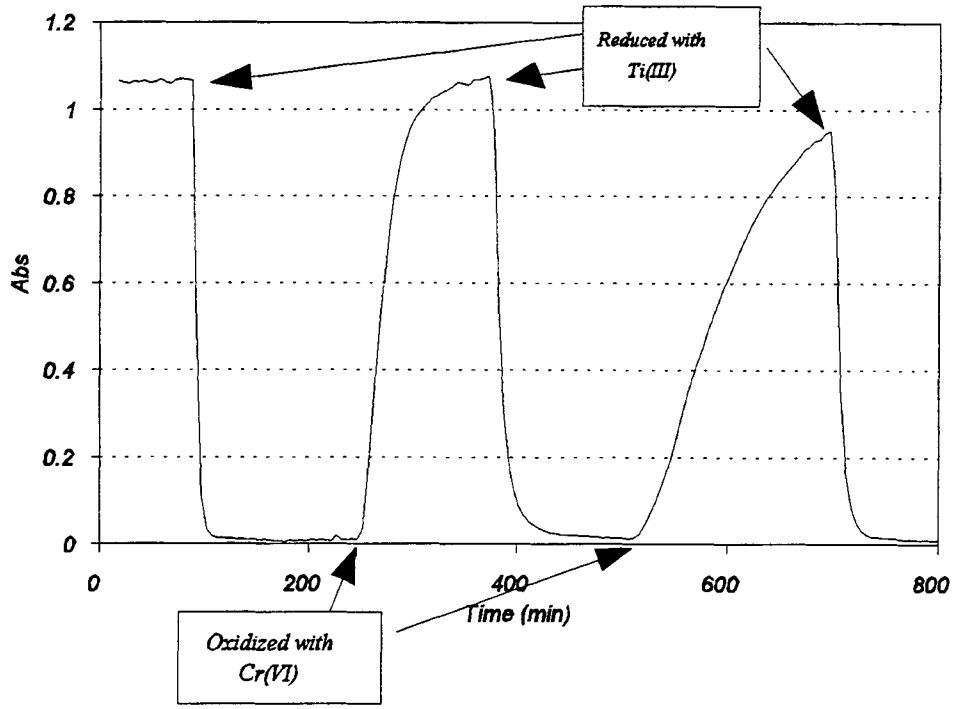

Figure 5.16 Redox cycling of immobilized thionine. The absorbance shown is corrected for the background of the gel by subtracting the absorbance at 790 nm.

The formal potentials ($E^{o'}$) for the free and immobilized indicators (Thi and PSaf) were determined in the following manner. The absorbance of the oxidized form of both the free (A_f) and the bound (immobilized) (A_b) indicator, the Pt electrode potential (E_H), and pH were measured. The measured absorbances (A_f and A_b), E_H, and pH were used to calculate the formal potential at the experimental pH for the free ($E_{m,f}$) and bound ($E_{m,b}$) indicator from equation 5.6. For the free and bound indicator, the determined E_m was then utilized to calculate the formal potential ($E^{o'}$) from equation 5.5. The calculated formal potentials for free and bound indicators are compared with the literature values in Table 5.4. The formal potentials of the free indicators are within 15 mV of literature values in agreement with the data presented earlier (Figure 5.14). For both indicators, immobilization results in a negative shift in the formal potential relative to the free indicator. However, the shift is only 14 mV for Thi and 19 mV for PSaf. The small change in formal potential is consistent with the slight change in the absorption spectra. Apparently, the electronic structure of the indicators is only slightly changed by immobilization on the gel.

5.3.3 Characterization of Oxygen Response

Experiments were conducted to determine how fast the Pt electrode, DO probe, and reduced thionine responded to oxygen introduced into the N_2 purge gas. Figure 5.17 shows the monitored parameters during a typical experiment as the E_H was increased in steps to 70, 85 and 100 mV. The O_2 flow was

Table 5.4 Formal potential for bound (immobilized) indicators.

	[1]Literature $E^{o'}$	[2]Observed $E^{o'}$ free indicator	[2]Observed $E^{o'}$ bound indicator
Thionine	74 mV	66 mV	52 mV
Phenosafranine	-243 mV	-267 mV	-286 mV

[1]Based on literature constants (2) and measured pH.
[2]Based on measured E_H and indicator speciation.

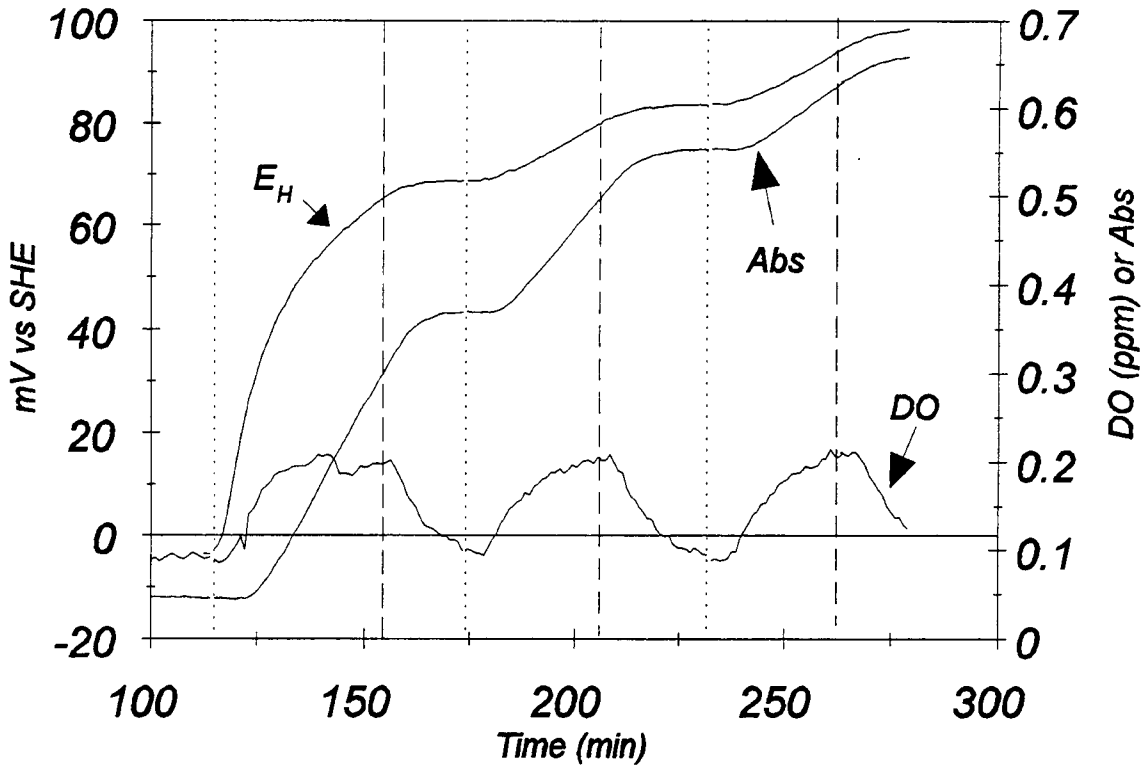

Figure 5.17 Monitored parameters during the determination of oxygen transfer efficiency from gas stream to solution. Thionine (13 μM) purged with N_2 (100 sccm) and reduced with Ti(III) (~8 μM) before addition of O_2 (0.49%) to gas stream. Dotted and dashed vertical lines indicate time where O_2 addition to the reactor was started and stopped, respectively.

automatically stopped when a given stat potential was reached, after which the measured DO decreased as the dissolved oxygen was swept out of the system by the continuing N_2 purge. Note that the DO levels approach 0.2 ppm which is the predicted DO in water in equilibrium with 0.5% O_2. The time necessary for the DO reading to reach a constant value is determined by the rate of O_2 transfer into solution, the consumption rate of O_2 by reduced thionine, and the response time of the DO probe. Other measurements with the DO probe (27) suggest that the response time of about 20 - 30 min observed in Figure 5.17 is primarily due to the response time of the DO probe.

The increase in the oxidized thionine concentration (absorbance) and the Pt electrode potential are correlated and continued until the majority of the oxygen was removed from solution. This again illustrates that the Pt electrode is poised by the thionine couple rather than the oxygen throughout this experiment (some reduced thionine remains at the end of the experiment). It appears that the maximum rate of oxidation occurs when the DO has reached its saturation value.

The delay in thionine oxidation during the first addition of oxygen is due to the presence of excess reducing agent at the beginning of the experiment. After this initial addition, the response time is similar for all three monitored parameters. Some of the delay in DO and absorbance response is due to the time for solution to flow from the reactor to the flow cells in the flow loop. (The flow rate is about 1 mL/min which would cause a delay of ~ 4 min.)

After each E_H step, the rate of absorbance increase was determined from a linear portion of the graph. This rate was utilized to calculate the rate of Thi oxidation in mol/min from

$$v(ox) = \frac{c_i A_{rate}}{A_i} \tag{5.10}$$

where c_i is the initial concentration of Thi, A_i is the initial absorbance of Thi (before reduction), and A_{rate} is the rate of increase in absorbance (A.U./min).

For three runs, the average rates of oxidation of thionine were 0.19, 0.12, and 0.069 μM/min at E_H values of 70, 80-85, and 90-100 mV, respectively. The rate of oxidation of reduced thionine is expected to be given by

$$v(ox) = k[thionine_{red}][O_2] \tag{5.11}$$

where k is the second order rate constant. Hence, the decrease in v(ox) with increasing E_H may be due to a decrease in the concentration of the reduced form of thionine.

When no oxygen is added to the N_2 purge stream, oxygen can still enter the system due to residual O_2 in the purified N_2 or an oxygen leak in the external loop or reactor lid. An increase in absorbance due to the formation of the oxidized indicator when no O_2 is included in the N_2 stream signifies oxygen is entering the reactor. Such increases were noticed in early experiments when short sections of Teflon tubing were used in the flow loop at the inlet and outlet of the spectrophotometer flow cell.

An oxygen leak can be quantified by the rate of increase in the concentration of the oxidized form of the indicator. In Figure 5.10c for example, the increases in absorbance after 300 min have slopes of 1.97 and 3.16

A.U./min which correspond to an increase in oxidized safranine O of 59 - 94 μM/min or 0.49 - 0.78 μM O_2/hr. In later experiments there were no noticeable oxygen leaks as shown in Figures 5.12 and 5.13. Overall, monitoring a reduced indicator provides an easy means to check the integrity of the connections in the external loop.

5.4 Conclusions

The approach of utilizing E_H as a master variable in complex environmental systems to determine the speciation of redox active components is not practical because many components do not couple with the Pt electrode nor with each other. However, the results presented here demonstrate that many redox indicators in solution couple with the Pt electrode and that the absorbance of the colored form of an indicator can be used to determine its redox state. Therefore, the indicator absorbance (speciation) can be used to predict the redox state of certain species of an environmental system if the species couple with the indicator with kinetics on the same time scale of the experiment.

The indicators studied encompass the potential range from -450 to 300 mV, except for a gap of about 100 mV at -150 mV. Figure 5.18 shows where transformations of indicators occur in relation to many environmentally relevant couples. Because the formal potential of phenosafranine and safranine O are below the E_H for methane production, the indicators with formal potentials more negative than -250 mV (benzyl viologen and methyl viologen) are probably not necessary. Because there are some environmental couples with formal potentials in the gap between indigo carmine and phenosafranine (E_H of -100 to -200 mV), it would be advantageous to find an indicator that would cover this potential range.

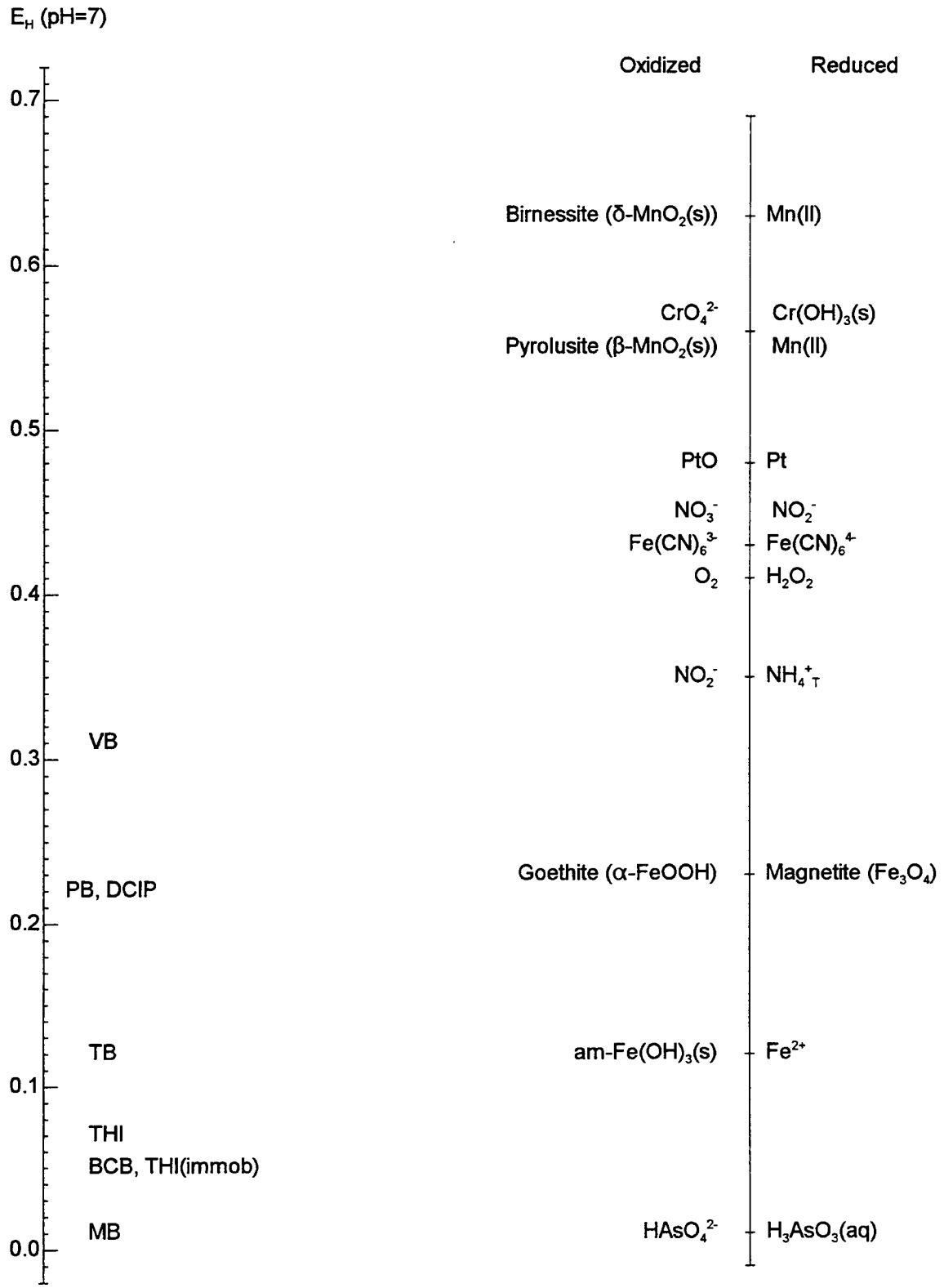

Figure 5.18 Potential scale showing location of redox indicators and important couples (9). Fe(II) and Mn(II) concentration assumed to be 10 μM.

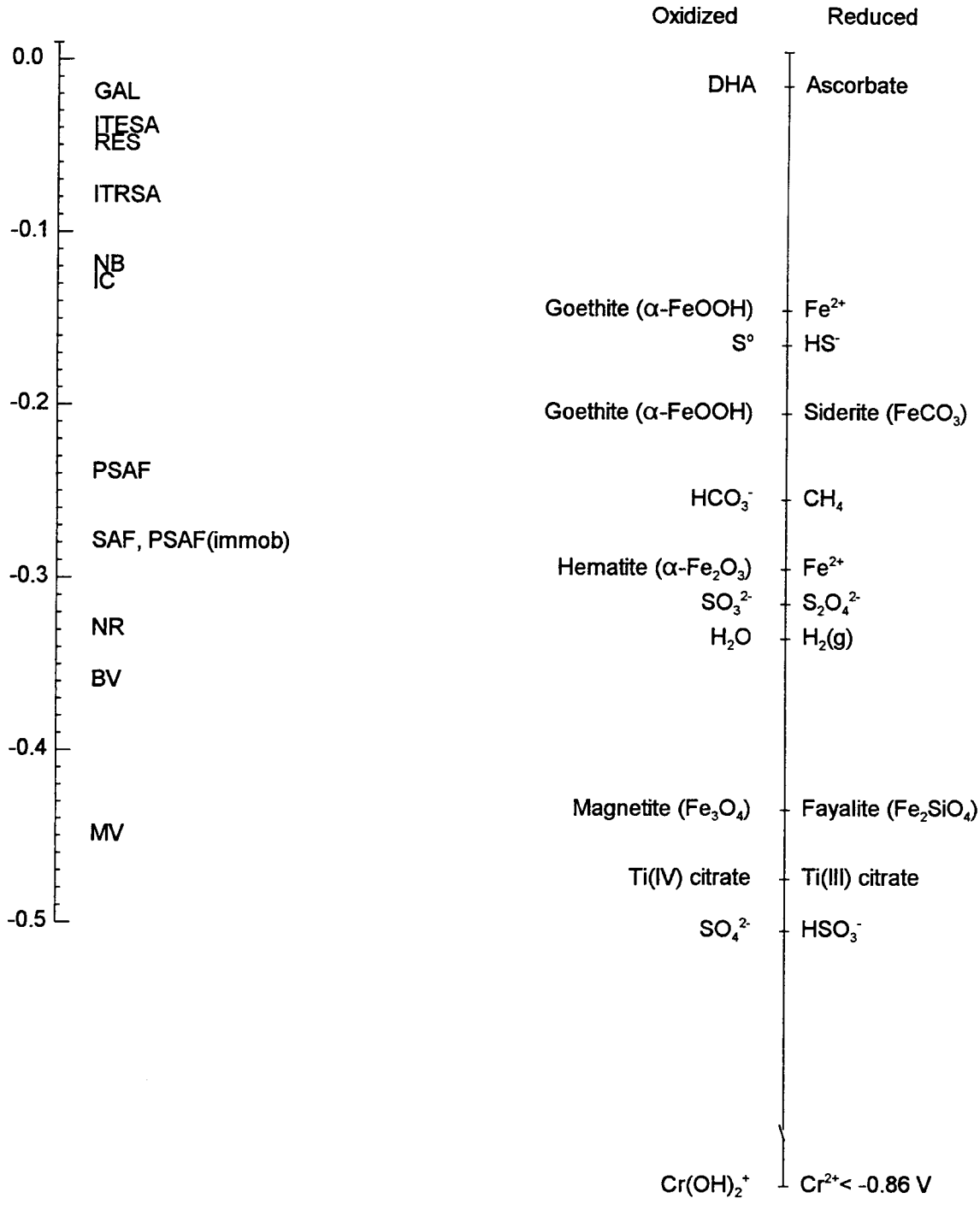

Figure 5.18 continued.

The studies of dissolved indicators also suggest that the indicators can be utilized to predict the prevalent forms of Fe and Cr present. For example, if an indicator that couples with Fe(II) (e.g., dichloroindophenol, methylene blue and thionine) remains oxidized, there is no soluble Fe(II) present (i.e., much less than the indicator concentration). Also, because all the reduced indicators couple with Cr(VI), if the indicator is reduced by the matrix, any chromium present must already be reduced. Even though these results illustrate the usefulness of indicators in solutions, adsorption of the indicators on the surfaces of solids precludes the use of indicators in most practical situations. Previous studies utilizing negatively charged indicators to minimize adsorption to sediments (5) were conducted with higher indicator concentrations (50 μM). When dichloroindophenol (DCIP) and indigo tetrasulfonic acid (ITESA) were added to sediment slurries at concentrations similar to those in the solution studies (5 μM), all the DCIP and most of the ITESA was adsorbed.

Two of the indicators tested in solution experiments, thionine and phenosafranine, were successfully immobilized on an affinity chromatography gel ($E^{o'}$ = 52 mV Thi_{immob}; $E^{o'}$ = -286 mV $PSaf_{immob}$) and were shown to be redox active and to couple with solution redox reagents. The immobilized indicators have an effective potential range of about 80 mV ($E^{o'}$ ± 38 mV) to change from 95% oxidized to 95% reduced (4). It was demonstrated that the immobilized indicators can be packed in a flow cell and monitored spectrophotometrically to determine their speciation. The electronic structure and electrochemical behavior of the indicators were only slightly affected by immobilization on the

gel. For both indicators, immobilization caused the formal potential to decrease (15 - 20 mV) and absorption spectrum to shift to higher wavelengths (20 - 40 nm) with respect to the free (unbound) indicators. These immobilized redox indicators should be useful for studying the redox characteristics of geochemical matrices in which adsorption of free indicators on solids would preclude their use. More immobilized indicators are needed to cover the environmental range (+400 to -300 mV).

There are two notable differences between the free indicators and bound indicators, the types of interactions allowed and the amount of indicator needed to study the system. The immobilized indicators can only interact with dissolved species in the present configuration. Therefore, the immobilized indicators can not take part in surface adsorption/desorption and redox reactions while the free indicators can experience such interactions. Also, a finite time is needed for the reductant or oxidant to reach the indicator in the flow loop as determined by the flow rate and the volume of the loop. However, the response time is probably more limited by redox kinetics and diffusion into the gel pores than by solution flow. Eventually, the immobilized indicators could be affixed to a fiber optic and included in the reactor which would eliminate the flow loop delay time and the need for a filter.

With either the free or immobilized indicator, it is important to consider the amount of indicator used to study the system. The amount of indicator utilized should be small compared to the amount of environmental couples present. The indicator itself should not affect the redox equilibria of the system. In order to

monitor the absorbance of the free indicators, concentrations between 5 and 33 μM were utilized, which are comparable to the concentrations of other species (oxidants and reductants). While the concentration of immobilized indicator in the spectrophotometric cell is higher than free indicator (170 μM compared to 5 μM), the volume of the cell is almost four orders of magnitude smaller than the volume of the reactor solution (60 μL compared to 1 L) resulting in less overall indicator (10 nmol compared to 6 μmol). Therefore, even though the concentration of immobilized indicator is higher than the free indicators for monitoring purposes, the total amount added to the system is lower. For calculations however, the total amount of oxidant or reductant delivered to the flow cell needs to be considered rather than the concentration in solution. For practical use, the flow loop should have a flow rate as fast as possible without leading to pressure problems, and a small volume to allow solution to reach the cell in a few minutes.

The percentage of available binding sites utilized to immobilize the indicators (0.5 - 0.9%) suggest that much higher loading could be achieved. If the loading is increased, the path length could be decreased. Conceivably, the path length could be decreased to the particle diameter (≈ 50 μm) if the indicator is immobilized on 10 - 20% of the available reaction sites. Indicators in this form are clearly a precursor for methodology that can be used in the field and ultimately combined with a fiber optic to develop a sensor.

The ability to utilize a reduced indicator to quantify the rate of oxygen addition to the system (either in the gas purge or in the flow loop) is also

significant. These results suggest the possibility of an oxygen sensor based on reduced immobilized indicators.

5.5 References

1. Clark, W. Mansfield *Oxidation-Reduction Potentials of Organic Systems*; Williams & Wilkins Company: Baltimore, 1960.

2. *Indicators*, Bishop, E., Ed., Pergamon Press: Oxford, 1972.

3. ZoBell, Claude E. *Bull. Am. Assoc. Petroleum. Geol.*, **1946**, *30*, 477.

4. Jacob, H. E. *Methods in Microbiology*, Norris, J. R.; Ribbons, D. W., Eds., Academic Press, Inc.: New York, 1970.

5. Tratnyek, Paul G.; Wolfe, N. Lee, *Environ, Toxicol. Chem.*, **1990**, *9*, 289.

6. McBride, Murray B. *Environmental Chemistry of Soils*; Oxford University Press: New York, 1994.

7. Hesse, P. R. *A Textbook of Soil Chemical Analysis*; Chemical Publishing Co., Inc.: New York, 1971.

8. Lindberg, R. D.; Runnells, D. D. *Science*, **1984**, *225*, 925.

9. Mobley, James; Oregon State University, unpublished report, **1992.**

10. Couch, Tara; Oregon State University, unpublished data, **1991**.

11. Sposito, Garrison *The Chemistry of Soils*, Oxford University Press: New York, 1989.

12. McKenzie, R. *Mineralogical Magazine*, **1971**, *38*, 493.

13. Zehnder, A. J. B.; Wuhrmann, Karl *Science*, **1976**, *194*, 1165.

14. Barteltt, Richmond; James, Bruce *J. Environ Qual*, **1979**, *8*, 31.

15. *Data Instructions, References, Reorder Information, for Spectra/Gel ® MAS Beads*, Spectrum: Houston.

16. Patai, Saul *The Chemistry of Acyl Halides*; Interscience: London, 1972.

17. Gleicher, G. J.; Private communication; Oregon State University, 1993.

18. *Organic Reactions, Volume 12*, Adams, R.; Blatt, A. H.; Boekelheide, V.; Cairns, T. L.; Cope, A. C.; Curtin, D. Y.; Niemann, C, Eds., John Wiley & Sons, Inc.: New York, 1962.

19. Sheehan, John C.; Hess, George P. *J. Am. Chem. Soc.*, **1955**, *77*, 1067.

20. Green, Floyd J. *The Sigma Aldrich Handbook of Stains, Dyes and Indicators*; Aldrich Chemical Company, Inc.: Milwaukee, WI, 1990.

21. Eary, L. Edmond; Rai, Dhanpat *Environ. Sci. Tech*, **1987**, *21*, 1187.

22. Fendorf, Scott E.; Zasoski, Robert J. *Environ. Sci. Tech.*, **1992**, *26*, 79.

23. Westall, John C.; Private communication; Oregon State University, 1993.

24. Sass, Bruce; Rai, Dhanpat *Inorg. Chem.*, **1987**, *26*, 2228.

25. Ingle, James D. Jr.; Crouch, Stanley R.; *Spectrochemical Analysis*; Prentice Hall: Englewood Cliffs, New Jersey, 1988.

26. Fessenden and Fessenden, *Organic Chemistry, 3rd Edition*; Brooks/Cole Publishing Company: Monterey, CA, 1986.

27. Jones, Brian D.; Private communication; Oregon State University, 1995.

Chapter 6
Redox Characterization of Soil

Teresa L. Lemmon and James D. Ingle Jr.*

Department of Chemistry
Oregon State University
Corvallis, OR 97331

6.1 Introduction

The redox status of soils affects the chemical speciation of many metal ions and thus their solubility, mobility and toxicity. For example, Cr(VI) is generally very soluble and highly toxic, whereas Cr(III) is very insoluble and not very toxic (1). (A review of Cr reactions in the environment is included in Appendix D.) Other priority pollutants that can exist in more than one oxidation state include As, Se, Ag, Cu, Hg, Sb and Tl.

The most common method of determining the redox status of a system is to measure oxidation-reduction (redox) potential with a Pt electrode (E_H). However, there are several problems with this approach. First, many environmental redox reactions do not reach equilibrium or couple with each other. Several redox couples may affect the measured potential such that it is a mixed potential. Finally, many redox reactions do not couple with the electrode surface (2). For these reasons, the potential measured at a Pt electrode cannot normally be used in thermodynamic equations to determine the solution speciation of redox-active components.

It is well known that microbiological activity in soils causes significant changes in the redox condition. The oxidation of organic carbon by aerobic and anaerobic organisms is accompanied by the reduction of a suitable electron acceptor. Generally, the most important electron acceptor is O_2 due to its ease of reduction, availability and diffusivity in soils (3). When a soil becomes flooded, the transport rate of O_2 in the soil decreases by as much as 5 orders of

magnitude. Aerobic activity rapidly depletes the residual O_2 that is soluble in water. At this time, the biological activity becomes anaerobic, and organisms capable of utilizing other inorganic electron acceptors, which are lower in free energy, become active. The reduction of inorganic components can occur through either direct or indirect reactions with the ultimate electron acceptor (2); not all reductions are directly caused by microorganisms.

Once a soil becomes waterlogged and the residual O_2 is consumed, a decrease in E_H and increase in pH is observed. Most reduction reactions consume H^+ (2, 4) as shown below:

$$O_2 + 4H^+ + 4e^- \rightleftharpoons 2H_2O \quad (6.1)$$

$$NO_3^- + 2H^+ + 2e^- \rightleftharpoons NO_2^- + H_2O \quad (6.2)$$

$$Fe(OH)_3\,(s) + 3H^+ + e^- \rightleftharpoons Fe^{2+} + 3H_2O \quad (6.3)$$

If the soil dries out and becomes aerated, the reactions 6.2 and 6.3 occur in the reverse direction, leading to more oxidizing conditions and subsequent production of H^+.

After reduction of O_2, the following electron acceptors are reduced sequentially; NO_3^-, Mn(IV) mineral solids, Fe(III) mineral solids, SO_4^{2-}, and CO_2 (3). Patrick and co-workers have conducted several studies to determine the E_H where transformations of these components and several redox-active elements (i.e., Cr, Se, As) begin to occur (3, 5 - 12). These studies confirm that the reaction order is sequential in both the oxidized to reduced half-cycle and the reduced to oxidized half-cycle (3).

To study redox transformations under specific E_H and pH conditions, a feedback-controlled reactor system is useful. Because most of the important redox reactions also involve H^+ as mentioned above, the reactions are affected by pH as well as E_H. Therefore, both the pH and E_H must be carefully controlled throughout each experiment.

A reactor system, similar to those described by Patrick (13, 14), was developed in this laboratory that allows control of pH and E_H. In addition, some of the solution is pumped from the reactor through an on-line spectrophotometric flow cell which contains an immobilized redox indicator. The change in absorbance of the immobilized indicator provides a unique method of measuring reducing or oxidizing conditions in addition to the Pt electrode. The purpose of this study was to determine the relationship between the measured E_H, the solution composition ($[Fe^{2+}]$, $[Mn^{2+}]$, $[PO_4^{3-}]$) and the speciation of the immobilized redox indicator.

6.2 Experimental

6.2.1 Instrumentation

The studies were carried out in an air-tight reactor system (see Figure 6.1) consisting of a 2-L glass bioreactor, stirrer, pH electrode, reference electrode, Pt electrode, dissolved oxygen (DO) probe, dispensing pumps, gas control system, and a personal computer (PC). This reactor system is discussed in detail in Chapter 4 and is briefly reviewed here. The electrodes, dispensing pumps, and solenoid valve are interfaced to the PC. The electrodes are used to monitor the pH, E_H, and dissolved oxygen concentration. The pumps add accurately small volumes of reagent (acid, base, oxidant or reductant) in response to the monitored pH or Pt electrode potential. They are used to change or maintain a selected experimental condition. The gas flow control system is used to purge the reactor with N_2 or a mixture of N_2 and O_2. The solenoid valve allows a controlled amount of O_2 to be mixed with the N_2 and bubbled in the reactor. There are two flow loops included in the system. The primary loop (A) contains a peristaltic pump and cross-flow filter which provide a filtered sample for the secondary loop. The secondary loop (B) includes a piston pump, DO probe in a flow cell, the spectrophotometer flow cell packed with the immobilized redox indicator thionine, and a 3-way valve for obtaining filtered samples for external analysis. A spectrophotometer (HP8452A diode array) is included to monitor the absorption spectra.

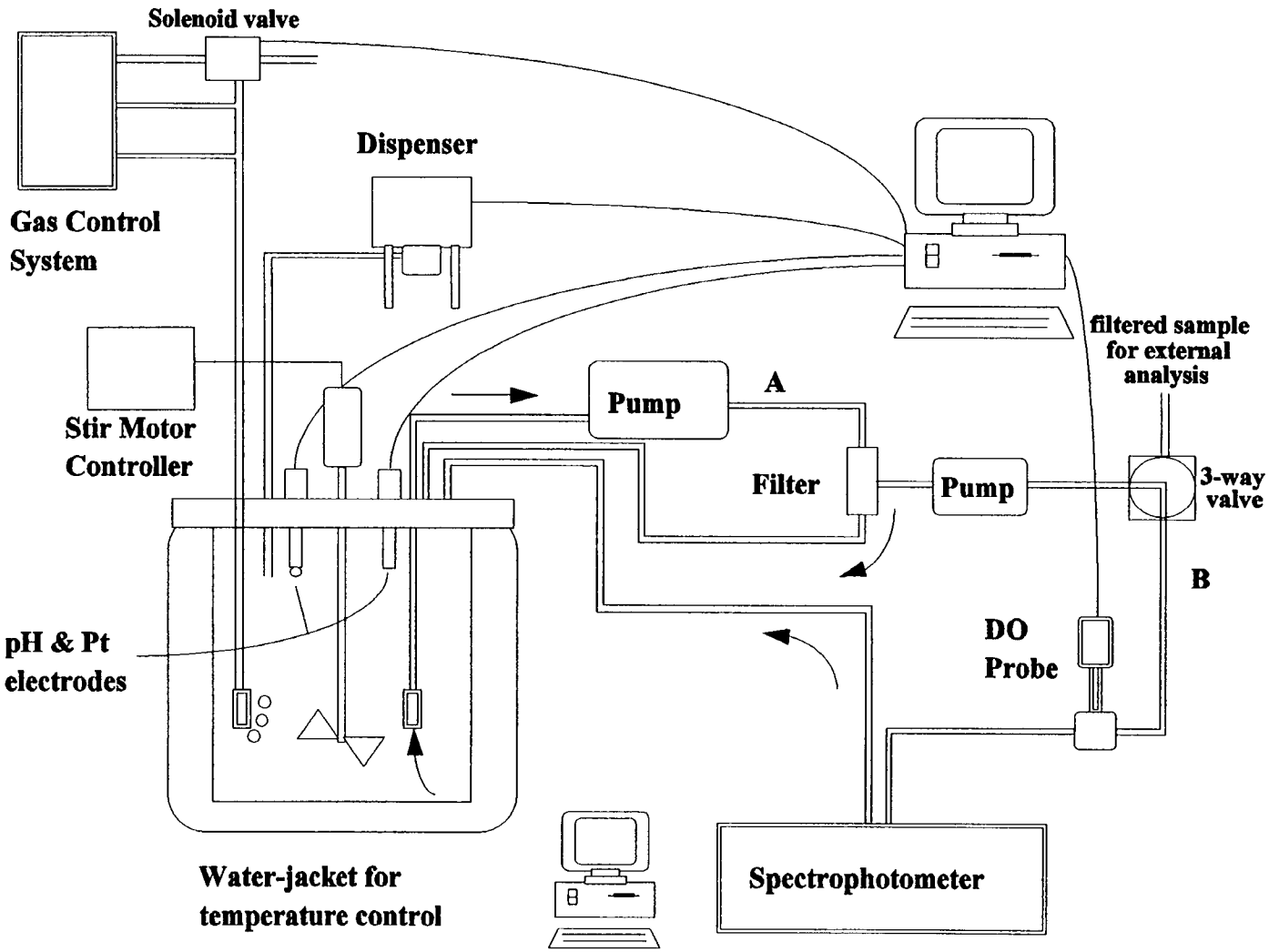

Figure 6.1 Schematic of reactor system. Arrows indicate direction of flow.

6.2.2 Soil Samples

Three different types of soil were studied (Aloha BC, Aloha A1, and Bashaw A1). Two experiments were conducted with the Aloha A1 soil. The soil samples were previously collected and thoroughly characterized as part of the Oregon Wet Soils Project by the National Resource Conservation Service (15). They are soils that were subjected to seasonal flooding and redox cycling. The three soil experiments conducted in the reactor were with two horizons of Aloha soil (A1 and BC) and one horizon of Bashaw soil (A1). The soil characteristics reported below were determined by the National Resource Conservation Service (15).

The Aloha soil samples were obtained by John Baham from Washington county, Oregon. Aloha BC soil (142-165 cm) is a dark brown silty clay loam soil with many fine, medium, and coarse distinct mottles (15). The structural grade is weak coarse prismatic with a firm, sticky, plastic consistency; few fine roots throughout and many fine tubular pores; few discontinuous distinct manganese or iron-manganese coats on faces of peds. The soil pH in water is 6.5. The soil is 21.9% (w/w) clay with an organic carbon content of 0.08% (w/w). The measured dithionite-citrate extractable Fe and Mn are 1.9 and 0.1%, respectively. The oxalate extractable Fe is 0.49% (w/w).

The Aloha A1 soil (0-6 cm) is described (15) as dark brown silt loam with moderate to medium granular structure. It has a friable, sticky, slightly plastic consistency and many fine roots throughout. There are many medium interstitial

pores and a few fine rounded iron-manganese concretions. The soil is 17% (w/w) clay, 4.36% (w/w) organic carbon, and has a pH of 5.7. The dithionite-citrate extractable Fe and Mn are 1.8 and 0.2% (w/w), respectively while the oxalate extractable Fe is 0.71 (w/w)%.

The Bashaw A1 soil has a much higher clay content, 52% (w/w), and organic carbon content, 12.5% (w/w) (15), and was obtained by Brian Jones from the Jackson Frazer Wetland located just north of Corvallis, OR. It is a very dark, grayish brown mucky silt loam with few fine prominent strong brown mottles. The consistency is soft, very friable, nonsticky and nonplastic. Many fine and very fine roots are present and there are very fine interstitial pores. Dithionite-citrate extractable Fe and Mn were determined to be 1.7 and 0.2% (w/w), respectively. Oxalate extraction values were not reported.

The Aloha soils were prepared by Mark Bos. The soil was spread out on plastic sheets and allowed to dry at room temperature for 48 hr. Then, it was lightly crushed with a rolling pin and sieved to 2 mm. The Bashaw soil was prepared by Brian Jones. The sieved soil (< 2-mm fraction) was ground further and sieved once with 0.5-mm mesh and twice with 0.25-mm mesh.

The concentrations of some major ions in a solution equilibrated with the Aloha BC soil were determined by Mark Bos and John Baham (16) to be 0.384 mM Ca^{2+}, 0.192 mM Mg^{2+}, 0.575 mM Cl^-, 0.287 mM SO_4^{2-}. The supernatant was equilibrated with successive batches of fresh soil until pH and conductivity remained constant before the ion analysis. A solution, denoted "pore water", was prepared from $CaSO_4$, $CaCl_2$, $MgCl_2$ and $MgSO_4$ such that the

concentrations were double those measured in the equilibrated solution. Aloha BC soils samples were mixed with the pore water so that the ionic strength (4 mM) was comparable to that in the original soil solution and sufficient for accurate potentiometric measurements.

To study the Aloha BC soil, a slurry was prepared from 125 g of soil (< 2-mm fraction) and 1 L of the "pore water", yielding a soil:water ratio of 1:8 (w/w). This soil was very low in organic carbon, so 1.25 g of coarsely ground wheat straw (17) was added (1% w/w soil).

The first study of the Aloha A1 soil was conducted on a slurry similar to the Aloha BC soil slurry; 125 g of soil (< 2-mm fraction) and 1 L of the "pore water" (1:8 w/w soil:water). The slurry used in the second study of Aloha A1 soil was prepared from 125 g of soil (< 2-mm fraction) and 1.25 L DI water (1:10 w/w soil: water). The lower ratio of soil to water was selected to help decrease the filtering problems. Calcium chloride was added to a concentration of 10 mM (1.85 g) to adjust the ionic strength. It is often chosen by soil scientists to adjust the ionic strength, decrease the electric double layer, and induce flocculation.

The Bashaw A1 soil was studied in a slurry prepared from 50 g of soil and 1 L of DI water in 10 mM $CaCl_2$ (1:20 w/w soil:water). The higher clay content of the Bashaw soil was a concern because it was difficult to maintain the flow in the filter loop with clay soils. For this reason, the lower soil:water ratio was selected. Nitrogen was added as NH_4Cl (1 mL of a 2 M solution) at the beginning of the experiment to ensure the system did not become nitrogen deficient. The amount to be added was determined by estimating the amount of carbon that could be

utilized for cell growth and assuming a 1:7 ratio N:C for cell growth as shown below. An upper limit for the N consumption was made by assuming that 50% of organic carbon was available and 5% of the available carbon could be used for cell growth:

$$\text{mol N} = \text{g soil} \times \%C/100 \times 0.50 \times 0.05 \times 1 \text{ mol}/12 \text{ g C} \times 1/7 \qquad (6.4)$$

where %C is the w/w% soil as organic carbon.

6.2.3 Reactor Studies

To begin an experiment, the soil slurry was prepared in the reaction vessel and the reactor lid was put in position to seal the system. The glass and Pt electrodes were inserted in the electrode ports and the N_2 purge (50 cm^3/min) was initiated. Then, the flow loops were assembled (see Figure 6.1). Typical flow rates were 20 mL/min in the primary loop (A) and 0.8 mL/min in the secondary loop (B). The computer program was started to begin monitoring the pH, E_H (measured at the Pt electrode) and DO (for detailed experimental setup, see Appendix C). In some cases, the initial pH was adjusted before selecting the program "pH-stat". In all the experiments, the E_H-stat was not selected initially, but was utilized later in the experiment.

For the pH-stat, the acid and base are added with the computer-controlled dispensing pumps (25 µL/stroke). The solutions dispensed were 1.2 M HCl prepared from concentrated HCl, and 1.0 M NaOH prepared from standardized 2.0 M NaOH solution.

Two approaches were used to adjust and maintain the E_H to a selected level during an experiment. The first approach utilizes mass flow controllers and the computer-controlled solenoid valve in the O_2 line (see Figure 6.1) to control O_2 level in the N_2 purge gas. The valve switches to the "on" position when the E_H decreases below the set point, then switches to the "off" position when the E_H has returned to the selected level. The other approach to E_H control is similar to the approach to pH control. An oxidizing solution of H_2O_2 (0.05 to 0.2 M) is added with a computer-controlled dispensing pump (25 µL/stroke). The hydrogen peroxide solutions were prepared from 30% reagent grade H_2O_2 solution (Spectrum Chemical MFG. CORP.).

In later experiments, the speciation of immobilized thionine was monitored in a spectrophotometric flow cell (1-mm path length, Hellma 170.700-QS). The thionine is immobilized on affinity gel beads, which are "packed" in a flow cell. The immobilization procedure and the assembly and packing of the flow cell are discussed in Chapter 5.

In some experiments, a variety of carbon sources were added in an attempt to increase the microbial activity and decrease the measured potential. Nitrogen was added as NH_4NO_3 or NH_4Cl. Specific details are given later.

Ion chromatographic analyses were conducted in other laboratories: phosphate, John Baham, Soil Science; acetate, Sheryl Stuart, Civil Engineering; cations (K^+, Na^+, Mg^{2+}, Ca^{2+}) and anions (SO_4^{2-}, Cl^-), Mark Bos, Chemistry. Soluble Fe(II) was monitored spectrophotometrically with the diode array spectrophotometer using the standard 1,10-phenanthroline method (details in

Appendix B), and soluble Mn(II) was measured by atomic absorption spectrophotometry on a Buck Scientific 200 atomic absorption spectrophotometer. To verify that the Fe was indeed Fe(II) (not Fe(III) colloidal particles), colorimetric measurements were performed without the addition of hydroxylamine hydrochloride to reduce the Fe(III) and no increase in measured Fe concentration was observed. In addition, samples were occasionally collected in N_2-purged septum vials. Because the Fe concentrations in samples collected in this manner were similar to concentrations measured in samples collected in open vials, no oxidation of Fe(II) occurs during the sampling time.

6.3 Results and Discussion

6.3.1 Aloha BC soil

The general experimental plan for the Aloha BC soil was to allow the soil solution to naturally become anaerobic and reducing and to maintain the E_H at various levels with the oxygen E_H-stat as the soil became anaerobic and reducing. An experimental time line is given in Table 6.1. The record of the measured pH and Pt electrode potential is shown in Figure 6.2.

After a 2-hr equilibration with 20% O_2 in N_2, the pH and E_H were 5.7 and ~500 mV, respectively. At this time, the pH was adjusted to 6 with 1 M NaOH utilizing the "pH shift" program option and a dispensing pump (25 µL/stroke). However, the pH-stat was not initiated. After 62 hr, the pH had increased to 6.3. The pH was again adjusted to 6 and the pH-stat was activated with only acid addition (1.2 M HCl, 25 µL/stroke). The pH was only adjusted when it was more than 0.05 pH above the set point.

After 150 hr, the potential was still above 300 mV. To stimulate microbial activity and attain reducing conditions, aliquots (1 to 5 mL) of 1 M glucose (see Table 6.1) were added with a syringe through the septum port in the reactor lid. Addition of 1 mL of 1 M glucose solution to the reactor increases the carbon content by 6 mmol C (or 0.06% w C/w soil). After each glucose addition, the E_H decreased for some time and then increased. With each addition of glucose, more was needed to cause a similar decrease in E_H. Also, the duration of the

Table 6.1 Aloha BC soil experiment summary. Glucose solution is 1 M.

Time (hr)	Action	Comments
23	Stat E_H at 250 mV:20% O_2	gas stream will become 20% O_2 when E_H decreases below 250 mV
62	Change to pH 6, initiate acid-stat	select pH change option and pH stat with acid (1.2 M HCl)
95, 96	Add Ti (III): 50 µL, 50 µL	no observable decrease in E_H
166	Add 1 mL of glucose soln 6 mmol C (0.06% w C/w soil)	after addition, E_H and pH both decrease, O_2 added to reactor when E_H decreased below 250 mV
190	Manually add 1 M NaOH to pH 6	no base added to increase pH on production of acid
230	pH stat with acid and base	pH stat with 1.2 M HCl and 1.0 M NaOH utilizing two dispense pumps
238, 258	Add 1 mL of glucose soln	E_H stat is at 250 mV: adjust gas composition to 1, 2, 3, and 4% O_2
260	E_H stat to 100 mV	change E_H stat level to 100 mV
278, 280	Add 1 mL glucose soln	
287, 303	Add glucose soln: 1 mL, 2 mL	O_2 added to reactor when E_H decreased below 100 mV
308	Add 2 mL of glucose soln	change E_H stat level to 0 mV
311, 313	Add glucose soln: 3 mL, 5 mL	
326, 328	Add glucose soln: 1 mL, 3 mL	
406	Add 1.8 g glucose	equivalent to adding 10 mL of 1 M glucose solution

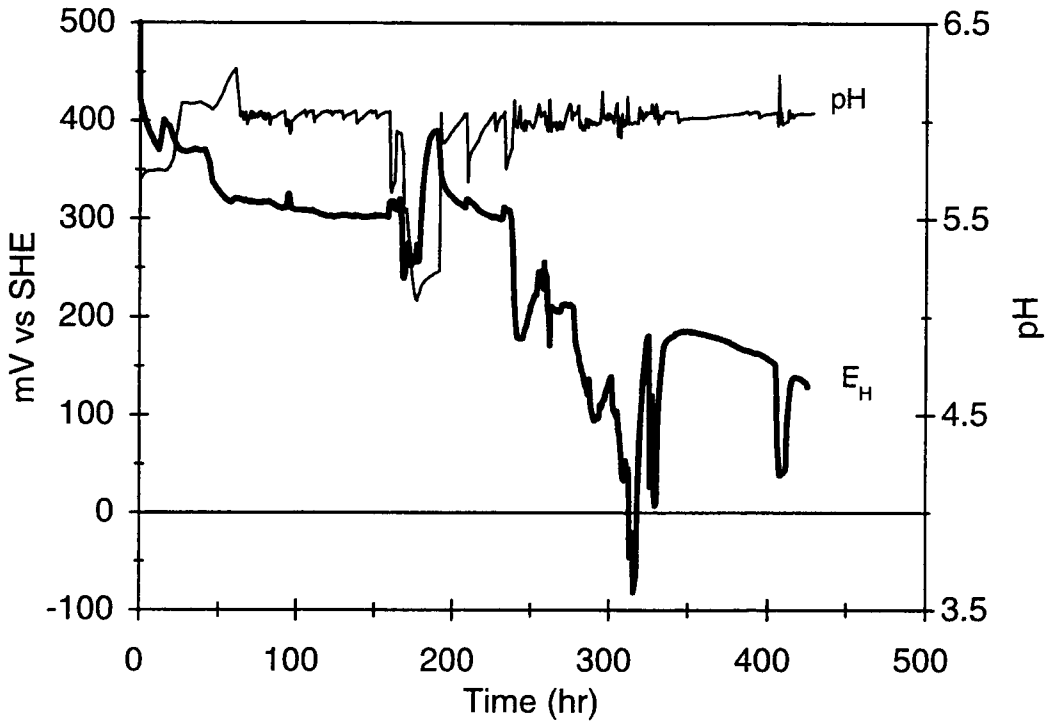

Figure 6.2 Potential measured at a Pt electrode and pH during the Aloha BC soil experiment. The ratio of soil:water in artificial pore water was 1:8.

effect shortened. Initially, with the addition of 1 mmol glucose, the E_H decreased for five or six hours before increasing again. At the end of the experiment, the E_H only decreased for 30 min with the addition of 10 mmol of glucose. The E_H-stat limited the E_H decrease to a particular level at several points in the experiment (e.g., 166, 238, 280, 320 hr). The E_H never decreased below 0 mV for more than 30 min and was greater than 100 mV for the majority of the experiment.

During the time period the E_H was lowered, the pH also tended to decrease and base was added to maintain the solution pH at 6.0. The pH decreased below 5.2 after the first addition of glucose because the pH-stat was configured to add only acid. The pH-stat configuration was then changed so either acid or base was added as needed. The observed decrease in pH is attributed to be due to the breakdown of glucose to organic acids. When the E_H began increasing, the pH increased and acid was added.

The amount of base added during the experiment tracked the amount of glucose added (see Figure 6.3). A total of 32 mmol of glucose were added to the reactor (1.8 % w C/w soil). The final concentration of acetate in solution was determined to be approximately 30 mM suggesting that the majority of glucose added was converted to acetic acid.

This experiment provided the first evaluation of the pH control, E_H control by addition of oxygen, and the filtering system with a soil sample. The oxygen E_H stat addition worked well, although the level of O_2 in the gas stream must be decreased from 20% to 1-4% to minimize the oscillations about the set point as

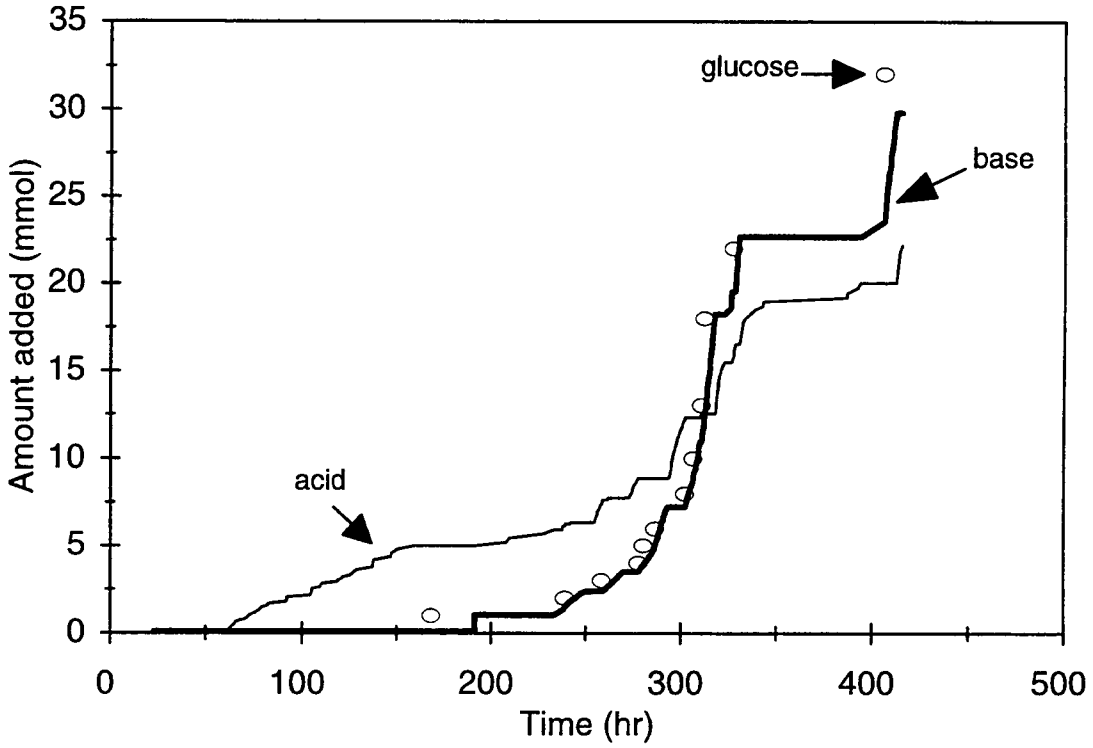

Figure 6.3 Total amount of acid, base and glucose added to the reactor during the Aloha BC soil experiment. The ratio of soil:water in artificial pore water was 1:8.

the E_H decreases. However, the oxygen content is easily adjusted with the gas flow controllers.

There were many problems with the flow loops and the cross-flow filter which became plugged after only a few minutes. The cylindrically shaped pieces of straw caused much of the difficulty. These pieces were able to enter the tubing easily, but became obstructions in the corners in the filter module. Many modifications were made which eventually led to the final configuration described in Chapter 4. Due to these problems, the flow loop was never used to make measurements.

Because the E_H did not go to a low enough value, it was decided to use a surface soil with higher organic carbon content.

6.3.2 Aloha A1 soil

6.3.2.1 First Experiment

In the first experiment with the Aloha A1 soil (Aloha A1 #1), the soil:pore water ratio was 1:8. Because the carbon content of this soil is higher, and the straw was the source of many of the filtering problems, no straw was added. The oxygen E_H stat was employed to maintain the E_H at various levels as the potential decreased. The solution concentration of Fe(II) and Mn(II) were measured at different E_H set points. Toward the end of this experiment, the measured E_H was then increased at separate times with either O_2 or H_2O_2 to test

and compare control with different oxidants. The pH was maintained at 6, which was near the initial pH of 5.97. The variation of the potential measured at the platinum electrode and the pH during the experiment is shown in Figures 6.4 and 6.5. Table 6.2 summarizes the reagent additions and E_H set points during the experiment.

During the first portion of the experiment (see Figure 6.4), the E_H decreased from 450 to -100 mV in about 300 hr. During this decrease, the oxygen E_H-stat was implemented at 250 mV to maintain the E_H at this level for several hours. This procedure was repeated when the potential reached 100 mV and -50 mV. When the E_H decrease slowed (130 hr), 1 mL of 1 M NH_4NO_3 was added manually with a syringe through the septum port in the reactor lid. This resulted in an increase in E_H for over 20 hr while apparently the nitrate was reduced. The E_H decreased slowly to -100 mV after another 80 hr.

In the second portion of the experiment (see Figure 6.5), O_2 was added to increase and maintain the measured potential at -50 mV (3 hr) at 2%, 50 mV (4 hr) at 5% and 100 mV (6 hr) at 7%. Finally, hydrogen peroxide (0.05 M, 25 µL/stroke) was added every 5 min to increase and maintain the potential at 0 mV (6 hr) and 100 mV (5 hr). As shown in Figure 6.5, the Pt electrode potential increased rapidly to the set point when O_2 or H_2O_2 was added and decreased as soon as the E_H-stat mode was terminated. A time interval of about 1.5 hr was required for the E_H to decrease half way to the natural E_H after the addition of O_2 was stopped (a, b, and c in Figure 6.5). When the addition of H_2O_2 was stopped,

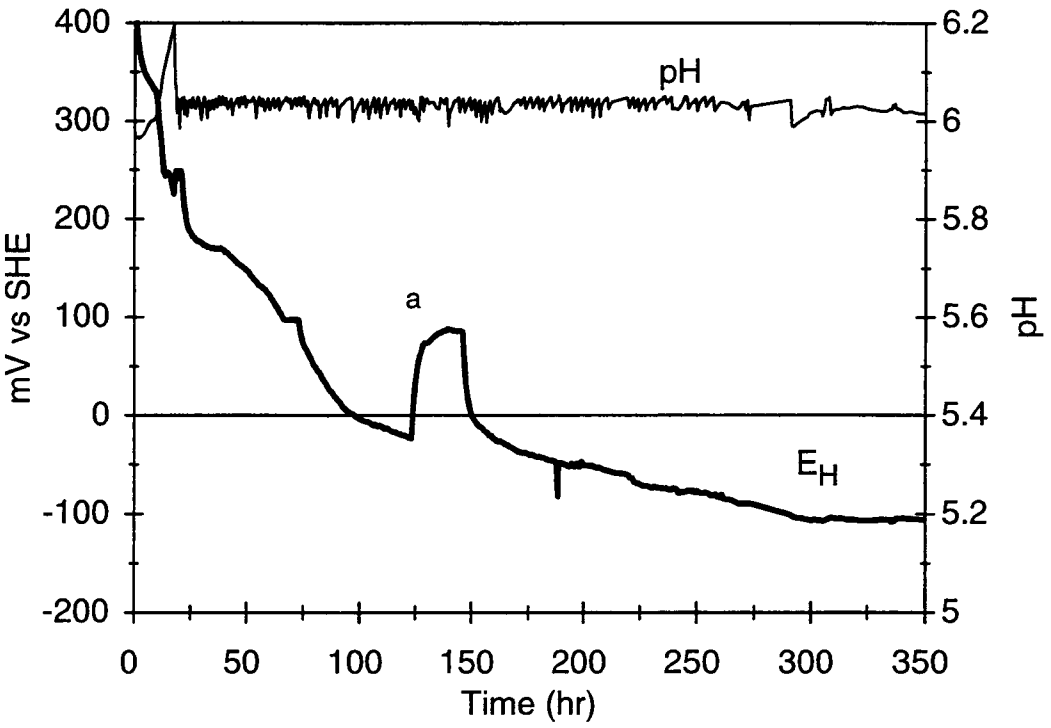

Figure 6.4 Pt electrode potential and pH during first 350 hr of the Aloha A1 #1 experiment. At (a), NH_4NO_3 was added. The ratio of soil:water in artificial pore water was 1:8.

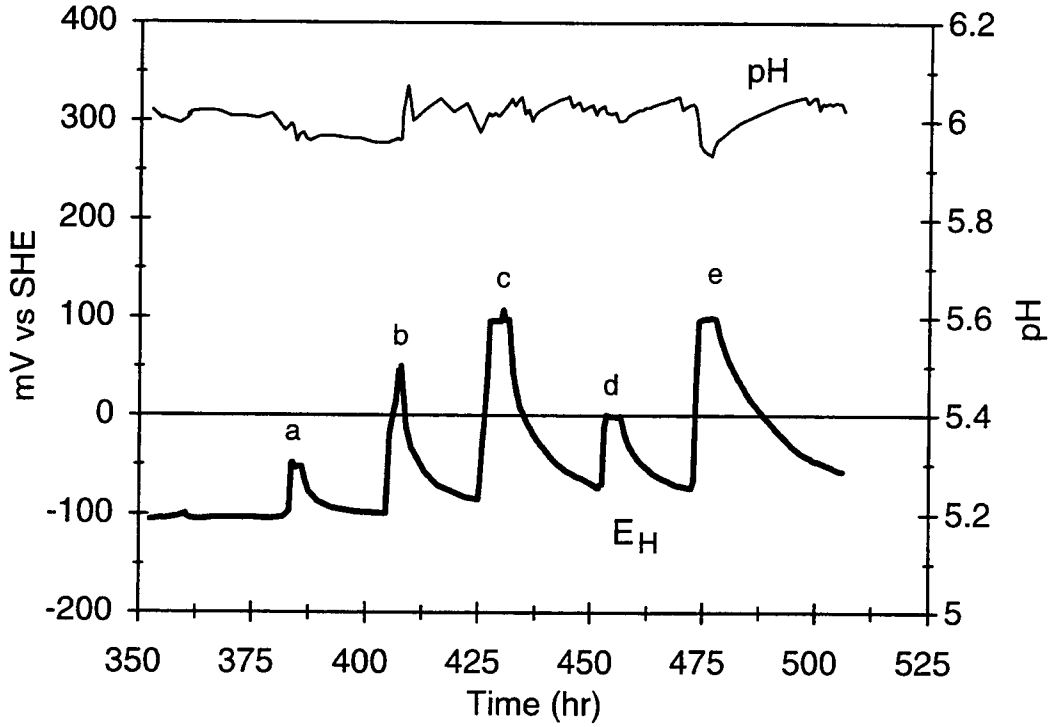

Figure 6.5 Pt electrode potential and pH during the last 150 hr of the Aloha A1 #1 experiment. The ratio of soil:water in artificial pore water was 1:8; (a) E_H stat to -50 mV with O_2; (b) E_H stat to 50 mV with O_2; (c) E_H stat to 100 mV with O_2; (d) E_H stat to 0 mV with H_2O_2; (e) E_H stat to 100 mV with H_2O_2.

Table 6.2 Summary of Aloha Al #1 soil experiment.

Time (hr)	Action	Comments
0	Stat pH to 6	select stat program to add acid and base as needed
2.5	Initiate O_2 E_H stat: 250 mV	gas composition initially 3% O_2, adjusted to 7% O_2 at 18 hr
21	Change E_H set point to 100 mV	gas composition 4% O_2
73	Change E_H set point to -50 mV	gas composition 2% O_2, E_H stat stopped at 199 hr
124	Add 1 mL 1 M NH_4NO_3	E_H increased 100 mV after addition
141	Add 1 mL starch slurry	starch slurry prepared to 6 M C
221, 241	Add 1 mL starch slurry	
383	Initiate O_2 E_H stat: -50 mV	stop E_H after 3 hr
388	Add 1 mL 1 M NH_4Cl	
404	Initiate O_2 E_H stat: +50 mV	stop E_H after 4 hr
426	Initiate O_2 E_H stat: 100 mV	stop E_H after 6 hr
451	Initiate H_2O_2 E_H stat: 0 mV	stat with 0.05 M H_2O_2: stop E_H after 6 hr
473	Initiate H_2O_2 E_H stat: 100 mV	stat with 0.05 M H_2O_2: stop E_H after 5 hr
499	add 1 mmol CH_3OH	
510	add 1 mmol benzoic acid	add solid benzoic acid

the potential decreases more slowly; 3 and 8 hr were needed for the E_H to decrease half way to the level before addition of H_2O_2 (d and e in Figure 6.5).

The average rate of H_2O_2 addition to maintain the E_H at 0 mV was 0.05 mmol/hr and the average redox buffer capacity was 2.5 mM/V. When the set point was increased to 100 mV, the addition rate of H_2O_2 increased to 0.13 mmol/hr and the redox buffer capacity increased to 3.2 mM/V. The higher rate of addition required to maintain the higher E_H could be due to renewed activity of aerobic or faculative microbes or Fe(III)-reducing microbes stimulated by H_2O_2. The increased rate of H_2O_2 addition could also be due to non-biological causes. At the higher E_H, the steady-state concentration of H_2O_2 or other oxidized species may be greater. The change in solution composition could increase the rate of dissolution or desorption of Fe(II).

The average delivery rate of O_2 into the reactor during this time period was 4 mmol/hr. The rate of H_2O_2 addition to maintain the same E_H was 0.13 mmol/hr. Although the reduction of O_2 to H_2O is a 4-electron transfer rather than a 2-electron transfer, the rate of addition of O_2 is much greater than that of H_2O_2. The consumption rate of O_2 is unknown, but it appears that only a small fraction of the O_2 delivered is consumed due to microbial activity.

As shown in Figure 6.6, the rate of addition of acid to maintain the pH at the set point was fairly constant before the addition of NH_4NO_3 and again after the E_H started to decrease again at about 150 hr. During the reduction of added nitrate, the rate of acid addition was much faster (almost 4 times greater). This higher rate is expected because most reduction reactions consume hydrogen

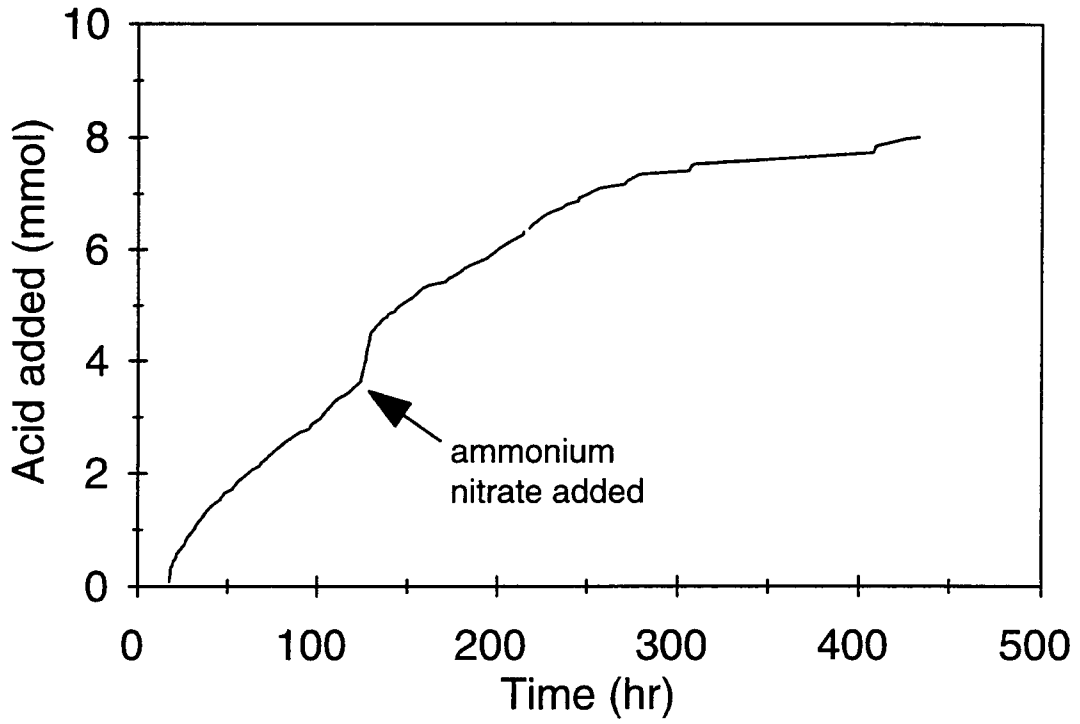

Figure 6.6 Total amount of acid added during Aloha A1 #1 experiment to maintain pH 6. The acid was added as 1.0 M HCl. The ratio of soil:water in artificial pore water was 1:8.

ions (2, 18, 19). Additional nitrogen was added at 388 hr as NH_4Cl (1 mmol) with no noticeable effect on the E_H. Several carbon sources, including starch (6 mmol as C), ethanol (1 mmol) and benzoic acid (1 mmol), were added throughout the experiment in an attempt to increase the microbial activity and decrease the redox potential further. However, none of the above carbon sources had a noticeable effect on the E_H.

The concentrations of Fe(II) and Mn(II) were determined when the E_H decreased to 450, 250, 100, -50, and -100 mV and are shown in Table 6.3. Manganese(II) (1.1 μM) was detected in the first sample at an E_H of 450 mV. Soluble Fe(II) (16.3 μM) was first detected at an E_H of 100 mV. Samples were also taken at two of the higher E_H values where O_2 or H_2O_2 (0.05 M) was added to increase the E_H. However, because the higher E_H was only maintained for a few hours, a steady-state condition had not been reached and the measured concentration of Fe did not change greatly during the second half of the experiment. The highest measured concentrations are 0.44 mM for Fe(II) and 0.50 mM for Mn(II).

6.3.2.2 Second Experiment

In the second experiment with Aloha A1 soil (Aloha A1 #2), the solution was prepared 1:10 (w/w) in 10 mM $CaCl_2$ and the variation in E_H and pH is shown in Figure 6.7. One possible reason that the E_H did not decrease further in the previous experiment was that the system was substrate limited. This

Table 6.3 Concentrations of Fe(II) and Mn(II) in the Aloha A1 #1 soil solution.

Time (hr)	E_H (mV)	Fe(II) (mM)	Mn(II) (mM)
2	450		1.1 μM
21	250		0.010
73	100	0.016	0.055
199	-50	0.043	0.25
380	-100	0.32	0.39
432	100	0.33	0.41
525	-50	0.44	0.50

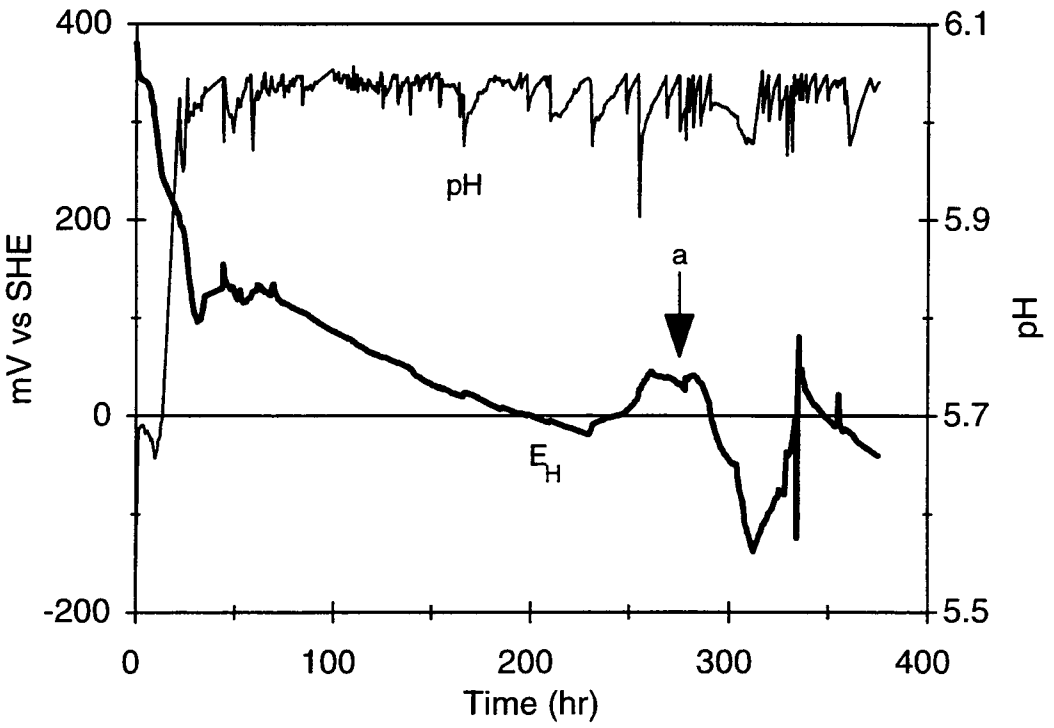

Figure 6.7 Pt electrode potential and pH during the Aloha A1 #2 experiment. The ratio of soil:water in 10 mM $CaCl_2$ was 1:10; (a) 2.5 g of compost added.

experiment was conducted to determine if a different carbon source added as a substrate could cause the slurry to reach more reducing conditions. The reagent additions are summarized in Table 6.4.

Many more carbon sources were added to stimulate the microbial activity in the soil and attain a more reducing condition (lower potential). The redox potential was not affected by the addition of each of the following at separate times: 15 mmol ethanol, 10 mmol acetate, and 5 mmol butyric acid. In this experiment, addition of 1 mmol glucose only resulted in 10 mV decrease in potential.

The greatest change occurred when 2.5 g of decomposed grass from the bottom of a compost pile (from the yard of J. D. Ingle) were added at 286 hr. The initial 10-mV increase in E_H for 5 hr may be due to O_2 associated with the compost. Then, the E_H decreased from 30 mV to -140 mV over a period of 34 hr and then immediately began increasing. Because the reducing conditions were not maintained, the carbon source must have been consumed. The E_H did not decrease when compost grass was added a second time (329 hr).

When the inorganic reductant, Ti(III) citrate, was added (339 hr), the E_H initially decreased by over 125 mV, but after 15 min was 80 mV higher than before the addition. This "spike" in potential was followed by a slow decrease of 90 mV over 18 hr before the experiment was terminated. The reason for this increase in E_H upon addition of Ti(III) is unknown.

Table 6.4 Summary of the Aloha Al #2 soil experiment.

Time	Action
21	Adjust pH to 6. Initiate pH stat with acid and base
140	Add 300 µL EtOH (5 mmol)
147	Add 300 µL EtOH (5 mmol)
158	Add 300 µL EtOH (5 mmol)
166	Add 5 mmol sodium acetate
186	Add 5 mmol sodium acetate
255	Add 5 mmol butyric acid
260	Add 1 mmol NH_4Cl
260	Add 1 mmol glucose
278	Add 2.5 g compost grass
329	Add 2.5 g compost grass
334	Add 150 µL of 250 mM Ti (III)

Samples were withdrawn for Fe(II) determination throughout the experiment and the results are listed in Table 6.5. The solution concentration again increased with time.

6.3.3 Bashaw A1 Soil

The measured E_H in the reactor slurry with the Aloha soils never fell below about -0.1 V (even after adding a carbon source). The filtered and circulated solution did not reduce the immobilized thionine, even though the E_H measured was less than the formal potential for the indicator (52 mV). For these reasons, a different type of soil was required to achieve "natural" (unstimulated) reducing conditions to determine if the solution would reduce the immobilized thionine. The Bashaw soil was selected because of its high organic content (12.5% w/w).

The dual-flow loop was employed throughout this experiment. In order to maintain the flow of soil solution in the primary loop, the cross-flow filter was sonicated in an ultrasonic water bath for approximately 15 min every 2 hr. Also, it was necessary to replace or shift the position of the Tygon tubing in the peristaltic pump every 3 days to prevent tubing rupture. The absorbance of the oxidized form of the immobilized thionine was monitored to determine the speciation of the indicator. In addition to E_H and pH, the concentrations of dissolved Fe(II), Mn(II), and phosphate were determined at various times during the experiment.

Table 6.5 Concentrations of Fe(II) in the Aloha A1 #2 soil solution.

Time (hr)	E_H (mV)	Fe(II) (mM)
138	50	0.056
158	26	0.036
212	-6	0.10
231	-16	0.15
260	42	0.16
303	-50	0.21
325	-78	0.24
333	-25	0.25

The 1150-hr (48-day) experiment consists of three distinct parts (see Figure 6.8). During the first part of the experiment (0 - 350 hr), the E_H was allowed to decrease to a potential of -125 mV, at which time the indicator was fully reduced (absorbance at 640 nm was 0.02 above the background). The slight increase in E_H at 110 hr was due to an O_2 leak. Then, during the second portion (350 - 780 hr) the E_H-stat based on addition of H_2O_2 solution with a dispensing pump (0.05 M, 25 µL/stroke) was utilized to increase the E_H in 25-mV increments of 24 to 48 hr duration while the speciation of the indicator and concentration of Fe(II) and phosphate were determined. Once the indicator was fully oxidized (780 hr, 400 mV) and the E_H-stat was stopped, the potential decreased and the indicator became 70% reduced (850 hr, 200 mV). Hydrogen peroxide was again added utilizing the E_H-stat, and the absorbance of indicator and concentration of dissolved Fe(II) were measured.

The net acid added (moles of acid minus moles of base) is shown in Figure 6.8. The initial pH of the soil in the $CaCl_2$ solution was 4.9, so base was added initially to increase the pH to 6. Base continued to be dispensed for 10 hr to overcome the acidity of the soil. After 15 hr, acid was added to maintain the solution pH. Addition of acid continued until the rate of change of E_H slowed at about -125 mV (350 hr). The consumption of acid during reduction is expected as discussed for the experiment involving Aloha A1 soil. During the time the E_H was fairly constant (300 - 350 hr), both acid and base were added as needed to maintain the pH at 6.

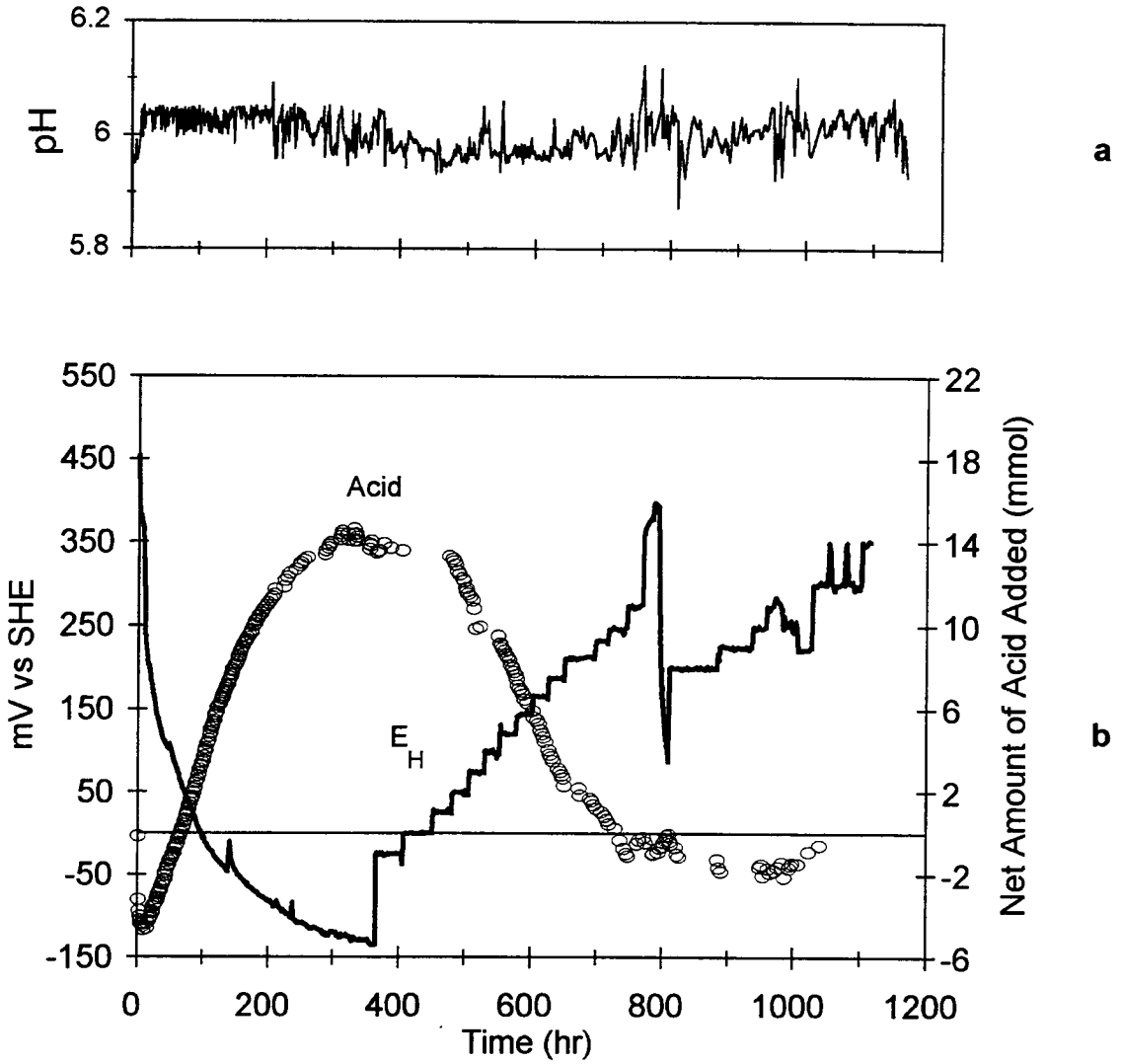

Figure 6.8 Monitored parameters during the Bashaw A1 soil experiment: (a) pH, (b) E_H and net amount of acid added (moles acid - moles base). The ratio of soil:water in 10 mM $CaCl_2$ was 1:20. Acid (1.0 M HCl) and base (1.0 M NaOH) were added to maintain pH 6.

During the second stage (350 - 780 hr), when the potential was increased with H_2O_2, the pH decreased and base was added by the pH-stat program. The reduction of H_2O_2 consumes acid while the oxidation of Fe(II) produces acid as shown in the half reactions below:

$$3H_2O + Fe^{2+} \rightarrow Fe(OH)_3 + 3H^+ + e^- \quad (6.5)$$

$$H_2O_2 + 2H^+ + 2e^- \rightarrow 2H_2O \quad (6.6)$$

The balanced equation is:

$$4H_2O + H_2O_2 + 2Fe^{2+} \rightarrow 2Fe(OH)_3 + 4H^+ \quad (6.7)$$

The oxidation of 3 mmol of Fe(II) (the measured decrease in Fe(II) between 400 and 700 hr) would result in the production of 6 mmol acid, and therefore the addition of 6 mmol base to maintain a constant pH. However, 12 mmol of base were added during this time period (see Figure 6.8). Therefore, the oxidation of Fe(II) accounts for about half the base added. The remaining base is probably added to balance the acid produced during the oxidation of other reduced species that were not monitored during the experiment (i.e., Mn, N). At 780 hr, the addition of H_2O_2 was stopped, the E_H began to decrease, and acid was again added to maintain the pH.

The rate of H_2O_2 addition was dependent on the E_H-set point as observed previously with Aloha A1 soil. The addition rate increased with increasing E_H, from 0.05 mmol/hr at an E_H of -25 mV to 0.6 mmol/hr at an E_H of 400 mV. At the slowest rate of H_2O_2 addition, the 3 mmol of Fe(II) present should be oxidized to Fe(III) in 30 hr. Because there is still measurable Fe(II) present throughout the remainder of the experiment (much more than 30 hr), Fe(II) may have been

continually produced by microbial reduction even while the H_2O_2 addition was continuing. It is also possible that some of the H_2O_2 was reduced microbially or reacted with another reductant present.

The redox buffer capacity value (Rcap) appears to be more dependent on the length of time H_2O_2 was added rather than the E_H. The Rcap values determined when H_2O_2 addition was initiated (~350 hr) were widely scattered and ranged from 3 - 7 mM/V. As addition of H_2O_2 continued, the measured Rcap values decreased (1 mM/V at 750 hr) and become less varied. When the E_H-stat was terminated and then started again (790 hr), the initial Rcap values were again larger and more scattered (2 - 3 mM/V). The decrease in Rcap with time of exposure to H_2O_2 could be due to a decrease in microbial activity. The increase in Rcap after H_2O_2 addition was stopped for 40 hr suggests that the system was recovering from the effects of H_2O_2.

6.3.3.1 Fe(II)

The variation of Fe and phosphate concentrations with the E_H value during the first 700 hr of the experiment is shown in Figure 6.9. The Fe(II) concentration increased as expected when the solution became more reducing. The appearance of Fe(II) in solution at an E_H of about 100 mV agrees with the results of previous studies by Patrick et al (1, 5, 6). They observed the onset of Fe(III) reduction in the 50 to 100 mV range. The maximum concentration of Fe(II) in solution (3 mM) represents 18% of the dithionite-citrate extractable Fe

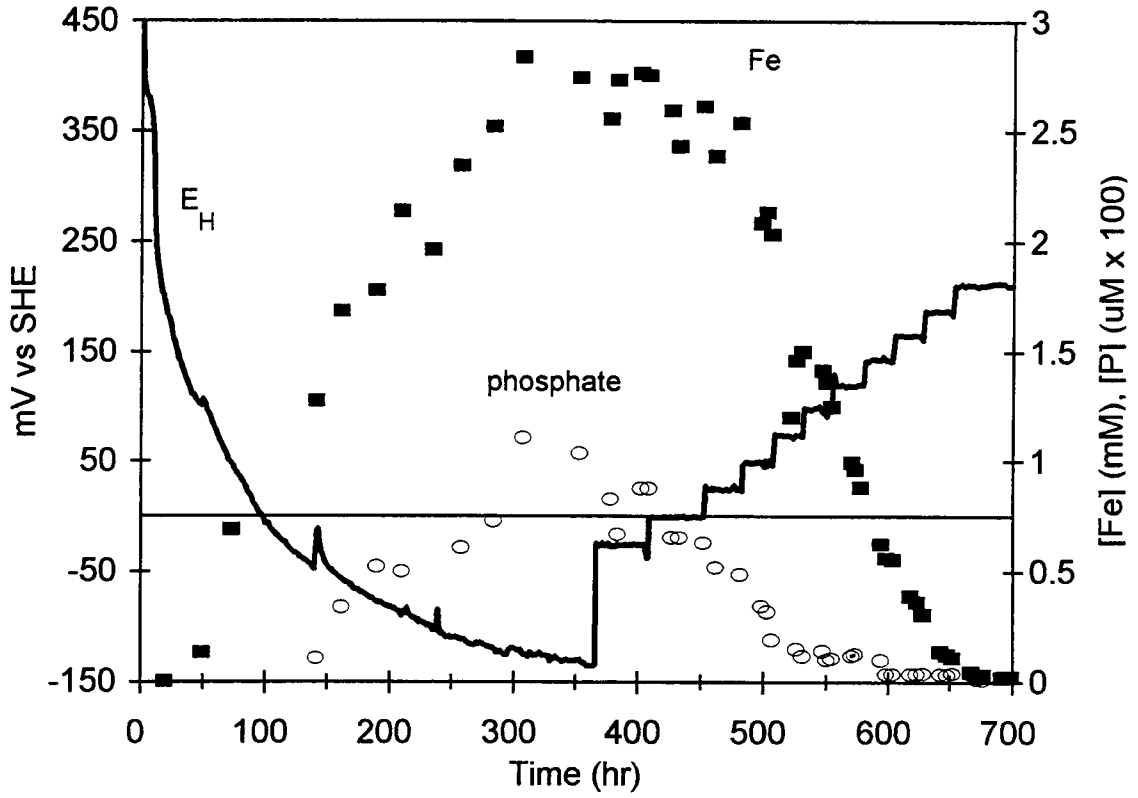

Figure 6.9 Measured concentrations of Fe(II) and phosphate in solution during the first 700 hr of the Bashaw A1 soil experiment. The ratio of soil:water in 10 mM $CaCl_2$ was 1:20.

present in the soil. (Dithionite-citrate extracted Fe is the total amorphous and crystalline Fe oxides available for reduction). The phosphate concentration also increased for about the first 350 hr, probably due to the reduction and dissolution of $FePO_4$ solids.

After 380 hr when peroxide was added to increase the E_H, the concentrations of both Fe and phosphate decreased as Fe(II) was oxidized and precipitated as $FePO_4$. Phosphate analysis was discontinued after 675 hr because the measured concentration was near or below the detection limit. A more detailed discussion of the correlation between E_H, Fe(II) concentration, and phosphate concentration is presented below.

During the initial decrease in E_H, there is a reasonably strong negative correlation between E_H and $[Fe^{2+}]$ ($r^2 = 0.8$) as seen in Figure 6.10. Likewise, a similar negative correlation is observed for the time period that the E_H is increasing ($r^2 = 0.97$), although the correlation line is shifted (i.e., the Fe(II) concentration is greater at a given E_H). Similar results were observed by Gotoh et al (6) when the time between the adjustment of the redox potential to a new level and sampling was less than two weeks. In this study, the E_H was held at the various levels for only one to two days, and thus the Fe was not given time to reach a steady-state. Note in Figure 6.9 that the Fe(II) concentration is reasonably constant from 250 to 450 hr where the E_H is below 50 mV.

Two more possible explanations for the different Fe(II) concentrations are based on the Pt electrode potential. Because the couple that is poising the electrode is not known, the electrode could be responding to different couples

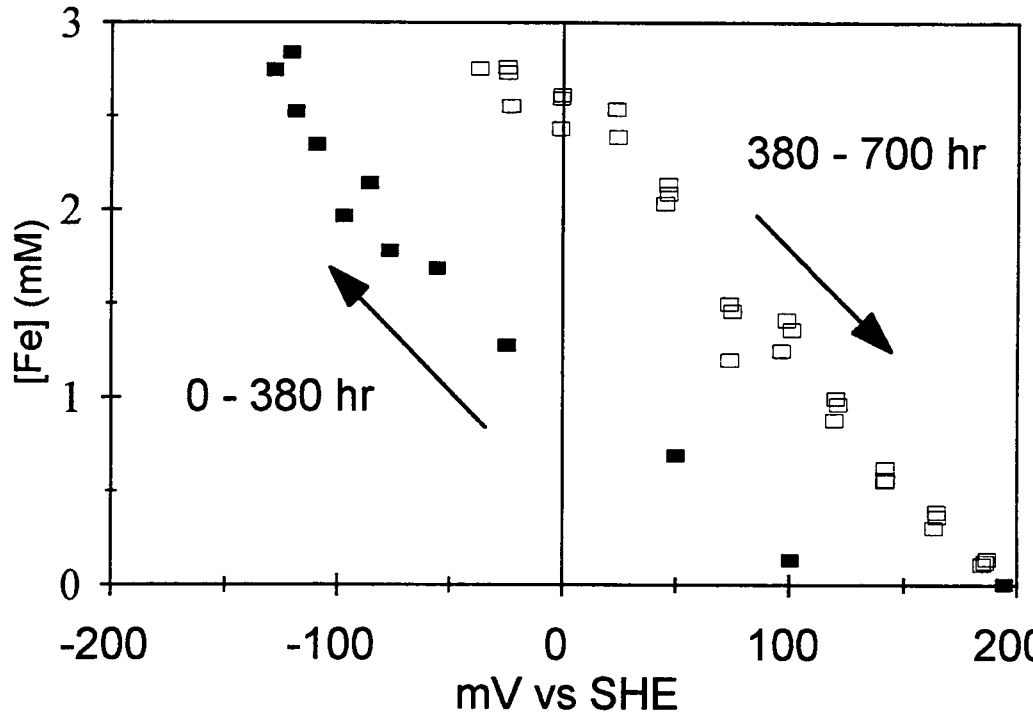

Figure 6.10 Correlation between solution concentration of Fe(II) and potential measured at a Pt electrode (below 200 mV) during the Bashaw A1 soil experiment. Data from first half during continuously decreasing E_H (■); data from second half with stepwise increasing E_H (□). The ratio of soil:water in 10 mM $CaCl_2$ was 1:20.

during the time when the E_H is decreasing and when the E_H is increasing. The Pt electrode could be responding to the added H_2O_2, resulting in a mixed potential. Another possibility is that the electrode could be poised by a different Fe(III) mineral during the two portions of the experiment. Iron(III) hydroxides freshly deposited on the electrode surface during the addition of H_2O_2 are likely to be more amorphous than the more aged Fe(III) hydroxides present during the first portion of the experiment. Doyle (20) concluded that Fe(III) minerals on the surface of the Pt electrode will poise the potential. Plots of E_H versus log[Fe^{2+}] were made and were very non-linear and the change in E_H is much greater than predicted by the log of the change in Fe(II) concentration. A linear plot would be expected if an Fe(III)-solid/Fe(II) couple poised the electrode.

After 700 hr, the E_H was increased in a few steps to 400 mV and then the E_H-stat was discontinued for 18 hr to allow the oxidized thionine to be reduced before starting again at about 800 hr as shown in Figure 6.11. The Fe(II) concentration increased rapidly when the E_H was allowed to decrease. However, over most of the time period from 700 - 1100 hr, the E_H was held above 200 mV and the Fe(II) concentration was 15 - 60 µM.

As shown in Figure 6.12, there is little correlation between soluble iron and potential (r^2 = 0.3) when the E_H was above 200 mV. If the Fe(III) mineral present is am-FeOOH (E° = 1.057 (21)), the Fe(II) concentration at pH 6 should be about 300 µM at 200 mV and 6 µM at 300 mV. The calculated Fe(II) concentrations would be lower for more crystalline (less soluble) iron hydroxides. For example, γ-FeOOH (lipidocrocite, E° = 0.96 (20)), would lead to Fe(II)

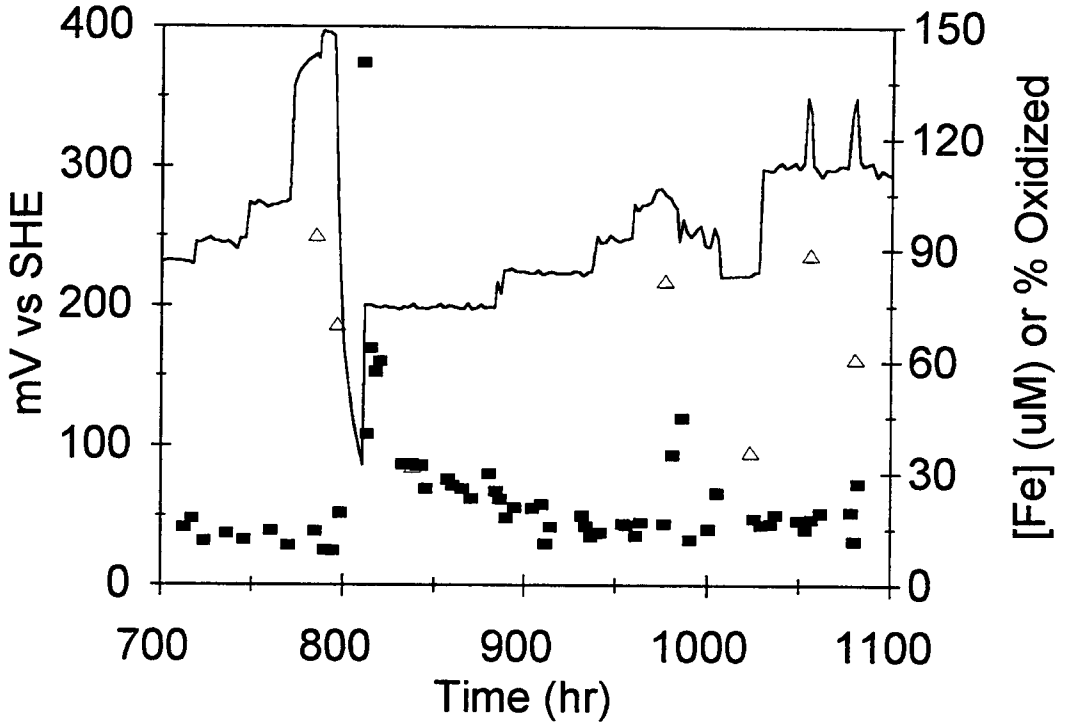

Figure 6.11 Measured concentrations of Fe(II) in solution (■) and percent of immobilized thionine oxidized (Δ) during the last 400 hr of the Bashaw A1 soil experiment. The ratio of soil:water in 10 mM $CaCl_2$ was 1:20.

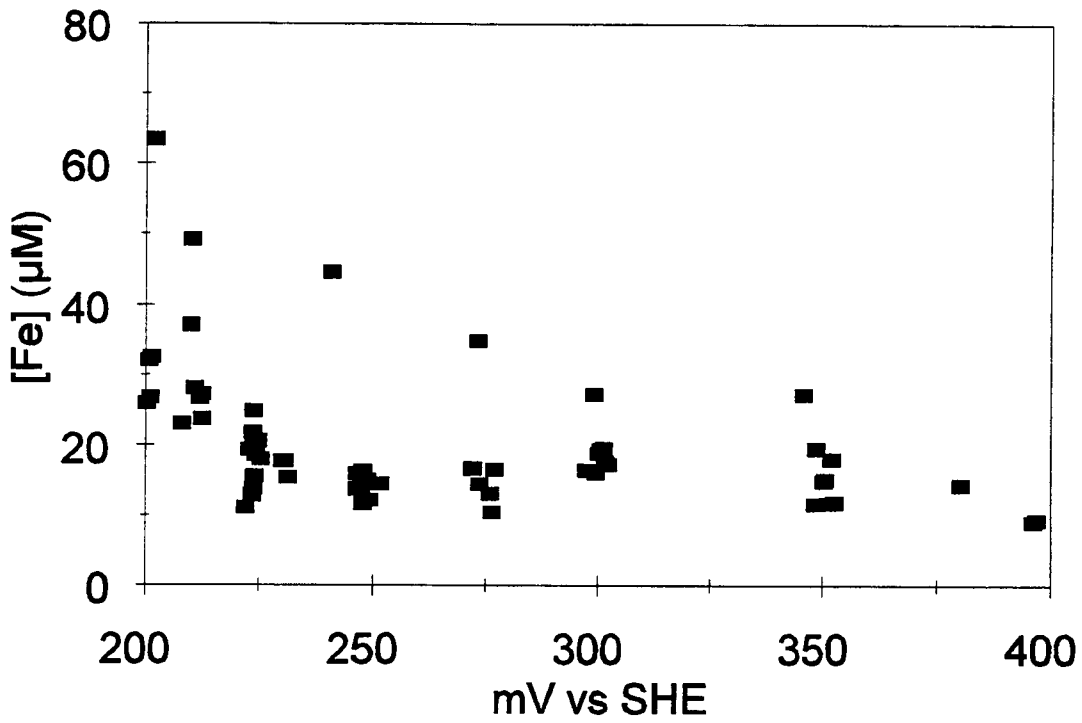

Figure 6.12 Correlation between solution concentration of Fe(II) and potential measured at a Pt electrode (above 200 mV) during the Bashaw A1 soil experiment from 700 to 1100 hr. The ratio of soil:water in 10 mM $CaCl_2$ was 1:20.

concentrations of 7 μM at 200 mV and 0.1 μM at 300 mV. The presence of measurable Fe(II) in solution at E_H levels above 300 mV may indicate that the system has not yet reached a steady-state in terms of the Fe speciation as discussed above. Presumably, if the system was maintained at the high E_H values for longer time periods, essentially all the Fe would be oxidized and no detectable Fe(II) would remain in solution. The decision to change to a new redox potential after 800 hr was based on the speciation of the immobilized indicator as discussed below.

The Fe(II) and phosphate concentrations in samples collected when the Fe(II) concentration was greater than 1 mM (log(Fe) < 0, Figure 6.13), are reasonably correlated ($r^2 = 0.82$). The average Fe:P ratio in the samples is 60:1, which is similar to that observed by others in weathered soils containing iron oxides with iron phosphate inclusions (22).

In samples collected after the Fe(II) concentration decreased below 1 mM, there is little or no correlation. This lack of correlation could be due to the slow kinetics of Fe redox transformations or of Fe-oxide and Fe-phosphate mineral formation. If the formation of phosphates occurs more slowly than the formation of oxides, the phosphate concentration would decrease more slowly relative to the Fe concentration. Another possibility is that the solution concentrations could be determined by the $FePO_4$ solubility.

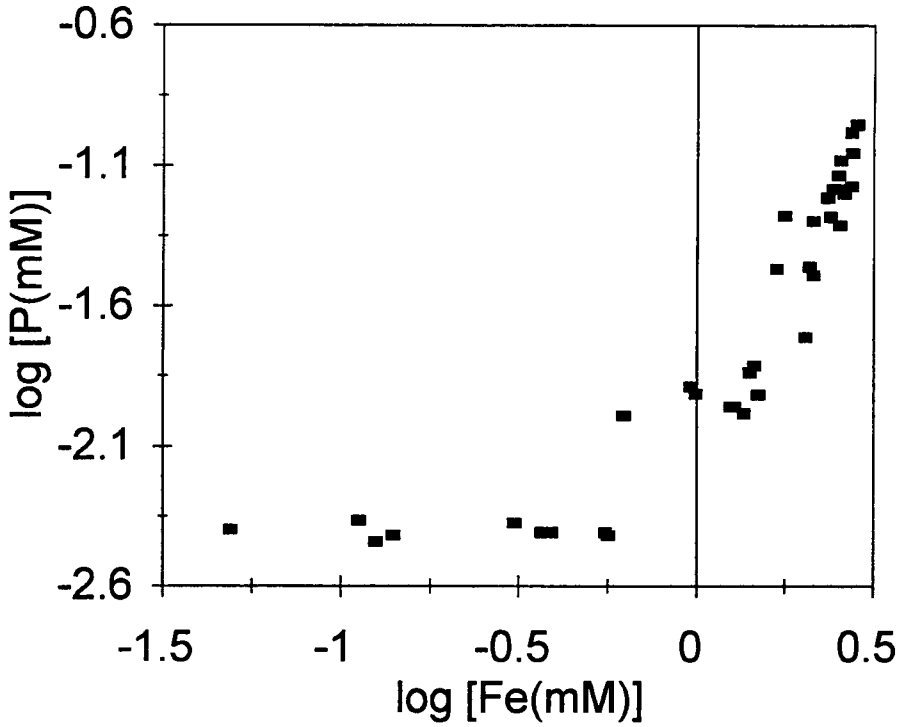

Figure 6.13 Correlation between solution concentration of Fe(II) and phosphate during the Bashaw A1 soil experiment. The ratio of soil:water in 10 mM $CaCl_2$ was 1:20.

6.3.3.2 Thionine

The absorbance of the immobilized thionine was also monitored throughout the experiment. As the E_H decreased, the absorbance of the oxidized form of immobilized thionine decreased as the thionine became reduced over the first 200 hr (see Figure 6.14). The formal potential of immobilized thionine is 52 mV (Chapter 5). The observed reduction of immobilized thionine during the first portion of this experiment occurs during the expected E_H range; 90% oxidized at 75 mV and 40% oxidized at 25 mV. However, the thionine was not fully reduced until an E_H of about -100 mV which is much lower than expected from the formal potential. The absorbance spectrum of the initially oxidized thionine (0 hr) and the fully reduced thionine (1050 hr) are shown in Figure 6.15.

During the middle and latter portion of the experiment (starting at 350 hr), H_2O_2 was added to increase the E_H in a stepwise fashion; the indicator was 54% oxidized at 210 mV (670 hr). As shown in Figure 6.11, once the indicator was fully oxidized and the addition of H_2O_2 was stopped (800 hr), the E_H decreased and the indicator became reduced again. Between 800 and 1100 hr, the E_H was then increased and decreased to determine where the transformation of immobilized thionine occurred relative to the measured E_H and Fe(II) concentration. All the indicator transformations during this time period occur at E_H values far above the formal potential of the immobilized thionine. As discussed previously, the system was not given sufficient time for the Fe(II) in

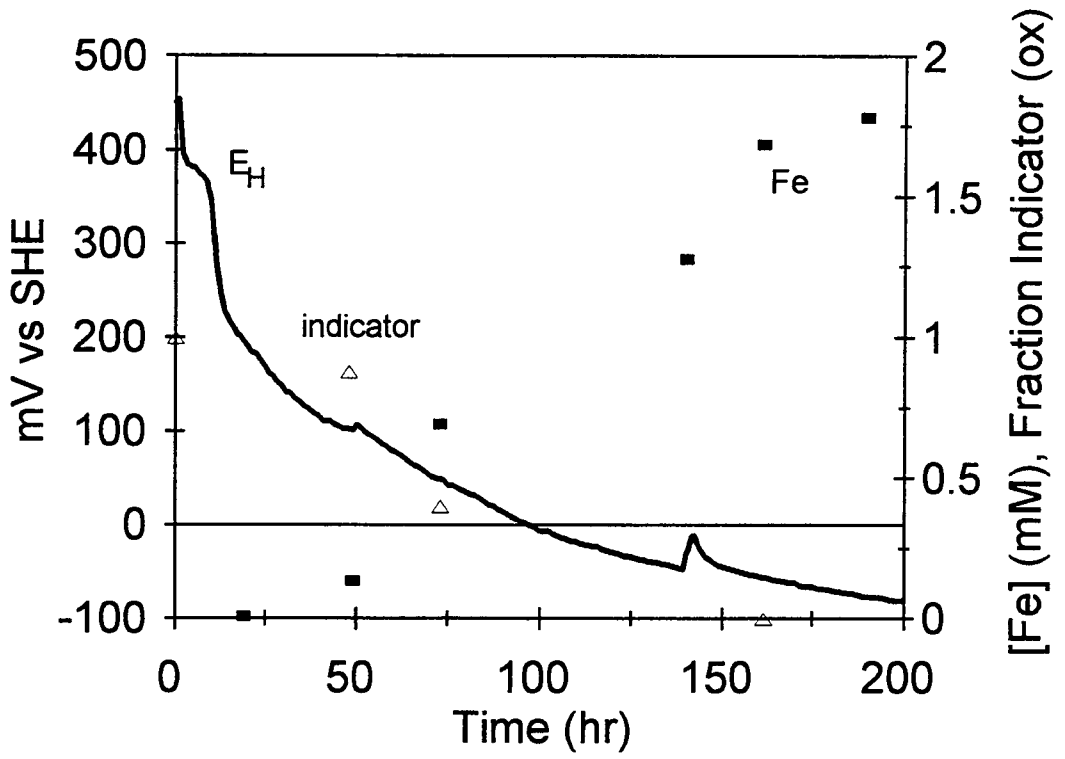

Figure 6.14 Measured concentrations of Fe(II) in solution (■) and the fraction of immobilized thionine oxidized (Δ) during the first 200 hr of the Bashaw A1 soil experiment. The ratio of soil:water in 10 mM $CaCl_2$ wais 1:20.

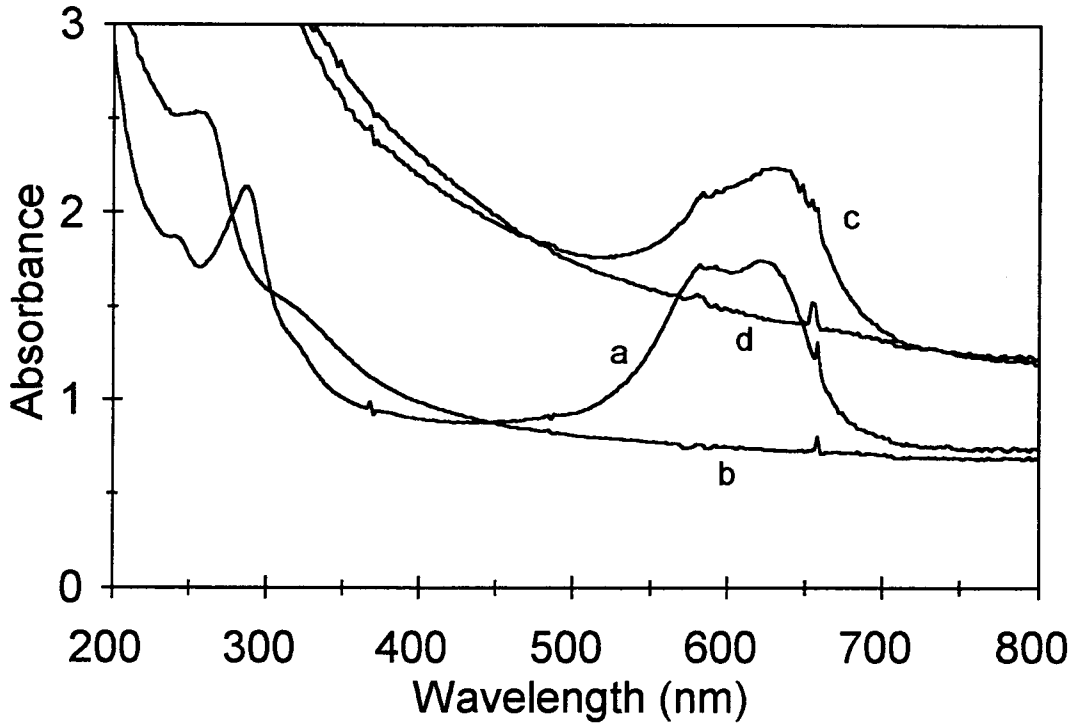

Figure 6.15 Absorbance of immobilized thionine during Bashaw A1 soil experiment. Absorbance spectrum (a) initial oxidized thionine (0 hr); (b) fully reduced thionine early in experiment (160 hr); (c) 89% oxidized (1050 hr); (d) fully reduced (1075 hr). The ratio of soil:water in 10 mM $CaCl_2$ was 1:20.

solution to reach a steady-state condition. Because there was still measurable Fe(II) at E_H levels above 100 mV, it is reasonable to expect some reduction of immobilized thionine to occur.

There is a correlation between [Fe(II)] measured in solution and the fraction of oxidized immobilized thionine ($r^2 = 0.64$) as shown in Figure 6.16. The correlation would be expected to be better if the system were given longer to equilibrate at each redox potential. The two points shown as open circles in Figure 6.16 indicate the only times when the DO concentration was above the deaerated condition (< 0.2 ppm) during the addition of H_2O_2 which can account for the high amount of oxidized thionine when the Fe(II) concentration is low.

The absorbance of oxidized thionine was also measured at 1035, 1079, and 1100 hr to be 6, 0, and 0% oxidized, respectively. These points were not included in Figures 6.11 and 6.16 because the absorbance was measured within 2 to 4 hr of resuming the flow in the external loop in the morning. It was often noted that the indicators became reduced overnight when the flow loop was turned off. It might be expected that the "effective E_H" for solution in the flow loop would be lower than for solution in the reactor because the H_2O_2 in the loop is not being replenished.

Over the entire Bashaw soil experiment, the immobilized thionine was 90% or more reduced whenever the E_H was below 0 mV or the Fe concentration was above 60 μM. Clearly, the indicator might be used to characterize redox conditions which are reducing enough to reduce the majority of the Fe.

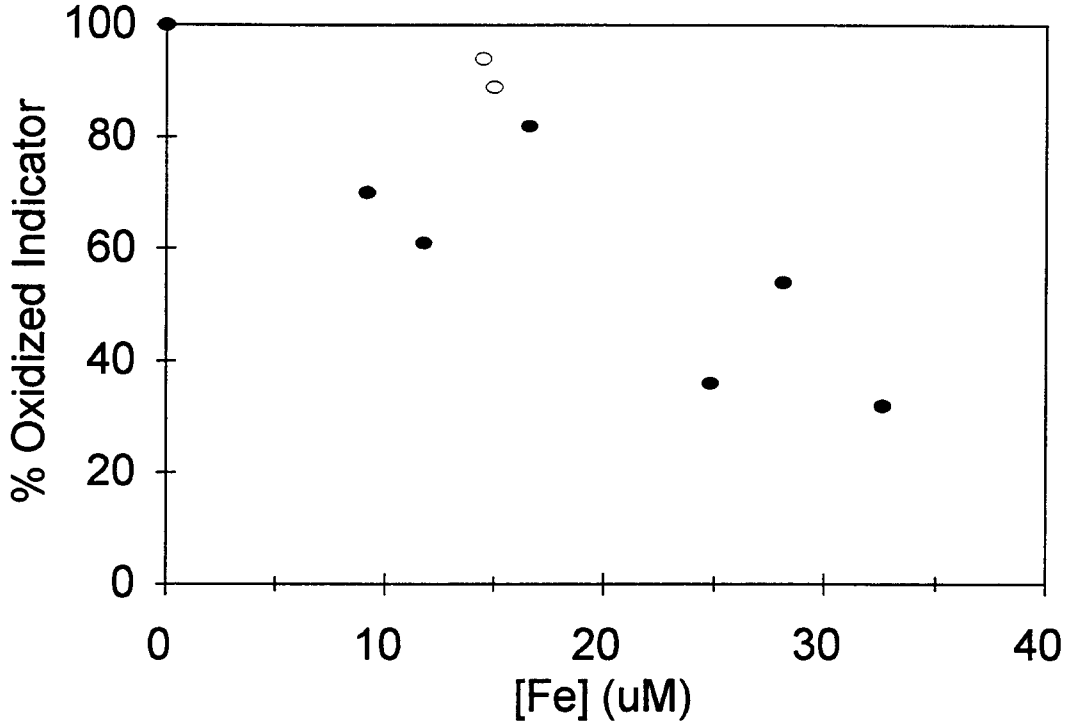

Figure 6.16 Correlation diagram for solution concentration of Fe(II) and % oxidized thionine during the Bashaw A1 soil experiment from 750 to 1100 hr. The DO concentration was below 0.2 ppm except where indicated by (o). The ratio of soil:water in 10 mM $CaCl_2$ was 1:20.

In a separate experiment, the immobilized thionine was reduced with Fe(II) solution. The experiment was similar to the solution experiments conducted previously (Chapter 5) where the reactor solution consisted of a phosphate buffer and Fe(II) was added to titrate the indicator. During the 7-hr experiment, immobilized thionine started to be reduced when the concentration of Fe(II) was 30 μM, and was completely reduced when the concentration was about 200 μM. These Fe(II) concentrations are higher than those observed to cause reduction of the immobilized thionine in the Bashaw soil experiment. However, the time of exposure to the solution during the soil experiment was much longer (days instead of hours), and therefore a greater amount of Fe(II) would be delivered to the indicator for a similar solution concentration.

During the Bashaw soil experiment, some of the filtered soil solution was collected in N_2-purged sample vials (3-mL) containing immobilized thionine in a small amount of phosphate buffer (~0.25 mL). The solution was collected at a time when the Fe(II) concentration was high enough (400 to 500 hr with an E_H of 0 to 25 mV) to reduce the immobilized thionine packed in the spectrophotometer flow cell. After shaking the vial to mix the immobilized thionine with the filtered soil solution, the vial was allowed to stand overnight. The gel settled to the bottom of the vial, and the top layer in contact with the solution became colorless, indicating reduction of the immobilized thionine. This demonstrates that soils could be characterized in a similar manner by adding soil solution to sample vials containing immobilized thionine.

There are problems with flow patterns and discoloration that occur when pumping filtered soil solution through the immobilized thionine. First, if the gel is not packed well, channels can develop which allow the solution to flow around the majority of the gel instead of through it. If this occurs, the flow cell must be removed from the loop and the cell repacked. The same gel can be used to repack the cell if care is taken when flushing the gel out of the cell.

A second problem is the gradual increase in background color of the gel as shown in Figure 6.15. As soil solution flows through the gel for several days, the gel becomes discolored to a light brown which results in a sloping background that increases as the wavelength decreases. The absorbance of the thionine peak can still be monitored, but because the peak occurs on a sloping background, the absorbance must be corrected. The indicator cycled back and forth between the fully oxidized and fully reduced forms during the experiment, so the absorbance of both forms at the wavelength of maximum absorbance were known. The absorbance allowed the speciation of the indicator to be estimated.

During an experiment in which the indicator speciation is not cycling back and forth, the background absorbance would have to be interpolated from the sloping baseline. The discoloration of the gel cannot be removed with base, and therefore the gel is discarded and replaced with new gel when the discoloration makes absorbance measurements difficult. Indicators that absorb at lower wavelengths would be difficult to use in this type of application because the

absorbance peak would be even more obscured by the increase in the background.

6.4 Conclusions

The reactor system designed works very well to control the solution pH and measured E_H of a soil slurry. The external flow loops and cross-flow filter provide a means for monitoring additional variables such as the absorbance of an immobilized indicator. Maintaining flow of a clay-type soil solution through the external loop over long periods of time is difficult and factors such as sonicating the filter module in an ultrasonic bath and replacing (or shifting) the Tygon tubing in the peristaltic pump are critical. The sonicator was controlled manually, but could be interfaced to the computer in a similar manner to the O_2 solenoid valve.

The measured concentration of Fe(II) has a strong negative correlation to the measured potential at a Pt electrode below 200 mV. However, the Fe(II) concentration was much greater for a given E_H when the E_H was forced higher by addition of O_2 or H_2O_2 relative to when the system was becoming more reduced due to microbial reduction. Because the redox potential was maintained at the various levels for time periods of less than 2 days, it is not surprising that the correlation line is shifted.

No specific organic substrate was found that increased microbial activity as indicated by a faster decrease in E_H or a lower E_H. The addition of partly decomposed grass from a compost pile did cause the E_H to become more negative but only for about 5 hr. The decrease in E_H was therefore a result of the addition of a consumable carbon source or actual reduced species in the

compost rather than an increase in the microbiological population. For the soils studied, reducing conditions were best achieved with a top soil with high organic content.

This is the first time the speciation of an immobilized redox indicator has been used to assess the redox status of a soil solution. However, there are some practical difficulties in utilizing the indicator to monitor redox transformations in the soil slurries; they can be overcome by careful packing of the flow cell and background correction of the absorbance. The immobilized thionine does couple with dissolved Fe(II), O_2, and Cr(VI) and therefore the measured absorbance can be used to estimate the overall redox status of the system. For example, if the indicator is reduced, any chromium present must also be reduced, and the concentration of Fe(II) must be greater than 30 μM. Likewise, if the indicator remains oxidized after exposure to the soil solution for several hours, it is possible for Cr(VI) to be present and the concentration of Fe(II) is below 200 μM. (If the indicator remains oxidized after several days, the Fe(II) concentration is below 30 μM.)

The redox transformation of the immobilized thionine did not always occur near its formal potential which was characterized previously. The indicator was initially reduced in a measured E_H range similar to the $E^{o'}$ of the immobilized indicator (52 mV). Later in the experiment, however, the indicator remained partially reduced at much higher E_H values. In the configuration used in this study, the indicator is isolated from the Pt electrode and therefore does not poise the electrode. The system is not in a steady-state condition during the oxidant

addition (H_2O_2 or O_2) as indicated by the rapid decrease in E_H when the E_H-stat is turned off. It appears that the addition of an oxidant creates an artificially high Pt electrode potential. The E_H could be responding to a transient concentration of H_2O_2 or O_2 during the E_H-stat.

To expand the E_H range of a soil which can be studied in this manner, more redox indicators need to be immobilized. Several immobilized indicators could be used to determine more specifically the redox condition of a soil and the redox speciation of more numerous redox-active components.

Suggested studies include those where the E_H is maintained at each potential for longer periods of time to allow the Fe to reach a steady state. This would enable a more detailed examination of the correlations among the E_H, indicator speciation, and the Fe(II) concentration. Also, the concentrations of additional redox-active solution species should be monitored throughout long-term soil experiments to determine where transformations of these species occur with respect to the speciation of immobilized thionine. Other geochemical matrix species of interest include Mn(II) (only measured in early soil experiments), NO_3^-, NH_4^+, Cr, As, and Se.

6.5 References

1. Ross, D. S.; Sjogren, R. E.; Bartlett, R. J. *J. Environ. Qual.*, **1981**, *10*, 145.

2. McBride *Environmental Chemistry of Soils*, Oxford Press: New York, 1994.

3. Patrick, W. H. Jr.; Jugsijunda, A. *Soil Sci. Soc. Am. J.*, **1992**, *56*, 1071.

4. Hesse, P. R. *A Textbook of Soil Chemical Analysis*, Chemical Publishing Co. Inc: New York, 1971.

5. Patrick W. H. Jr.; Gotoh, S. *Soil Sci. Soc. Amer. Proc.*, **1972**, *36*, 738.

6. Gotoh, S; Patrick, W. H. Jr. *Soil Sci. Soc. Amer. Proc.*, **1974**, *38*, 66.

7. Patrick, W. H. Jr.; Henderson, R. E. *Soil Sci. Soc. Am. J.*, **1981**, *45*, 855.

8. Charoenchamratcheep, C.; Smith, C. J.; Satawathananont, S.; Patrick, W. H. Jr. *Soil Sci. Soc. Am. J.*, **1987**, *51*, 630.

9. Masscheleyn, Patrick H.; Delaune, Ronald D.; Patrick, W. H. Jr. *Environ. Sci. Technol.*, **1990**, *24*, 91.

10. Masscheleyn, P. H.; Delaune, R. D.; Patrick, W. H. Jr. *J. Environ. Qual.*, **1991**, *20*, 522.

11. Masscheleyn, Patrick, H.; Delaune, Ronald D., Patrick, William H. Jr. *Environ. Sci. Technol.*, **1991**, *25*, 1414.

12. Masscheleyn, Patrick H.; Pardue, John H.; Delaune, Ronald D.; Patrick, W. H. Jr. *Environ. Sci. Technol.*, **1992**, *26*, 1217.

13. Patrick, William H. Jr. *Nature*, **1966**, *212*, 1278.

14. Patrick, W. H. Jr.; Williams, B. G.; Moraghan, J. T. *Soil Sci. Soc. Amer. Proc.*, **1973**, *37*, 332.

15. Soil Survey Staff, **1992**, Open File Rpt. CP92-OR216 and CP91-OR220, National Resource Conservation Service, Lincoln, NE.

16. Bos, Mark; Baham, John; Private communication; Oregon State University, 1994.

17. Westall, J. C. ; Private communication; Oregon State University, 1994.

18. Thurman, E. M. *Organic Geochemistry of Natural Waters*, Nujhoff and Junk Publishing: Dordrecht, 1985.

19. Stumm, W., and Morgan, J. J. *Aquatic Chemistry*, Wiley-Interscience: New York, 1981.

20. Doyle, Roger W. *American Journal of Science*, **1968**, *266*, 840.

21. Pankow, James F. *Aquatic Chemistry Concepts*, Lewis Publishers: Chelsea, Michigan, 1991.

22. Mayer, T. Ph.D. Thesis, Oregon Graduate Institute, Hillsboro, OR, **1995**.

Chapter 7
Conclusions

This thesis has discussed the development of two reactor systems used to study redox transformations of inorganic and organic matrix components, inorganic and organic contaminants, and organic redox indicators. These reactor systems allow investigation of soil samples at different environmental redox levels (as measured with a Pt electrode) under well controlled, quasi steady-state conditions. The redox condition can be controlled during an experiment by addition of either a solution (e.g., H_2O_2) or a gas (e.g. O_2) as selected by the user.

The most unique aspect of the reactor systems presented here, compared to previously developed redox control systems, is the external loop system which provides a continuously filtered and recirculated solution for on-line measurements. This is critical for spectrophotometric measurements and allows other sensors to be added. Another innovation includes the in-situ standardization of the sulfide electrode which circumvents the potential problem of sulfide oxidation if a sample is removed from the reactor before sulfide determination. Finally, the approach of using a pH-stat to maintain a nutrient concentration is unique to the reactor system described in Chapter 3.

Several extensions to the reactor systems are suggested. First, the gas flow controllers could be computer-controlled via a DAC computer board. This would allow the ratio of O_2 present in the N_2 stream to be adjusted automatically

to an appropriate level when controlling the E_H using the gas-controlled E_H-stat mode. Second, the incorporation of an electrochemical cell for on-line cyclic voltammetry would enable a more detailed investigation of the electrochemical characteristics (e.g., redox reversibility) of the system components. Finally, the inclusion of on-line gas analysis for H_2, CH_4, CO_2, and H_2S in the head space would be beneficial to monitor sulfate reduction (production of H_2S) and methanogenesis (production of CH_4).

The usefulness of twelve redox indicators in solution to evaluate the redox potential was demonstrated. Unlike many environmental redox couples, the redox indicators couple with a Pt electrode to poise its potential. The speciation of the indicators with a formal potential above 0 mV can be used to predict the prevalent forms of Fe and Cr present. A series of indicators is needed because each indicator is only effective over a small range of redox potential (~80 mV). Therefore, an individual redox dye can demonstrate only whether the E_H is above or below the formal potential of the dye.

Because the redox indicators adsorbed on solid surfaces, methods were developed to immobilize two indicators with amine substituents, thionine and phenosafranine, on an affinity chromatography gel with aldehyde coupling groups. These immobilized indicators are redox active and couple with solution redox reagents, which allows the redox status of systems containing a solid phase to be evaluated. The electronic structure (absorbance spectrum) and electrochemical behavior (formal potential) of the indicators were only slightly affected by immobilization on the gel.

More immobilized redox indicators are needed to cover the environmental range of +400 to -300 mV ($E^{o'}$ = 52 mV, Thi_{immob}; $E^{o'}$ = -286 mV, $PSaf_{immob}$). Several approaches are possible to increase the number of immobilized indicators available as many available redox indicators do not have a primary amine substituent.

One option is try other affinity chromatography gels which utilize different functional groups than aldehydes for binding. Other functional groups present on one or more of the tested indicators that could be used for immobilization are alcohol, methoxy, and sulfonate.

Secondly, indicators could be synthesized similar to existing ones (such as indigo carmine) with a primary amine or other functional group attached to the ring. For example, if a primary amine group is added to a ring, the indicator could be immobilized by the method developed and described here. Addition of hydrophilic substituents (i.e., polar or ionic groups) to the rings of nile blue may eliminate the pressure problems that occur when pumping water through the packed cell. Although the formal potential of an indicator changes somewhat when functional groups are added, the new formal potential could be determined by the titration method described in Chapter 5.

For the first time, the speciation of an immobilized redox indicator has been used to assess the redox status of a soil solution. Because immobilized thionine couples with dissolved Fe(II), O_2, and Cr(VI), the redox state of these species can be estimated from the measured absorbance (speciation) of the thionine. However, because the observed redox state of the immobilized

thionine changed over a large apparent E_H range (100 - 350 mV), further experiments are needed to characterize more precisely at what potential oxidation and reduction of the indicator occurs.

Immobilized phenosafranine was not tested in the soil solutions because the E_H did not become reducing enough. It should be evaluated with the acetate and PCP degrading anaerobic consortium discussed in Chapter 3 to test its effectiveness as an indicator of methanogenesis. The "natural" E_H of this culture is about -250 mV which is near the formal potential of immobilized phenosafranine (-286 mV).

A very strong negative correlation between the concentration of dissolved Fe(II) and the measured E_H was shown to exist when the E_H was below 300 mV. However, when the E_H was forced higher by the addition of an oxidant (O_2 or H_2O_2), the Fe(II) concentration was greater for a given E_H than when the soil was becoming more reduced due to microbial reduction. It appears that the addition of an oxidant creates an artificially high Pt electrode potential during the short time of oxidant addition used in the experiments presented in this thesis. The Pt electrode could be responding to a transient concentration of H_2O_2 or O_2 during the E_H-stat. Although these results confirm that the speciation of Fe can be used to track redox conditions over a certain E_H range in a soil solution, it is clear that use of a redox indicator for on-line or in-situ measurements would be simpler.

The next steps in sensor development are to combine the immobilized indicators with fiber optics and to employ the sensor in the field. The

immobilized indicator could be placed between two fiber optic cables to allow the absorbance changes to be monitored in-situ.

Finally, further studies are necessary to understand the redox conditions in soil solutions more fully. For example, the species responsible for the reduction and reoxidation of the immobilized indicator need to be verified. In addition, the redox potential in the external loop can be monitored and compared to the redox potential in the reactor which might demonstrate the importance of solids in determining the potential measured at a Pt electrode. This will be a step toward solving the greatest puzzle in redox measurements: what is poising the Pt electrode?

Bibliography

Anderson, Linda D.; Kent, Douglas B.; Davis, James A. *Aabstract: American Chemical Society Meeting*, **1992.**

Barteltt, Richmond; James, Bruce *J. Environ Qual*, **1979**, *8*, 31.

Bartlett, R. J.; Kimble, J. M. *J. Environ Qual*, **1976**, *5*, 379.

Bloomfield C.; Pruden, G. *Envion. Pollut. Ser. A*, **1980**, *23*, 103.

Bos, Mark; Private communication; Oregon State University, 1994.

Charoenchamratcheep, C.; Smith, C. J.; Satawathananont, S.; Patrick, W. H. Jr. *Soil Sci. Soc. Am. J.*, **1987**, *51*, 630.

Chemical Attenuation Rates, Coefficients in Leachate Migration: Vol 1, Rai, D.; Zachara, J. M., Electric Power Research Institute Report EA-2485-3, 1984.

Chromium Reactions in Geologic Materials, Rai, D.; Zachara, J. M., Electric Power Research Institute Report EA-2485-3, 1988.

Clark, W. Mansfield *Oxidation-Reduction Potentials of Organic Systems*; Williams & Wilkins Company: Baltimore, 1960.

Couch, Tara; Oregon State University, unpublished data, **1991**.

Cox, B. X.; Linton, Richard W. *Environ. Sci. Technol.* **1985**, *19*, 345

Data Instructions, References, Reorder Information, for Spectra/Gel® MAS Beads, Spectrum: Houston.

Eary, L. E.; Rai, Dhanpat *American Journal of Science*, **1989**, *289*, 180.

Eary, L. E.; Rai, Dhanpat *Environ. Sci. Tech.*, **1988**, *22*, 972.

Eary, L. Edmond; Rai, Dhanpat *Environ. Sci. Tech*, **1987**, *21*, 1187.

Fendorf, Scott E.; Zasoski, Robert J. *Environ. Sci. Tech.*, **1992**, *26*, 79.

Fendorf, Scott E.; Sparks, Donald L *Abstract: American Chemical Society* Meeting, **1992.**

Fessenden and Fessenden, *Organic Chemistry, 3rd Edition*; Brooks/Cole Publishing Company: Monterey, CA, 1986.

Fetzer S.; Conrad R. *Arch. Microbiol.*, **1993**, *160*, 108.

Frevert, Tönnies; *Arch. Hydrobiol.*, **1979**, *11*, 278.

Frevert, Tönnies; *Schweiz. Z. Hydrol.*, **1984**, *46/2*, 269.

Geochemical Behavior of Chromium Species, Rai, D.; Zachara, J. M., Electric Power Research Institute Report EA-4544s, 1986.

Gleicher, G. J.; Private communication; Oregon State University, 1993.

Gotoh, S.; Patrick, W. H. Jr. *Soil Sci. Soc. Amer. Proc.*, **1974**, *38*, 66.

Green, Floyd J. *The Sigma Aldrich Handbook of Stains, Dyes and Indicators*; Aldrich Chemical Company, Inc.: Milwaukee, WI, 1990.

Griffin, R. A.; Au, Anna K.; Frost, R. R. *J. Environ. Sci. Health*, **1977**, *A12*, 431.

Grove, J. H.; Ellis, B. G.; *Soil Sci. Soc. Am. J.*, **1980**, *44*, 238.

Hanke, M. E.; Katz, Y. J. *Arch. Biochem.*, **1943**, *2*, 183.

Hesse, P. R. *A Textbook of Soil Chemical Analysis*; Chemical Publishing Co., Inc.: New York, 1971.

Hostettler, John D. *American Journal of Science*, **1984**, *284*, 734.

Indicators, Bishop, E., Ed., Pergamon Press: Oxford, 1972.

Ingle, James D. Jr.; Crouch, Stanley R.; *Spectrochemical Analysis*; Prentice Hall: Englewood Cliffs, New Jersey, 1988.

Jacob, H. E. In *Methods in Microbiology, Vol 2*; Norris, J. R.; Ribbons, D. W., Eds., Academic Press, Inc.: New York, 1970.

James, Bruce; Bartlett, Richmond J. *J. Environ Qual*, **1983**, *12*, 173.

James, Bruce R.; Bartlett, Richmond J. *J. Environ. Qual.*, **1983**, *12*, 177.

Jee, Hae Sung; Nishio, Naomichi; Nagai, Shiro *J. Gen. Microbiol.*, ***1987***, *33*, 401.

Jee, Hae Sung; Mano, Tarumi; Nishio, Naomichi; Nagai, Shiro *J. Ferment. Technol.*, **1988**, *66*, 123.

Knight, B. C. J. G. *Biochem. J.*, (London), **1930**, *24*, 1075.

Lindberg, R. D.; Runnells, D. D. *Science*, **1984**, *225*, 925.

Ljungdahl, Lars G.; Wiegel, Juergen *Manual of Industrial Microbiology and Biotechnology*, A. L. Deamin and N. A. Solomen Eds.; American Society for Microbiology: Washington D. C., 1986.

Lovley, Derek R. *Geochimica et Cosmochimica Acta*, **1988**, *52*, 2993.

Lovley, Derek, R.; Chapelle, Francis H.; Woodward, Joan C. *Environ. Sci. Technol.*, **1994**, *28*, 1205.

Lovley, D. R.; Goodwin, S. *Science*, **1988**, *52*, 2993.

Manceau, A.; Charlet, L. *Abstract: American Chemical Society Meeting*, **1992.**

Masscheleyn, Patrick H.; Pardue, John H.; Delaune, Ronald D.; Patrick, William H. Jr. *Environ. Sci. Technol.*, **1992**, *26*, 1217.

Masscheleyn, P. H.; Delaune, R. D.; Patrick, W. H. Jr. *J. Environ. Qual.*, **1991**, *20*, 522.

Masscheleyn, Patrick H.; Delaune, Ronald D.; Patrick, W. H. Jr. *Environ. Sci. Technol.*, **1990**, *24*, 91.

Masscheleyn, Patrick, H.; Delaune, Ronald D., Patrick, William H. Jr. *Environ. Sci. Technol.*, **1991**, *25*, 1414.

McBride *Environmental Chemistry of Soils*, Oxford Press: New York, 1994.

McKenzie, R. *Mineralogical Magazine*, **1971**, *38*, 493.

Mobley, James; Oregon State University, unpublished report, **1992.**

Organic Reactions, Volume 12, Adams, R.; Blatt, A. H.; Boekelheide, V.; Cairns, T. L.; Cope, A. C.; Curtin, D. Y.; Niemann, C, Eds., John Wiley & Sons, Inc.: New York, 1962.

Owen, W. F.; Stuckey, D. C.; Healy, J. B. Jr.; Young, L. Y.; McCarty, P. L. *Water Research*, **1979**, *13*, 485.

Patai, Saul *The Chemistry of Acyl Halides*; Interscience: London, 1972.

Patrick, W. H. Jr.; Henderson, R. E. *Soil Sci. Soc. Am. J.*, **1981**, *45*, 855.

Patrick, W. H. Jr.; Gotoh, S. *Soil Sci. Soc. Amer. Proc.*, **1972**, *36*, 738.

Patrick, William H. *Nature*, **1966**, *212*, 1278.

Patrick, W. H. Jr.; Jugsujinda, A. *Soil Sci. Soc. Am. J.*, **1992**, *56*, 1071.

Patrick, W. H. Jr.; Williams, B. G.; Moraghan, J. T.; *Soil Sci. Soc. Amer. Proc.*, **1973**, *37*, 332.

Rai, Dhanpat; Sass, Bruce, Morre, Dean A. *Inorg. Chem.*, **1987**, *26*, 345.

Ross, D. S.; Sjogren, R. E.; Bartlett, R. J. *J. Environ. Qual.*, **1981**, *10*, 145.

Sass, Bruce; Rai, Dhanpat *Inorg. Chem.*, **1987**, *26*, 2228.

Schroeder, David C.; Lee, G. Fred *Water Air and Soil Pol.*, **1975**, *4*, 355.

Sheehan, John C.; Hess, George P. *J. Am. Chem. Soc.*, **1955**, *77*, 1067.

Smith, Michael J.; Manahan, Stanley, E. *Analytical Chemistry*, **1973**, *45*, 836.

Sposito, Garrison *The Chemistry of Soils*, Oxford University Press: New York, 1989.

Stollenwerk, K. G.; Grove, D. B. *J. Environ. Qual.*, **1985**, *14*, 396.

Stumm, W., Morgan, J. J. *Aquatic Chemistry*, Wiley-Interscience: New York, 1981.

Thurman, E. M. *Organic Geochemistry of Natural Waters*, Nujhoff and Junk Publishing: Dordrecht, 1985.

Tratnyek, Paul G.; Wolfe, N. Lee, *Environ, Toxicol. Chem.*, **1990**, *9*, 289.

Vainshtein, M. B.; Gogotova, G. I. *Microbiology,* **1987**, *56*, 23.

Walden, W. C.; Hentges, D. J. *Appl. Microbiol.*, **1975**, *30*, 782.

Westall, John C.; Private communication; Oregon State University, 1993.

Zehnder, A. J. B.; Wuhrmann, Karl *Science*, **1976**, *194*, 1165.

ZoBell, Claude E. *Bull. Am. Assoc. Petroleum. Geol.*, **1946**, *30*, 477.

Appendices

Appendix A

Instrumentation

Dispensing Pumps

The FMI dispensing pumps were modified with GrayHill solid state relays (140 VAC, 3 A) to allow computer control with TTL logic. The original and modified circuit diagrams are shown in Figure A.1. When the added toggle switch is in the "MAN" position, the pump functions as purchased. When the switch (b) is in the "TTL" position, the mode switch in "Singles" and 5-V power supplied to the circuit box, the pump will perform one stroke cycle for each logic pulse. The logic lines are all normally high in the program (ensured by a 5 kΩ pull-up resistor in the interface box) so that one complete dispensing cycle is accomplished when the digital output pulses low and returns to high. The mini toggle switch (d) was added to allow continuous pumping without depressing the pendant switch. With the switch in either side position, the pump runs continuously. The dispensing pump needs to be in Singles mode when using toggle switch (d) for continuous pumping. If the dispensing pump is in the continuous mode there is excessive noise in the electrode readings.

Interface Box

The interface box shown in Figure A.2 is connected to the CIO board in the computer with a ribbon cable. There is no electronic circuitry contained in

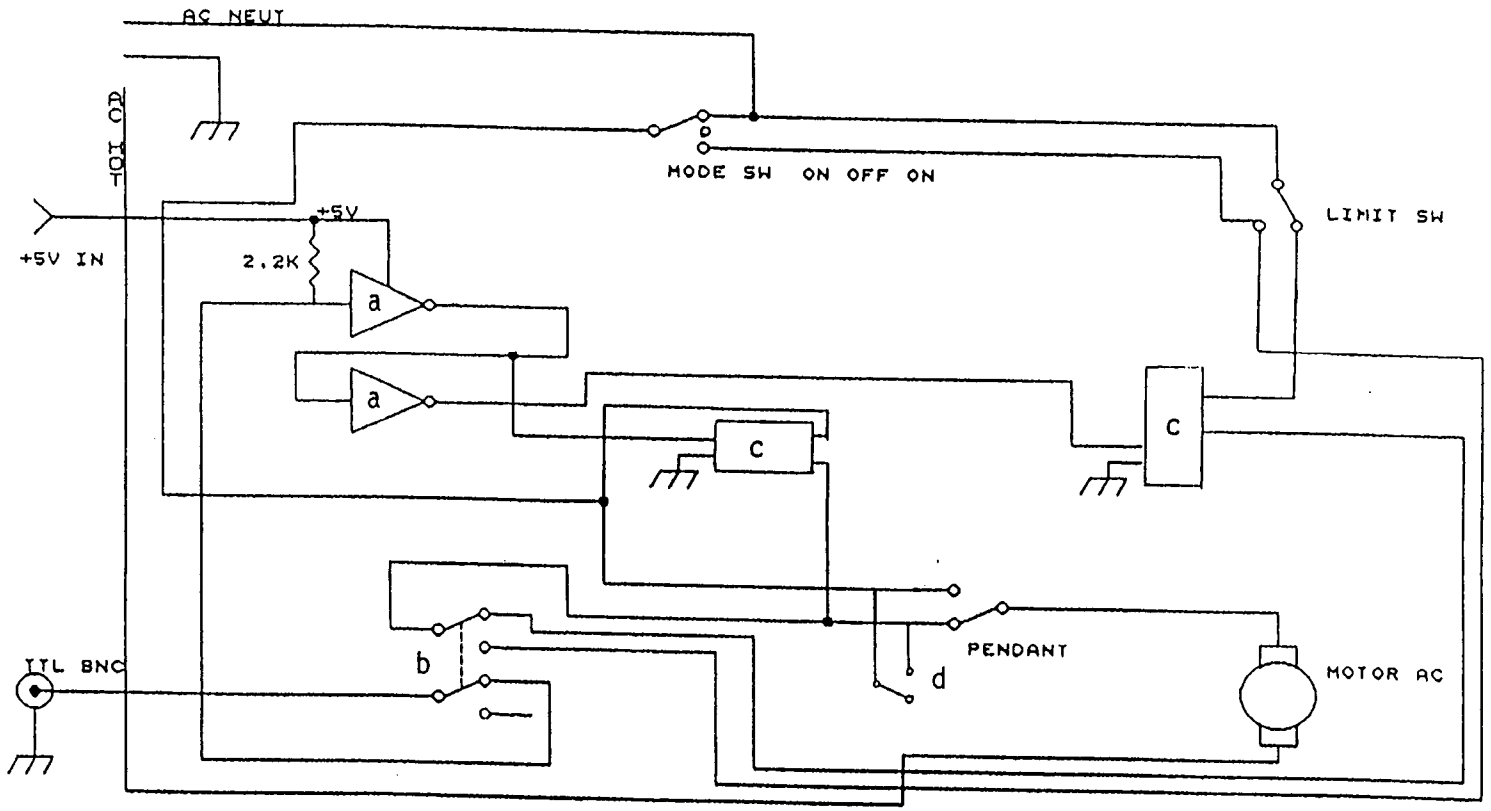

Figure A.1 Circuit diagram for computer controlled dispense pump: (a) 7404 inverter; (b) DPDT switch - up (shown) is TTL control, down is MANual control; (c) solid state relay; (d) SPTT switch to allow continual pumping. Switch (d) is shown in center position for controlled dispensing; both side positions are tied together although only one is shown.

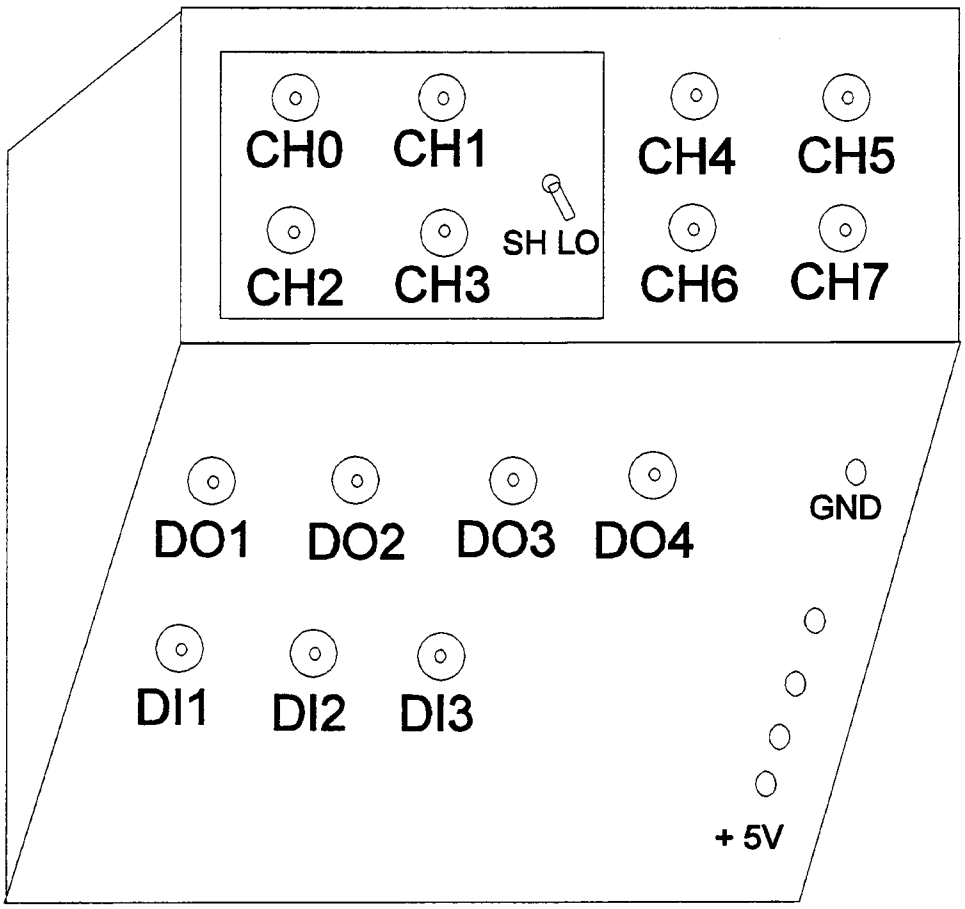

Figure A.2 Interface box attached to computer board with ribbon cable: eight BNC connectors for ADC ports; seven BNC connectors for digital input and output; four banana plugs for +5 V; one banana plug for ground.

the box, only signal connections. The "pinout" for the CIO board is shown in Figure A.3. The multiplexer provides an input impedance of 10 MΩ for each analog input. All eight ADC channels are brought out to insulated BNC connectors to allow differential inputs. Channels 4-7 are configured only for differential input while channels 0-3 have a toggle switch to choose between differential and single-ended input. In the single-ended input mode, all channels share the same common by connecting all lo inputs together in the interface box. In this mode, the same reference electrode (connected to a low input) can be used for potentiometric measurements on all four channels. The digital input/output lines are uninsulated BNC connectors. Finally, there are four 5-V banana plug connectors and one ground.

The signal connections for the system described in Chapter 3 are as follows: pH and reference electrode into pH meter (Orion 407A); recorder output of pH meter to CH0; Pt electrode #1 to CH1, Pt electrode #2 (if applicable) to CH3; sulfide ISE to CH2; digital output 1 (DO1) to the sodium acetate/acetic acid dispensing pump; DO4 to the dispensing pump for redox reagents; DO4 is changed to the sodium sulfide dispensing pump to calibrate the sulfide electrode at the end of the experiment. DO2 and DO3 are reserved for sodium acetate and sodium sulfate solutions; two options that are available but not utilized. The recorder output jacks of the pH meter are pin jacks with full scale output of ± 114 mV. A BNC connector was added and connected at a point above a voltage divider to give full scale output of ± 1V (allowing the signal to be increased without increasing the noise). Several Pt electrodes used are

combination electrodes in which only the Pt half cell is used. This is accomplished by connecting the standard pin (indicator half) to a standard to BNC adaptor (Fisher Scientific, 13-670-498), but not connecting the reference pin. The range for the ADC channels (assigned in the program) are as follows: pH channel, ±0.5 V (0.25 mV or about 0.002 pH resolution)); Pt and sulfide electrode channels, ± 1 V (0.5 mV resolution).

The signal connections for the system described in Chapter 4 are as follows: pH and reference electrodes into Chemtrix Type 60A pH meter #1; recorder output of pH meter #1 to CH3; standard jack of Pt electrode to standard to BNC adaptor (reference pin not connected) to CH1; DO probe to Chemtrix Type 60A pH meter #2; recorder output of pH meter #2 to CH4; DO1 to the acid dispensing pump; DO2 to the base dispensing pump; DO3 to the dispensing pump for other reagents (matrix component etc.); DO4 to the dispensing pump for E_H control with a liquid or to gas solenoid valve for E_H control by O_2 addition. The range for the ADC channels is 0-1 V (0.25 mV or 0.0025 pH resolution) for the pH and DO channels and ±1 V (0.5 mV resolution) for the Pt electrode channel.

Delrin reactor lid

Figure A.4 shows a machine drawing of the Delrin lid constructed for the reactor system described in Chapter 4. To obtain an air-tight seal around the 12-mm diameter electrodes, two O-rings (1/2" x 1/16"W, 3/4" x 1/16"W) and two

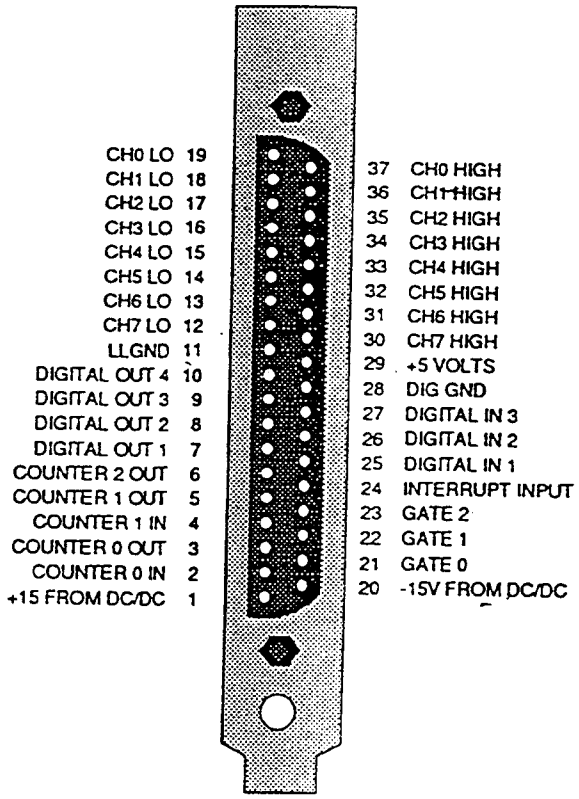

Figure A.3 ADC board analog connector.

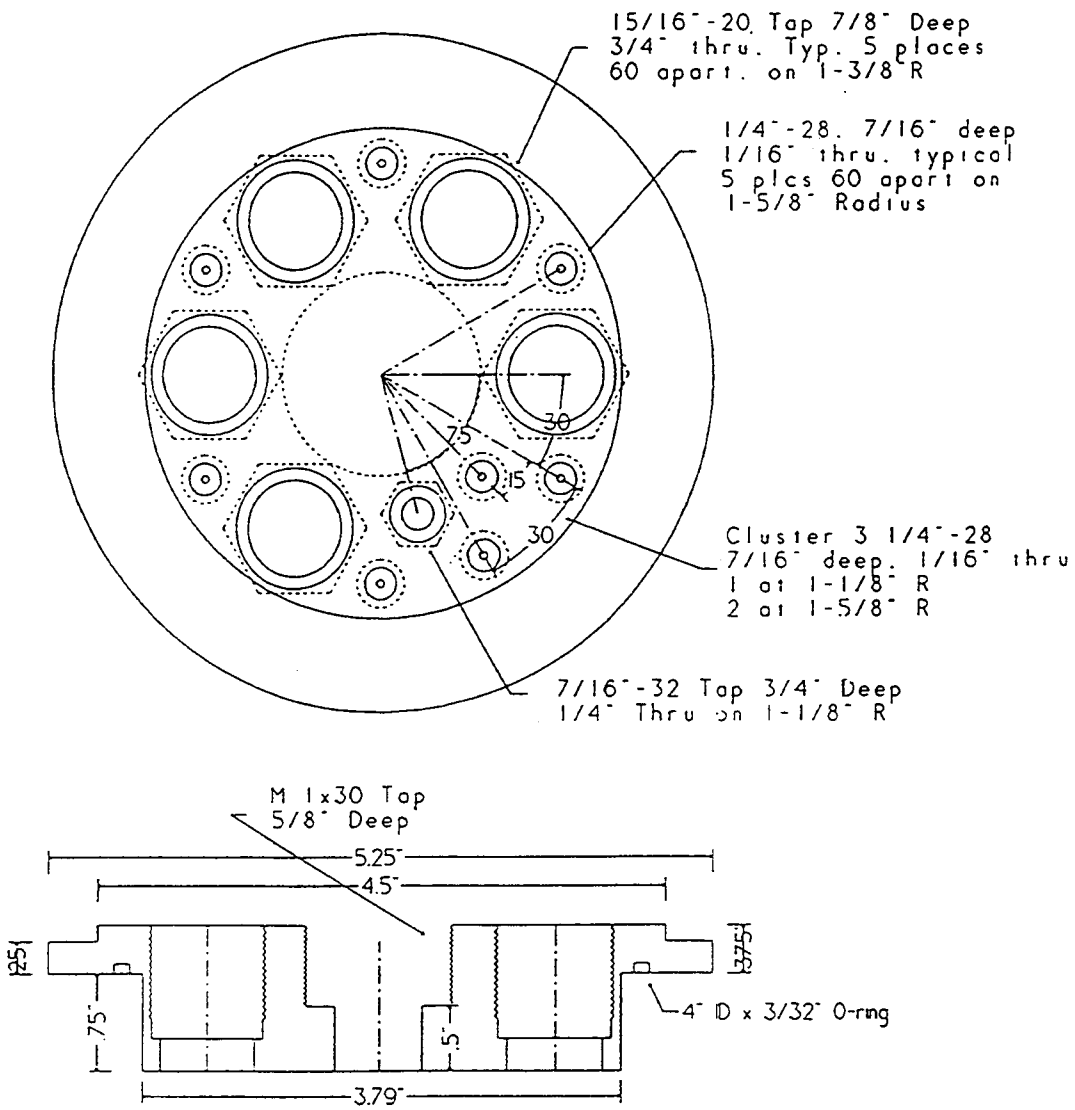

Figure A.4 Machine drawing of Delrin reactor lid. Fittings include: center tap for stirrer motor; five electrode ports; eight ports with 1/4"-28 tap for inlet/outlet of liquids/gases; one thermometer port.

Delrin disks are needed as shown in Figure A.5. The pH electrode has a slightly smaller diameter, so a smaller O ring is needed (3/8" x 1/16"W). The 1/4"-28 thread holes are for inlet/outlet of gases and liquids. Four of the eight have been opened up to 1/8" through holes. The larger tapped hole (7/16"-32) is the thermometer port. The center tap is for the stirring motor.

Delrin filter module

Diagrams of the Delrin filter module are shown in Figure A.6. To minimize plugging of the flow path and leaking around the edges, the module is assembled in the following way (Figure A.7): 1) bottom plate of filter module; 2) Teflon ring made from Teflon film (PTFE, 0.005" thick, 47-mm OD, approximately 37 mm ID); 3) fluorocarbon mesh (Spectra-Mesh macroporous filters, 70-μm pore, 47-mm diameter); 4) Durapore filter (Millipore, 0.65 μm, 47-mm diameter); 5) fluorocarbon mesh; 6) Teflon ring; 7) filter module top plate.

Computer controlled solenoid valve

A three-way solenoid valve is interfaced to the computer to control addition of O_2 (or other gas) to the reactor. The circuit diagram is shown in Figure A.8 and includes a solid state relay (Grayhill, 140 VAC, 3A) and an inverter. The box includes circuitry to control two separate valves. When the valve is not powered (not connected, or connected with TTL line high), gas flow is to the room. When the valve is powered (connected with TTL line low), gas

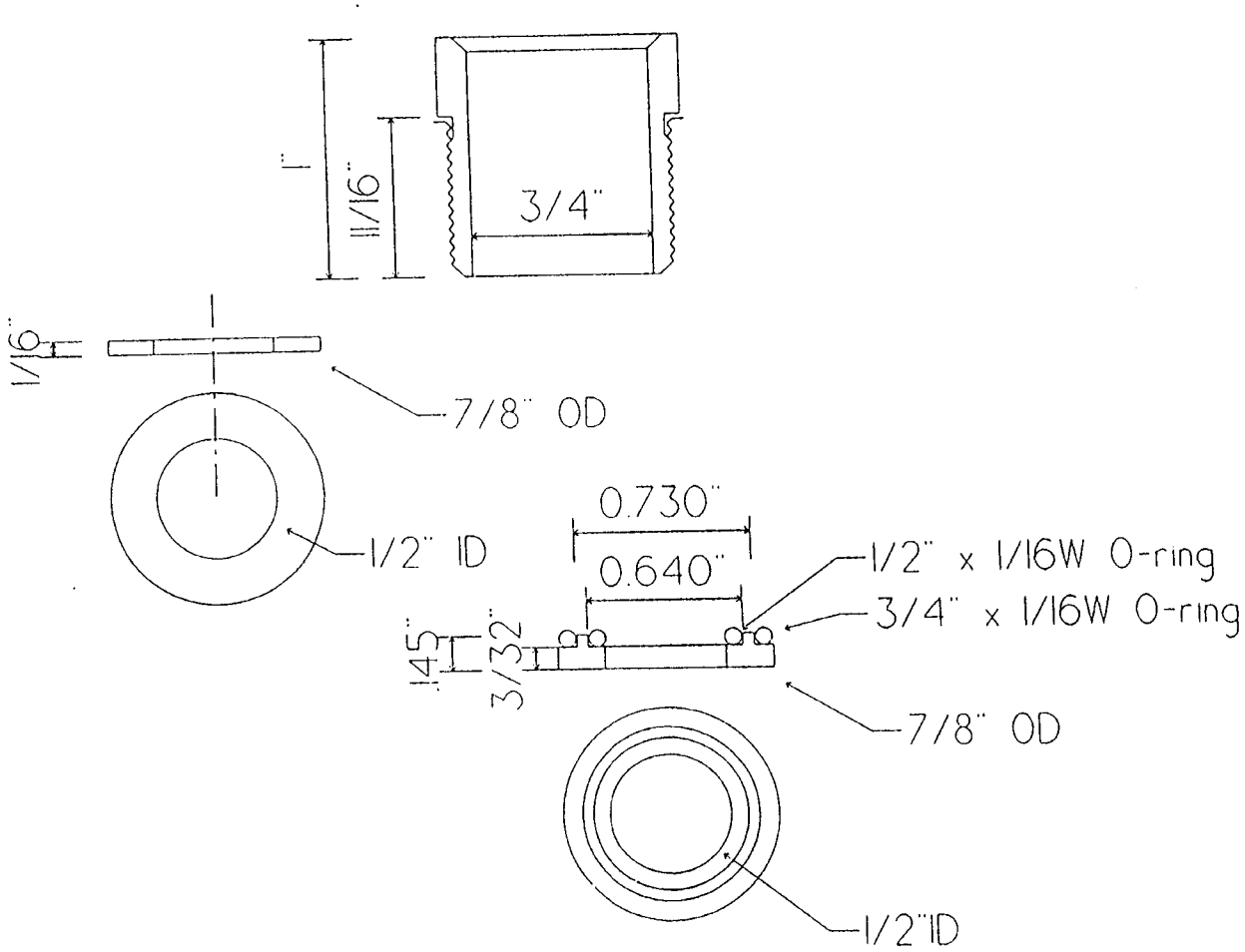

Figure A.5 Electrode fitting assembly.

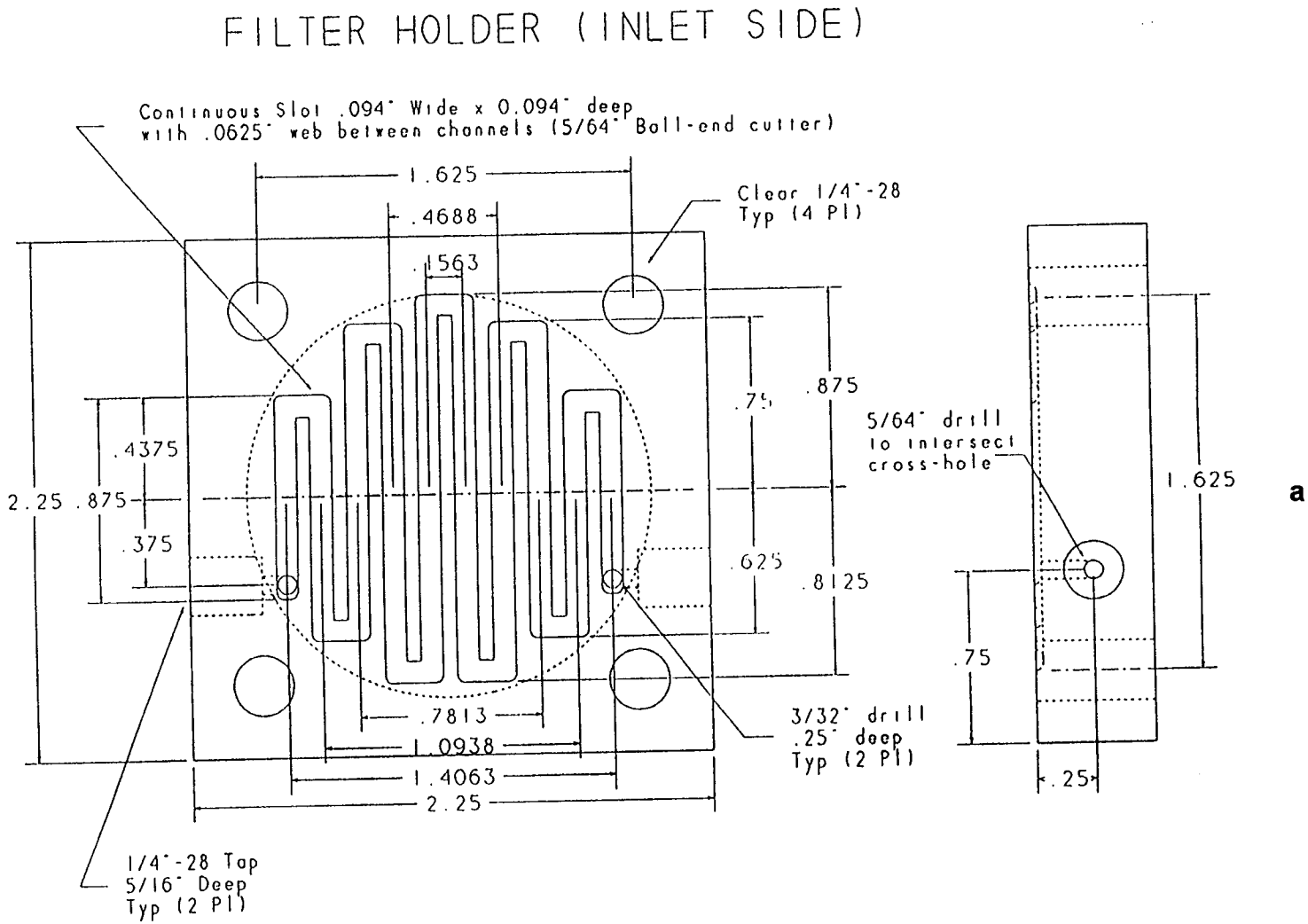

Figure A.6 Machine drawing of Delrin filter holder: (a) inlet side; (b) outlet side.

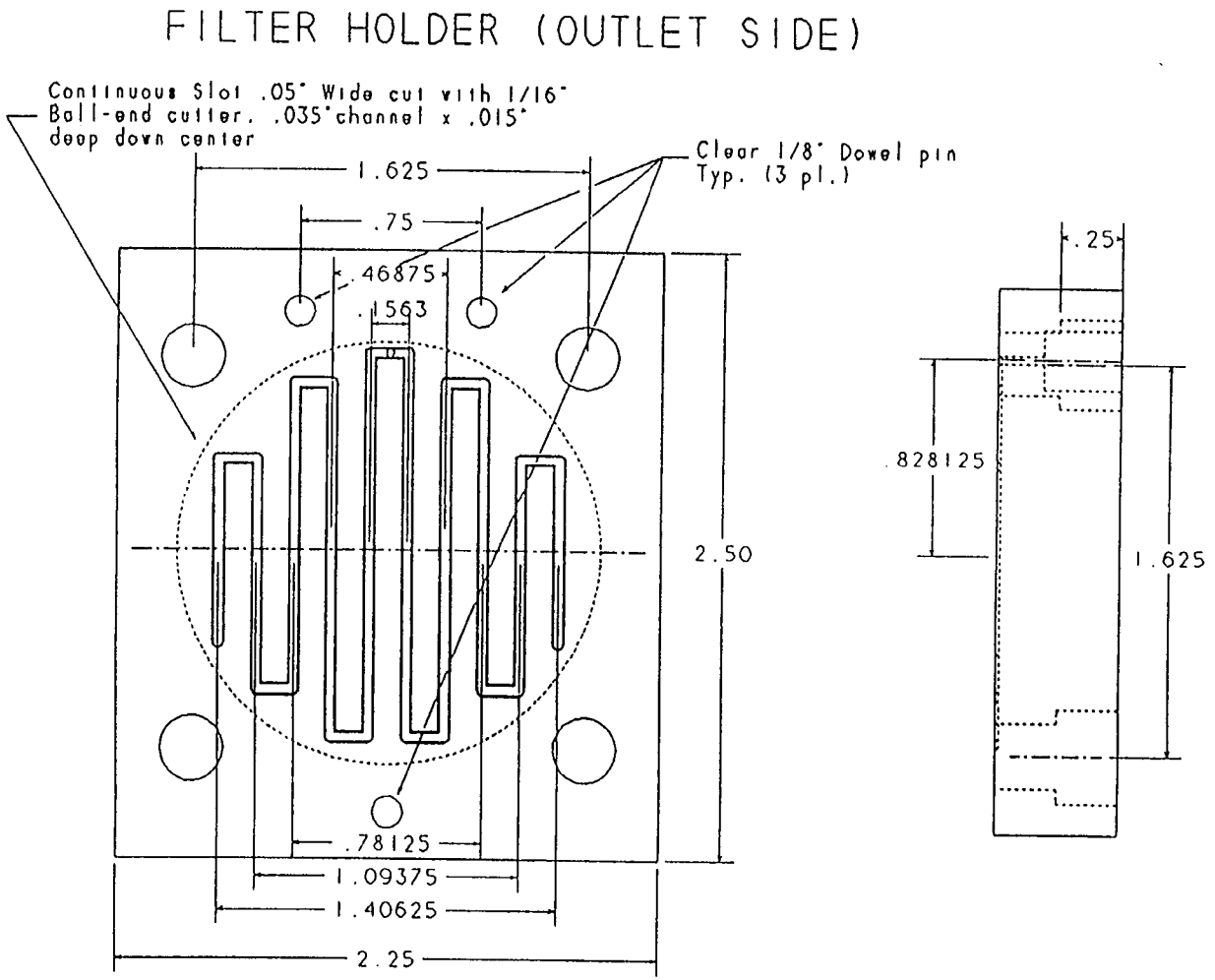

b

Figure A.6 continued.

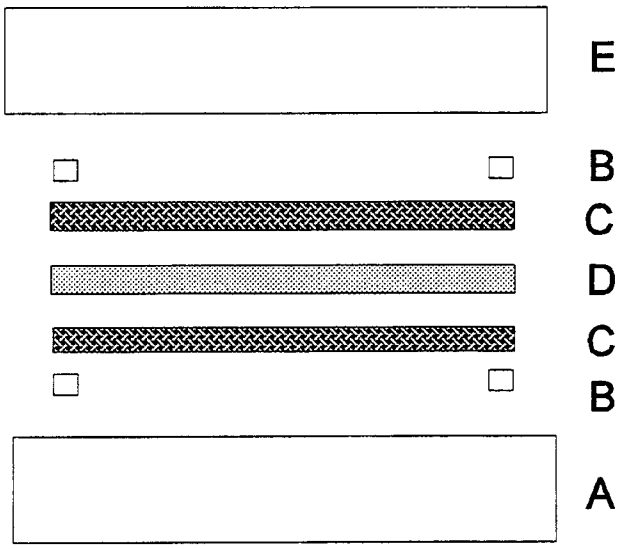

Figure A.7 Assembly of cross-flow filter: (A) filter holer inlet side; (B) Teflon ring; (C) fluorocarbon mesh; (D) Durapore filter; (E) filter holder outlet side.

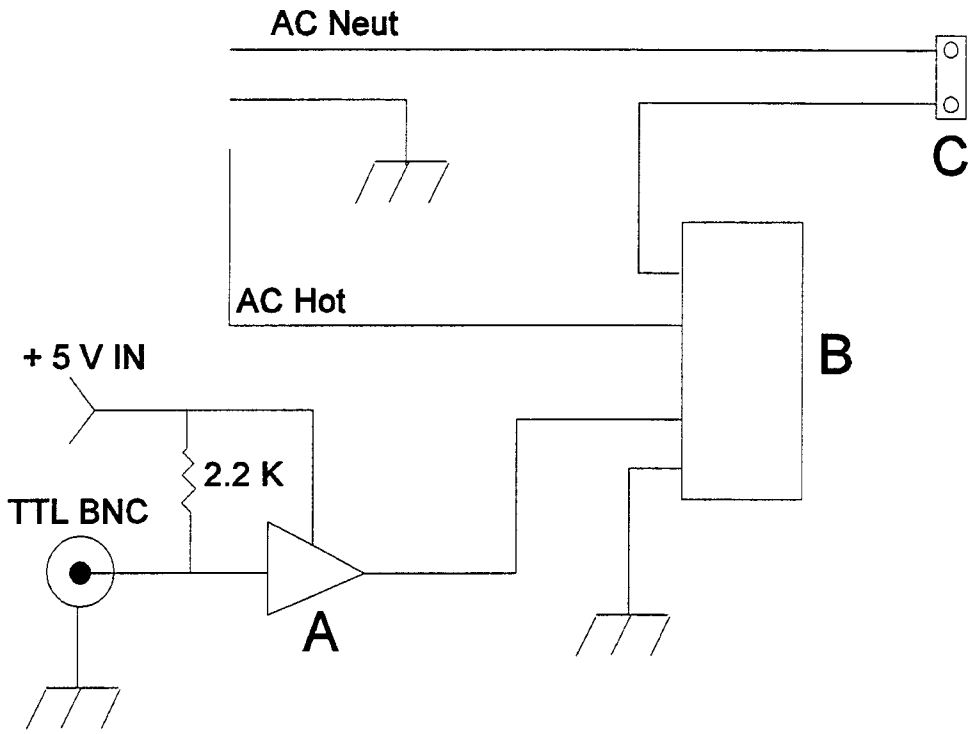

Figure A.8 Circuit diagram for computer controlled solenoid valve: (A) 7404 inverter; (B) solid state relay; (C) plug for solenoid valve.

flow is into the reactor. A three-way valve is used instead of an on/off valve because the flow meter sensor can overheat if no gas is allowed to flow. This allows program logic parallel to the dispensing pump control -- all logic lines are held normally high.

Appendix B

Colorimetric Procedures

Chromium (VI)

Prepare the s-diphenylcarbazide color reagent solution as follows:

1. Dissolve 0.04 g s-diphenylcarbazide in 20 mL of 95% ethanol.
2. Add 24 mL of 85% H_3PO_4 to 56 mL of DI water.
3. Add H_3PO_4 solution (2) to ethanol solution (1).

To determine the concentration of Cr(VI) in a standard solution or a sample, add 1 mL of the above color reagent to 10 mL of sample. Allow the color to develop for 20 min before measuring the absorbance at 540 nm. A standard of 0.96 μM Cr(VI) results in an absorbance of approximately 1.

Soluble Iron

Prepare the following reagents:

1. Hydroxylamine hydrochloride, 10% w/v.
2. Sodium acetate/acetic acid buffer, 1 M.
3. 1,10-phenanthroline, 0.5% w/v.
4. Iron standard, 50 ppm.

In a 10-mL volumetric flask, add the standard (1 mL) or the sample (0.2 - 4.0 mL), hydroxylamine hydrochloride (0.2 mL), sodium acetate/acetic acid buffer (0.4 mL), and 1,10-phenanthroline (0.4 mL). Mix well after addition of

each reagent and dilute to volume. The absorbance is measured at 508 nm after 10 min.

Appendix C

Detailed Experimental Procedure

There are many steps to setting up an experiment in the reactor. They are divided into the following areas: electronic connections, calibrations, packing of the spectrophotometer flow cell, solution preparation, assembly of the reactor lid, assembly of flow loops and data collection.

Electronic Signal Connections

The pH electrode and the reference electrode are connected to a pH meter. The signal from the recorder output is sent to the ADC board channel 2 on the interface box via a BNC cable. The platinum electrode is connected to channel 1 on the ADC board via a standard to BNC adapter. The reference pin of the redox electrode is not used. The low input signals for channels 0-3 are tied together in the interface box when the toggle switch is in the SH LO position. This allows the pH and Pt electrode potentials to be measured against the same reference electrode and eliminates ground loop problems that can occur with two reference electrodes. The dissolved oxygen (DO) probe is attached to a 2nd pH meter and the recorder output is sent to channel 4 of the ADC board.

The dispensing pumps are controlled by digital output (DO) from the ADC board. Each pump is connected to a DO port (with a BNC cable) and the 5-V power supply (with a banana plug) on the interface box. The digital lines are all normally high (a pull-up resister is located inside the interface box). To make an

addition, the digital lines are pulsed low, then high. The in-house modification of the pumps include solid-state relays, an inverter and the circuitry that allow the pumps to be controlled by TTL signals from the computer. The acid pump is controlled by DO1, the base by DO2, and the redox reagent by DO4. If adding gas to control the redox potential, the three-way solenoid valve is connected to DO4.

Calibrations

Replace the inner (saturated AgCl) and outer (10% KNO_3) filling solutions of the reference electrode. Check the potential of the reference electrode vs a saturated calomel electrode (SCE) in a solution with suitable ionic strength (either buffer is OK). The potential should be within a few millivolts. The pH electrode is calibrated manually in buffers of pH 4 and 7. The potential measured in each buffer should be noted as well as the pH. If the slope of the electrode response changes significantly (Orion specifications: 53 - 60 mV/decade), the problem should be investigated further before continuing. Once the meter has been calibrated to read the buffers correctly, the voltage at the recorder output is measured with the program CHPHCAL.BAS. The DO probe is calibrated according to the manufacturer's instructions, and the voltage output is measured by the program DOCAL.BAS. The Pt electrode potential is corrected for the reference electrode (241 mV) before writing to the data file or

the display screen. The reference voltage can be input at the start of the program if a different reference electrode is being used.

The dispensing pumps also need to be calibrated so the actual volume delivered with each pulse is known. The stroke volume is calibrated by weighing the water delivered in 20 strokes.

Spectrophotometer flow cell

To confine the indicator gel to the flow cell, a piece of nylon mesh (Spectrum 30 um) is placed in the outlet fitting of the cell. A tool (similar to a cork borrer) is used to cut the correct size disc. The mesh is positioned between two rubber gaskets that allow the fitting to seal. The two short sections of inlet and outlet tubing are connected to the cell and the indicator gel is packed by drawing the slurry through the inlet tubing into a 5 mL syringe located on the outlet side of the cell.

Solution Preparation

Solutions of 1 M HCl and 1 M NaOH are prepared for the pH-stat. The 0.05 M hydrogen peroxide solution is not prepared until needed. The delivery lines (PEEK tubing 0.0625" OD, 0.03" ID) are thoroughly flushed with the reagents and the pumps are placed in singles mode. The reactor solution is prepared by adding one liter Millipore deionized water, the soil, and $CaCl_2$ to the

reactor. The typical soil:water ratio is 1:20 and the $CaCl_2$ concentration in the reactor is 10 mM.

Assembly of Reactor Lid

To include the gas purge filter, the tubing must first be placed through one of the liquid ports in the reactor lid before the filter can be attached. This must be done before the lid is sealed to the reactor vessel. The pH, reference and Pt electrode are placed in three of the electrode ports in the reactor lid. The Delrin disks and o-rings must be used to obtain an air-tight seal. A smaller o-ring is used with the pH electrode since the electrode diameter is smaller. The Chemiinert septum valve occupies the fourth electrode port (replace septum as needed). The final electrode port is where the inlet filter fitting is located. This fitting allows the inlet filter to be removed and cleaned if needed during an experiment without opening the reactor and exposing the contents to atmospheric oxygen. The other liquid ports are used for the inlet/outlet of the flow loops, the reagent addition tubing and the gas outlet line. The outlet gas is bubbled first through a saturated solution of sodium sulfite (about 3 g per 25 mL) which serves as an oxygen scavenger and then through a flask of DI water. This DI water is always in equilibrium with the head space in the reactor and can be added to the reactor to maintain the volume as made necessary by sampling.

Assembly of flow loops

The first step is to assemble the Delrin filter module as follows: bottom half of filter module, Teflon o-ring, fluorocarbon mesh, Durapore filter, fluorocarbon mesh, Teflon o-ring, top half of filter module. There are two flow loops in the system; the primary loop which includes the peristaltic pump and the filter module, and the filtered secondary loop which consists of the piston pump, the pressure gage, the spectrophotometer flow cell and the DO flow cell. The smaller toggle vavle on the piston pump allows continous pumping. NOTE: the dispensing pump needs to be in Singles mode. The tubing for the primary loop is PEEK tubing (0.125" OD, 0.080" ID) except for the section of Tygon tubing (size 14) at the peristaltic pump. The secondary loop is entirely PEEK tubing (0.0625" OD, 0.03" ID). All tubing connections are standard 1/4" - 28 thread. It is imperative that all tubing connections be tight so no oxygen can enter the system.

Data collection

Take an initial scan of the indicator gel before starting the flow loops. The second 1-mm flow cell with water is used as the blank. Start the primary flow loop, dial set to 1.8 (~20 mL/min), and the secondary flow loop, dial on micro ∏-petter set to 75 (~0.8 mL/min). Begin the nitrogen purge at 50 sccm. Initiate data collection program.

During the experiment, the Tygon tubing for the peristaltic pump needs to be replaced or moved every three days. The flow through the primary loop should be checked periodically. If the flow stops, the filter module may need to be removed from the loop and cleaned. When the Tygon tubing is replaced, it is a good idea to clean the filter module as well. The secondary loop should not be left pumping overnight. When it is operating, the filter module needs to be sonicated every few hours for at least 15 min and ice aded to the bath to prevent overheating.

The reference electrode filling solutions should be replaced every week. To remove the reference electrode, loosen the Delrin fitting enough to allow the electrode to be gently pulled out. Immediately place a Teflon rod plug in the electrode port. Check the potential of the reference electrode versus a SCE electrode both before and after replacing the filling solutions.

Appendix D

Chromium Reactions in the Environment

Chromium is a heavy metal that is widely used in industry (i.e. tanning, electroplating, pulp products and ore refining) and thus is often present in waste sludges disposed of in landfills, on land surfaces or in waste ponds and lagoons. Chromium oxidation states range from -2 to +6, but under E_H/pH conditions found in soils and groundwaters, only the +3 and +6 oxidations states are stable. Cr(III) exists under reducing and moderately oxidizing conditions (a wide range of E_H and pH) while Cr(VI) is only stable under strongly oxidizing conditions. The mobility and toxicity of Cr are dependent on its oxidation state. Cr(III) has no established toxicity and is therefore considered a low health risk. However, Cr(VI) compounds are toxic and known carcinogens that can be absorbed by ingestion, skin contact and inhalation (1, 2). Chromium present as Cr(III) is relatively immobile in water and soil systems due to precipitation as $Cr(OH)_3$ and $(Cr,Fe)(OH)_3$ solids, adsorption to surfaces and complexation with insoluble organic matter while Cr(VI) compounds are more mobile.

As can be seen from the above discussion, the environmental chemistry of Cr is very complex. Rai et al (3, 4, 5) have published several reports that summarize the reactions of Cr in the environment and provided newly determined equilibrium constants for many of these reactions. The reactions of interest are the oxidation of Cr(III), reduction of Cr(VI), precipitation/dissolution

of Cr(III) and precipitation/dissolution of Cr(VI). These reactions are summarized below.

Rai et al (3) concluded that either $Cr(OH)_3(s)$ or Cr(III) in a solid solution with Fe hydroxides are the solids that control the solubility of Cr(III) in environmental systems. They conducted studies to determine the solubility (6, 7) and hydrolysis constants (6) of Cr(III) solids. The dominant species were concluded to be $CrOH^{2+}$ at pH < 6.5, $Cr(OH)_3^0$ at pH between 6.5 and 11, and $Cr(OH)_4^-$, above pH 11. The solubility of $Cr_xFe_{1-x}(OH)_3$ solids prepared with various mole fractions of Cr (x) were studied (7), and it was observed that the concentration of Cr(III) in solution varied with the mole fraction (x). This indicates that Cr and Fe do form a solid solution. In addition, the concentration of $CrOH^{2+}$ in equilibrium with $Cr_xFe_{1-x}(OH)_3$, at the low chromium concentrations expected in geological environments, is several orders of magnitude lower than predicted by $Cr(OH)_3$ solubility.

Dissolved oxygen and manganese oxides are the only naturally occurring oxidizing agents capable of oxidizing Cr(III) to Cr(VI) (8). Schroeder and Lee (9) studied the oxidation of Cr(III) by dissolved oxygen (DO). They conclude that oxidation by DO is sufficiently slow that Cr(III) is more likely to be involved in other reactions before oxidation by DO can occur.

Bartlett and coworkers (10, 11, 12) were the first to observe oxidation of Cr(III) to Cr(VI) in soils containing oxidized manganese. The increase in [Cr(VI)] was accompanied by an increase in [Mn(II)], indicating Mn(IV) is acting as the

electron acceptor. The oxidation of Cr(III) was not observed in soils that were low in Mn or in soils for which the predominant form of Mn present was Mn(II).

More extensive studies of Cr(III) oxidation by various forms of MnO_2 have been performed by Eary and Rai (6), Fendorf and Zasoski (13), Fendorf and Sparks (14), and Manceau and Charlet (15). Eary and Rai (6) examined Cr(III) oxidation by β-MnO_2(s) (pyrolusite). This mineral is the most chemically pure and crystalline form of MnO_2(s). The results are as follows: 1) oxidation is unaffected by DO; 2) oxidation of Cr(III) increases almost proportionally to an increase in surface area of β-MnO_2; 3) the rate of oxidation is initially rapid and then decreases; 4) the rate of oxidation is independent of the Cr(III) concentration; 5) in neutral and basic solutions (pH 6.3, 8.3, 10.1), oxidation of aqueous Cr(III) is slow and limited by the low solubility of $Cr(OH)_3$. The authors suggest that the adsorption of aqueous Cr(VI) anions to the positively-charged surface of the oxide is the cause of the decrease in rate of oxidation with time. This conclusion is disputed by other workers (13, 14) because the extent of oxidation increased at lower pH values which contradicts an expected stronger adsorption by negative Cr(VI) species on the more positively-charged surface.

Fendorf and Zasoski (13) and Fendorf and Sparks (14) studied the extent of oxidation of Cr(III) by δ-MnO_2 (birnessite), a common naturally occurring form of MnO_2. They also observed a decrease in extent of oxidation as pH increased and proposed that surface precipitation of chromium hydroxide prohibits the extent of oxidation. When the pH is less than 4, the release of Mn(II) is a direct measurement of the oxidation rate of Cr(III).

In early studies, it assumed that the removal of Cr(VI) was due to either adsorption (16) or reduction (17) alone. Neither precipitation nor a combination of adsorption and reduction was considered. The removal of Cr(VI) can be attributed to the sum of; 1) Cr(VI) reduction and subsequent precipitation of chromium hydroxide, 2) Cr(VI) precipitation, and 3) Cr(VI) adsorption. Chromium(VI) can be reduced in soil and groundwater by Fe(II) (18, 19), dissolved sulfides (9) and easily oxidized organic matter (20). The reactions are all favored by low pH and low dissolved oxygen content.

Removal of Cr(VI) from soils has been studied by several groups (11, 12, 20, 21, 22). The amount removed decreased when the pH of the soils was increased with $CaCO_3$ (20) as expected since increased pH should decrease Cr(VI) reduction. Because addition of sulfate and phosphate had no affect on the removal of Cr(VI) in the soils not treated with $CaCO_3$, it was proposed that removal was due to reduction rather than precipitation.

Reduction of Cr(VI) by aqueous Fe(II) reaches completion within 1- 2 min but is not stoichiometric in moderately basic solutions that have high phosphate concentrations (18). The ratio of products, Fe(III) to Cr(III), is greater than the expected value of 3. This is attributed to the increased rate of Fe(II) oxidation by O_2 under these conditions. Because the equilibrium activity of Cr(III) was found to be lower than those predicted by the solubility of $Cr(OH)_3$, it was determined that the precipitates formed were a solid solution of $(Cr,Fe)(OH)_3(s)$.

The abundance of Fe(II) containing minerals in soils and sediments represent a large source of Fe(II) for reduction of Cr(VI). The kinetics of

chromate reduction by hematite (3% Fe(II), 62% Fe_{total} by weight) and biotite (12% Fe(II), 15% Fe_{total} by weight) were studied to determine what factors affect the rate of the redox reaction (19).

Complete reduction of 10^{-4} M Cr(VI) occurred in both solutions, but was much faster in the hematite solution (less than one hour) than in the biotite solution (within 12 hr). Fe(II) ions in solution were not detected until after the complete reduction of Cr(VI), indicating that Fe(II) was the reducing species. Both the rate of reduction and total amount of Cr(VI) reduced were dependent on pH. As pH increased, the rate and amount of reduction decreased in hematite and biotite solutions due to slower dissolution of the minerals and increased rate of Fe(II) oxidation by dissolved oxygen.

From the above results, it was concluded that reduction of Cr(VI) occurs in the aqueous phase, not on the surface. Therefore, the effective oxidation potential of the Fe(II) minerals can be defined by the $Fe^{2+}/Fe(OH)_3(s)$ redox couple. It was also observed that the concentrations of Cr(III) in acidic solutions were similar to those predicted by the solid solution $(Cr_{0.25},Fe_{0.75})(OH)_3$ indicating the formation of this precipitate.

In a recent study (23) of Cr(VI) reduction by suboxic core material, it was observed that the degree of reduction was dependent on the composition and amount of fines present. The percentages of Fe(II)-minerals and organic content, which enhance Cr(VI) reduction, increase with smaller grain size. It is therefore suggested that composition and amount of fines is the key to understanding Cr(VI) reduction in aquifers.

Most Cr(VI) solids are very soluble (3) and therefore unimportant in determining the concentration of aqueous Cr(VI) in geological environments. However, the low solubility of $BaCrO_4$ and the presence of barium in soils and minerals suggests that $BaCrO_4$ may control the concentration of aqueous Cr(VI) in soil solutions. Because the observed concentrations of Ba and Cr(VI) are often several orders of magnitude below those predicted by the solubility of $BaCrO_4$, it was determined that a solid solution of $BaCrO_4$ and $BaSO_4$ controls the solubilities (5).

Rai et al (5) investigated the behavior of Cr in several soils (rather than pure minerals) and observed all of the above discussed reactions to take place. They also determined that more than one reaction is important in all of the soils.

References

1. Cox, B. X.; Linton, Richard W. *Environ. Sci. Technol.* **1985**, *19*, 345

2. Ross, D. S.; Sjogren, R. E.; Bartlett, R. J. *J. Environ. Qual.*, **1981**, *10*, 145.

3. *Chemical Attenuation Rates, Coefficients in Leachate Migration: Vol 1*, Rai, D.; Zachara, J. M., Electric Power Research Institute Report EA-2485-3, 1984.

4. *Geochemical Behavior of Chromium Species*, Rai, D.; Zachara, J. M., Electric Power Research Institute Report EA-4544s, 1986.

5. *Chromium Reactions in Geologic Materials*, Rai, D.; Zachara, J. M., Electric Power Research Institute Report EA-2485-3, 1988.

6. Rai, Dhanpat; Sass, Bruce; Moore, Dean A. *Inorg. Chem.*, **1987**, *26*, 345.

7. Sass, Bruce; Rai, Dhanpat *Inorg. Chem.*, **1987**, *26*, 2228.

8. Eary, L. Edmond; Rai, Dhanpat *Environ. Sci. Tech*, **1987**, *21*, 1187.

9. Schroeder, David C.; Lee, G. Fred *Water Air and Soil Pol.*, **1975**, *4*, 355.

10. Bartlett, Richmond; James, Bruce *J. Environ Qual.*, **1979**, *8*, 31.

11. Bartlett, R. J.; Kimble, J. M. *J. Environ Qual*, **1976**, *5*, 379.

12. James, Bruce; Bartlett, Richmond J. *J. Environ Qual*, **1983**, *12*, 173.

13. Fendorf, Scott E.; Zasoski, Robert J. *Environ. Sci. Tech.*, **1992**, *26*, 79.

14. Fendorf, Scott E.; Sparks, Donald L *Abstract: American Chemical Society* Meeting, **1992.**

15. Manceau, A.; Charlet, L. *Abstract: American Chemical Society Meeting*, **1992.**

16. Griffin, R. A.; Au, Anna K.; Frost, R. R. *J. Environ. Sci. Health*, **1977**, *A12*, 431.

17. Grove, J. H.; Ellis, B. G.; *Soil Sci. Soc. Am. J.*, **1980**, *44*, 238.

18. Eary, L. E.; Rai, Dhanpat *Environ. Sci. Tech.*, **1988**, *22*, 972.

19. Eary, L. E.; Rai, Dhanpat *American Journal of Science*, **1989**, *289*, 180.

20. James, Bruce R.; Bartlett, Richmond J. *J. Environ. Qual.*, **1983**, *12*, 177.

21. Bloomfield C.; Pruden, G. *Environ. Pollut. Ser. A*, **1980**, *23*, 103.

22. Stollenwerk, K. G.; Grove, D. B. *J. Environ. Qual.*, **1985**, *14*, 396.

23. Anderson, Linda D.; Kent, Douglas B.; Davis, James A. *Abstract: American Chemical Society Meeting*, **1992.**